OPTIMISING A WATER TRANSMISSION SCHEME IN UNITED ARAB EMIRATES

Sustainability and Cost-Effectiveness Perspectives

MSc. Thesis Energy Science
J.L. Swanenberg
4167112

Deltares
Enabling Delta Life

Utrecht University

Optimising a Water Transmission Scheme in United Arab Emirates

Sustainability and Cost-Effectiveness Perspectives

by

J.L. (Joyce Liselot) Swanenberg

Copernicus Institute of Sustainable Development

In partial fulfilment of the requirements for the degree of

Master of Science
in Energy Science

at Utrecht University, UU

Date:	July, 2019	
Student number:	4167112	
Supervisor UU:	Prof. Dr. Madeleine Gibescu	Utrecht University
Second reader UU:	Assistant Prof. Dr. Elena Fumagalli	Utrecht University
Supervisor Deltares:	Sam van der Zwan	Deltares

Abstract

A considerable portion of costs and greenhouse gas (GHG) emissions associated with the transmission of fresh water is related to energy usage. Optimising the costs and GHG emissions of energy consumption by scheduling the pumping cycle and by the use of storage areas is a multi-objective mixed integer nonlinear programming (MINLP) problem that contains multiple constraints. The solution space and running time of this type of problem can be very large. To solve this problem and to improve the operational sustainability of a water transmission scheme (WTS) as profitable as possible and by fulfilling to the demand of water, a mixed integer linear programming (MILP) model is made with the software OpenModelica and RTC-Tools. The model is made and analysed for a WTS located in the emirate Abu Dhabi, United Arab Emirates (UAE), but can be applied to other portions of a WTS. Multiple scenarios are conducted related to electricity prices (flat rate versus Time of Use (ToU) rates), GHG emissions factors (average (AV) versus time-dependent (TD) GHG emissions factors), carbon taxes and the influence of the infrastructure of the WTS on the pump schedule. The results show that when switching to ToU electricity tariffs and/or TD GHG emissions factors and thereby using the capacity of the storage areas, remarkable costs and/or GHG emissions savings are possible. Also, including a carbon tax has a positive effect on switching the pump schedule to day time (solar availability in UAE). However, when the proportion of solar power is small compared to the other power sources, the necessary carbon tax is disproportional high. Furthermore, a sensitivity analysis is performed to test the robustness of the GHG emissions intensities and the water flow speed through the system. Finally, recommendations are made to shift the model to a continuous model to further reduce the solution space.

Preface

This thesis is part of my Master's programme Energy Science at the Faculty of Geosciences at Utrecht University, research group Energy and Resources of the Copernicus Institute of Sustainable Development. Over the last six months I have been working on it at Deltares in Delft in collaboration with my supervisors at both Deltares and Utrecht University. I would like to thank several people for their support and contribution to this research.

I am really grateful for the opportunity Deltares gave me to perform my thesis here. It ended up being an enjoyable and interesting experience. Thank you Sam van der Zwan for initiating this project and for sharing your passion and knowledge of water systems with me. Thank you Tjerk Vreeken for helping me with the questions I had about the software and the many errors I experienced. You really helped me understanding the tool much better than I would have accomplished by myself. Also thank you TRANSCO for providing me with the data of your water infrastructure network and the water flows through your network. I hope the results of this project give you an insight in how the pump schedule reacts on different electricity prices and GHG emissions factors and how this can result in costs and GHG emissions savings for you.

I would also like to thank Madeleine Gibescu, my supervisor from Utrecht University. Although the topic is not your research expertise, I hope you enjoyed supervising me and that you gained some knowledge about water transmission systems. I always had pleasant meetings with you and I want to thank you for your feedback you provided on the delivered products.

Finally, I would like to thank the colleagues and fellow students at Deltares for the good discussions we had about our projects but also for the enjoyable coffee breaks and lunches. I enjoyed working together on our projects.

I hope you will enjoy reading my thesis.

Joyce Liselot Swanenberg
Utrecht, July 2019

List of Figures

List of Tables

Abbreviations & Symbols

List of Abbreviations

Symbol	Description	Units
AADC	Al Ain Distribution Company	–
ADDC	Abu Dhabi Distribution Company	–
ADWEA	Abu Dhabi Water and Electricity Authority	–
ADWEC	Abu Dhabi Water and Electricity Company	–
BST	Bulk Supply Tariff	–
EI	Emission Intensity	–
GHG	Greenhouse Gas	–
MIGD	Million Imperial Gallons per Day	–
MILP	Mixed Integer Linear Programming	–
MINLP	Mixed Integer Non-Linear Programming	–
MO	Multi-objective	–
RTC-Tools	Real Time Control Tools	–
SO	Single-objective	–
ToU	Time of Use	–
TRANSCO	Transmission and Despatch Company	–
TUoS	Transmission Use of System	–
UAE	United Arab Emirates	–
WDS	Water Distribution System	–
WSS	Water Supply System	–
WTS	Water Transmission System	–

List of Symbols

Symbol	Description	Units
$\#_{tanks}$	Number of tanks in tank farm	–
ϵ	Pipe roughness	mm
η	Efficiency	%
ω	Angular velocity	rad/s

π	Pi	–
ρ	Density of water	kg/m^3
ϑ	Kinematic viscosity	m^2/s
A	Cross sectional area	m^2
AV_{factor}	Average GHG emissions factor	kg CO_2-eq/kWh
C	Resistance coefficient	s^2/m^5
C_{tot}	Total costs	AED
CP	Carbon price	AED/kWh
CT	Carbon tax	AED/kg CO_2-eq
d	Diameter of pipe	mm
$d_{modelled}$	Diameter of modelled pipeline	mm
$Distr_{source}$	Distribution per power source	%
E_{tot}	Total emissions	kg CO_2-eq
EI_{source}	Emissions intensities per source	kg CO_2-eq/kWh
EP	Electricity price	AED/kWh
f	Friction factor	–
f_{GHG}	GHG emissions factor	kg CO_2-eq/kWh
g	Gravitational acceleration	m/s^2
H	Head	m
H_b	Level of bottom of tank compared to sea level	m
H_{cp}	Counter pressure	m
H_{dyn}	Dynamic head	m
H_{stat}	Static head	m
h_{tank}	Height of tank	m
H_{total}	Total head	m
H_{valve}	Height of valve	m
$HQ.H_{max}$	Maximum water elevation (max. level of water in the tank compared to sea level)	m
$HQ.H_{min}$	Minimum water elevation (min. level of water in the tank compared to sea level)	m
k	Relative roughness	–
L	Length of pipeline	km
M	Torque in drive shaft of pump	Nm
n	Speed of pump	rpm
n_{pumps}	Number of pumps	–

P	Power	kW
P_{demand}	Demand profile of UAE	kW
p_{elec}	Electricity price	AED/kWh
$P_{pump,mir}(t)$	Power of pumping station Mirfa at timestep t	kWh
$P_{pump,shu}(t)$	Power of pumping station Shuweihat at timestep t	kWh
P_{source}	Power generation by different power sources	kW
$P_{tot}(t)$	Total power at timestep t	kWh
Q	Discharge	m^3/s
r_{tank}	Radius of tank	m
Re	Reynolds number	–
TD_{factor}	Time-dependent GHG emissions factor	kg CO_2-eq/kWh
TP	Total price (EP + CP)	AED/kWh
v	Speed of flowing water	m/s
$V_{modelled}$	Volume of modelled pipeline	m^3
V_{single}	Volume of single pipeline	m^3
V_{tank}	Volume of individual tanks	m^3
V_{total}	Volume of tanks modelled together	m^3
$WL_{mir,max}$	Max. water level storage area Mirfa	m
$WL_{mir,min}$	Min. water level storage area Mirfa	m
WL_{mir}	Water level storage area Mirfa	m
$WL_{mus,max}$	Max. water level storage area Mussafah	m
$WL_{mus,min}$	Min. water level storage area Mussafah	m
WL_{mus}	Water level storage area Mussafah	m
$WL_{shu,max}$	Max. water level storage area Shuweihat	m
$WL_{shu,min}$	Min. water level storage area Shuweihat	m
WL_{shu}	Water level storage area Shuweihat	m

Contents

I

Background

---

1 Introduction

1.1. Background

The growing demand of fresh and clean water together with population growth and an increased water consumption per capita result in one of the most important issues facing civilisation today: water scarcity (Simonovic, 2002; Jones et al., 2018). 40% of the global population faces severe water scarcity, rising to 60% by 2025. Moreover, two-thirds of the global population (four billion people) face severe water scarcity at least one month per year (Mekonnen & Hoekstra, 2016). Besides that, the World Economic Forum list the water crisis in the top ten risks in terms of potential impact, behind failure of climate change mitigation and extreme weather events (Forum, 2019). These statistics are in direct conflict with Sustainable Development Goal 6: 'Ensure access to water and sanitation for all' (UN, 2019). Countries and areas facing water scarcity therefore need to re-think and re-develop their fresh water resource planning and management (Jones et al., 2018), including supply enhancement strategies (Gude, 2017) and strategies for transporting the water from places where it is abundant to places where it is scarce. To transport the water to water-scarce areas, the water must flow from the supply source, for instance a desalination plant, through a Water Supply System (WSS) where it will end at the customers.

A WSS consist of two main parts: the Water Transmission System (WTS) and the Water Distribution System (WDS). The WTS usually connect the fresh water reservoir of a treatment plant with a central storage in the distribution area. In case of long distances or height differences in the landscape, pumping stations or interim storages may be required. The WDS consist of smaller pipes that directly supply water to the customers through numerous connections. Although the systems differ, their main objectives are common: 1) the supply of adequate water quantities, and 2) maintaining the fresh water quality (Trifunovic, 2006). The global growing demand of fresh water and therefore the need of an increasing usage of WTSs and WDSs leads to a rise in electricity usage and greenhouse gas (GHG) emissions since a larger amount of fresh and desalinated water must be transported. The electricity usage and the corresponding GHG emissions of WSSs are mainly generated from system operations related to pumping (Wu, 2011b). Research conducted by Tarantini and Ferri (2001) shows that pumping (used for water treatment and for distribution) accounts for the highest environmental impact of the water system of Bologna, Italy. A research of the South Australian Water Corporation shows similar results, where pumping accounts for 46% of the GHG emissions of their total activities across South Australia (Kelly, 2007). However, the impact of pumping on the environment is dependent on the height differences in the landscape and the distance the water must transport. For a country such as The Netherlands, pumping may have a smaller impact compared to for example Australia because of the smaller transport distances and the smaller height differences. Besides pumping, other components also have an influence on the electricity usage and the GHG emissions of WSSs. Among them, the electricity tariff schedule of the specific country (peak hours, power source mix) and the drivers of the WSSs (electric motors, gas turbines, solar panels, etc.) have a large influence (Stokes et al., 2014; Wu, 2011a). Although the importance of the global access to fresh and clean water in line with Sustainable Development Goal 6 is clear and must be pursued, the minimisation of electricity usage and GHG emissions of WSSs are important criteria for improving the sustainability of water systems (Filion, 2008). The minimisation of electricity usage due to the higher efficiency of pumps will also result in the minimisation of economic costs, meaning that more water can be transported with lower costs. Because of the lower price, water will be available for more people, which is again in line with Sustainable Development Goal 6. Hence, to reduce the electricity usage and GHG emissions of WSSs, the system must be optimised.

Optimising the operation of WSSs is done with the help of an optimisation algorithm. Here, the performances of different operation combinations are modelled and evaluated to find the best solutions and with that the lowest electricity usage and GHG emissions of the system (Stokes et al., 2014). An optimisation algorithm can consist of a single-objective (SO) optimisation algorithm (e.g. minimising the economic costs of the system) or a multi-objective (MO) optimisation algorithm (e.g. minimising the GHG emissions of the system along with the economic costs of the system). Primary focus has been on the optimisation of the different WSSs infrastructure design options (e.g. pump types, pump sizes, pipe sizes, storage sizes/locations) (Planells-Alandi et al., 2005; Amborse, 2002; Basupi et al., 2014; Dandy et al., 2008; Ghimire & Barkdoll, 2009; Kang & Lansey, 2011; MacLeod et al., 2011; Wu, 2009a). Less attention is given to:

1. The impact of pump operational management (e.g. pump scheduling, storage trigger levels, variable speed pumps) (Basupi et al., 2014; Cabrera et al., 2010; Ramos et al., 2011);
2. The impact of policy drivers which may affect the optimal trade-offs between economic costs and GHG emissions (e.g. carbon costs, economic discount rate, emissions discount rate) (Kang & Lansey, 2011; Kumar & Karney, 2007; MacLeod et al., 2011; Roshani et al., 2012; Wu, 2009a);
3. The interaction between the water supply infrastructure and the energy generating infrastructure (e.g. power source consideration, single average tariff/GHG emission factor value versus time-dependent tariff/GHG emission factor structure) (Biehl & Inman, 2010; Bunn & Reynolds, 2009; Herstein et al., 2009; Ramos et al., 2011; Wu, 2011b);
4. The demand pattern variations (e.g. daily, weekly, seasonally) (Planells-Alandi et al., 2005; Basupi et al., 2014; Ghimire & Barkdoll, 2009; Herstein et al., 2009; Ramos et al., 2011).

Besides the many different optimisation components for WSSs, trade-offs between them can occur as well. For instance, a trade-off can occur between the design phase and the operation phase of a WSSs, such as the minimisation of pipe sizes to reduce the investment costs (design phase), and the minimisation of pump energy to reduce the operational costs (operation phase) (Stokes et al., 2014). When taking into consideration a MO optimisation algorithm for WSSs, trade-offs can also occur between the different objectives, for example by changing the time-of-use of pumps while taking into consideration the electricity tariffs and the emissions intensities, where pumps can both alter the GHG emissions as well as the economic costs. Especially when the fluctuations of electricity tariffs and emissions factors do not coincide, trade-offs will be evident (Stokes et al., 2014; Wu, 2011a).

1.2. Problem definition

As section 1.1 illustrates, the importance of optimising the fresh water resource systems accounts not only for the economic costs of the system. The importance also rises due to the growing water scarcity issue along with the need of reducing the corresponding GHG emissions.

The United Arab Emirates (UAE) faces the issue of water scarcity together with the need to reduce their GHG emissions. The UAE is located in the southern part of Arabian Peninsula with a total area around 82,800 km^2. It consists of seven emirates: Abu Dhabi (AUH), Dubai (DXB), Sharjah (SHJ), Ajman (AJM), Fujairah (FUJ), Ras Al Khaimah (RAK) and Umm Al Quwain (UAQ) (Dweiri et al., 2018). The UAE is an oil-rich country with an economy mainly depending on oil, gas and other fossil fuels. According to the latest data of the Carbon Dioxide Information Analysis Centre (CDIAC) available online (2014), the UAE together with other Gulf states have the highest CO_2 emissions per capita of the world. The per capita fossil-fuel CO_2 emission rate of UAE was 23.3 metric tons of CO_2 in 2014 (rank number 6/220), compared to 9.9 metric tons of CO_2 per capita for the Netherlands (rank number 25/220) (CDIAC, 2014). Despite a long history of a fossil fuel energy mix together with high GHG emissions, the country now aims to achieve a more sustainable infrastructure by generating power through renewable energy. This is also in line with the Green Key Performance Indicators (Green KPIs) of the UAE: a list of 41 indicators which serve as a first attempt at capturing green economy performance in the country, such as the energy consumption per capita, the carbon intensity of energy and the total GHG emissions (MOCCAE, 2019). For example, the UAE Energy Strategy 2050 targets an energy mix of 44% clean energy (mainly solar power), 38% gas, 12% coal, and 6% nuclear (AE, 2019).

Besides the need of reducing UAEs GHG emissions, they are also facing a water scarcity concern. This is because their climate is defined by very high summer temperatures (46 °C average) together with a high humidity (Shahin & Salem, 2015). This arid climate plays a significant role in UAEs water resources availability,

since conventional approaches (e.g. rainfall, river runoff) are limited. This is because first, precipitation rates, the main source of recharge for water resources such as groundwater and surface water, are low and irregular. The annual average rainfall varies from 103 to 273 mm since 1998 (Sherif et al., 2014). Second, the evaporation rate, which reduces the amount of surface water, is high. Third, groundwater levels are low due to heavy pumping in the past (Murad et al., 2007) and are expecting to dry out within the next 16 to 36 years (Shahin & Salem, 2015). Because of the arid climate conditions together with the rising water demand due to the increasing population and the economic development, UAE experiences a lack of sufficient quantities of water. Therefore, unconventional water resources such as desalination plants play a key-role in narrowing the water demand-supply gap in UAE (Jones et al., 2018).

The UAE has multiple desalination plants. The locations of those desalination plants are important, since 1) it must be located near sea water to decrease the costs of sea water intake, 2) it must be located near a power source for running the plant and for making use of the excess heat of the power plant, 3) the project must take into account the impact on the environmental surrounding, and 4) it must be located as close as possible to the customers to decrease the costs of transmission and distribution (Dweiri et al., 2018). However, locations with all four requirements in the optimal state are not possible and therefore, trade-offs must be made. This results in the fact that the desalination plants are spread out over the UAE (Figure 1.1), and so WSSs are necessary to supply the water across the country. However, as section 1.1 already appoint, the electricity usage and the GHG emissions of WSSs must reduce in order to mitigate global warming.

This research focusses on the WTS of the largest Emirate of UAE: Abu Dhabi. The transmission of water from the production companies to the two distribution companies (Al Ain Distribution Company (AADC) who supplies water in the Al Ain Municipality area, and Abu Dhabi Distribution Company (ADDC) who supplies water to customers in the rest of the Emirate) is executed by the Transmission and Despatch Company (TRANSCO). TRANSCO is a subsidiary of Abu Dhabi Water & Electricity Authority (ADWEA) and their core business is the planning, construction and operation of a safe, reliable and efficient water (and electricity) transmission network. The WTS of TRANSCO (Figure 1.1) consists of over 3,000 km of pipeline. Pumping stations at production, transfer and terminal stations are used to pressurise the system and are supported by storage reservoirs (RSB, 2019a). Primary focus has been on developing the system to fulfil the increasing demand of water. TRANSCOs goal now is to optimise their system in order to a) improve the sustainability of their system, b) make it as profitable as possible, and c) by still fulfilling to the (future) demand of water.

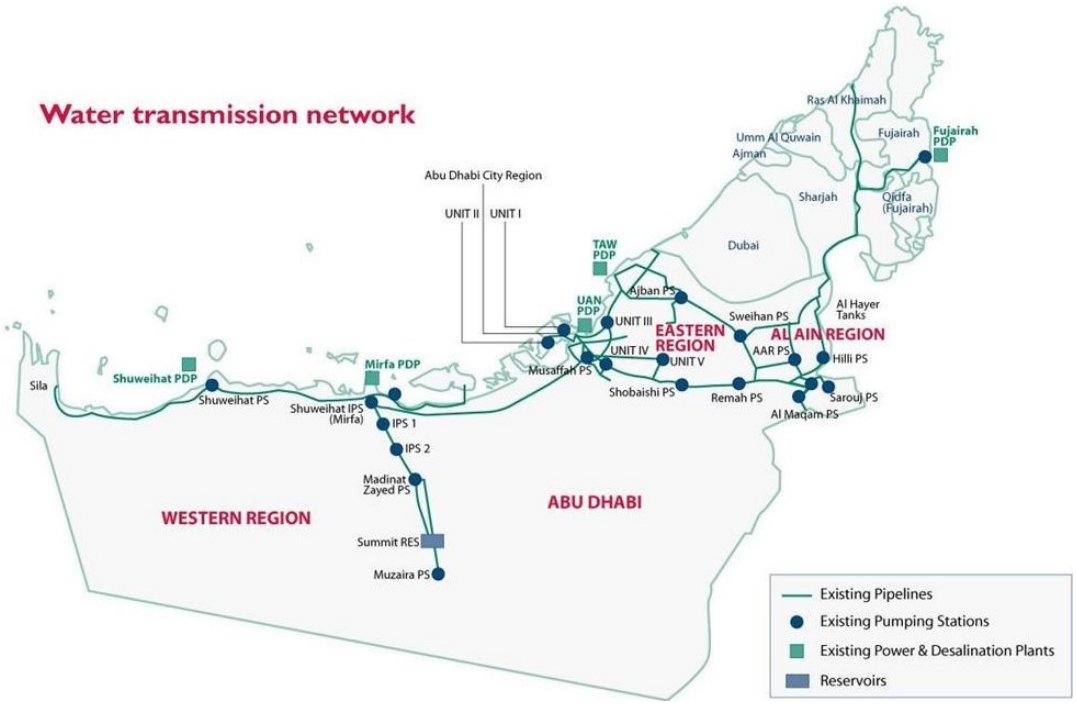

Figure 1.1: The Water Transmission Network of TRANSCO.

1.3. Research question

Based on the outlined problem in section 1.2, the following research question is posed:

What is the optimal trade-off between operational costs and sustainability performance of TRANSCOs Water Transmission System, while fulfilling the water demand in the Emirate Abu Dhabi, United Arab Emirates by 2030-2050?

To answer the research question, a quantitative analysis is conducted. This analysis refers to an optimisation model that establishes the operational electricity usage, GHG emissions and expenditures related to electricity use of TRANSCOs water network. Available data from TRANSCO and literature are utilised to substantiate the model. Due to the strict time limitations of this research, the focus is on optimising the Shuweihat water transmission scheme, which starts at Shuweihat and ends at Mussafah with Mirfa as intermediate pumping station. The Shuweihat water transmission scheme has a dual transmission line of approximately 230 km (Deltares, 2015b). The method of the optimisation is however general and can be applied to other portions of the WTS.

1.4. Social and scientific relevance

The added value for this research is found in the fact that it is a complex multi-criteria optimisation in which multiple components (described in section 1.1) of a WTS are researched together from a system perspective. Since optimising a WTS consists of multiple components, this study gives a first impetus for mapping all of the facets of TRANSCOs WTS. The social relevance of this study is ascribed to the relation between fulfilling the water demand while also taking into consideration the sustainability goals of UAE, and how this alters the current economic costs for TRANSCO. In addition, this study includes the predicted future renewable energy mix of UAE in the WTS (forecast to 2030, 2050). Scientifically, this study gives insight in how the energy market and water management can achieve a better collaboration (smart water management). This study is based on creating a quantitative understanding for indicating the electricity usage, GHG emissions and economic costs regarding a WTS. The different components individually are often named in literature, but quantitative assessments of multiple components together are limited. In addition, the model can be used to further expand the optimisation of TRANSCOs WTSs. Finally, the knowledge and results can be used for the optimisation of WTSs in general.

1.5. Research outline

Chapter 2 of Part I introduces the theoretical framework and research components considering a WTS. Part II introduces and discusses the methodology used in this research. It consist of four chapters, which are Chapter 3: Base case (unoptimised) configuration, Chapter 4: Internal model, Chapter 5: Optimisation model, and Chapter 6: Scenarios. Part III shows the results of this research. It consist of five chapters, which are Chapter 7: Electricity tariffs, Chapter 8: GHG emissions factors, Chapter 9: Policy driver carbon tax, Chapter 10: Infrastructure influence, and Chapter 11: Sensitivity analysis. Part IV describes the discussion and recommendations (Chapter 12) and the concluding remarks (Chapter 13).

2

Theoretical background

This chapter provides the theoretical background of this research. The chapter consists of five sections. Section 2.1 introduces the theoretical framework. Sections 2.2 till 2.5 highlight each set of input elements of the theoretical framework by explaining their research components and characteristics.

2.1. Theoretical framework

The theoretical framework that is used in this research is derived from Stokes et al. (2014) and displayed in Figure 2.1. The framework has four input components, which may consist of sub-components. The four input components are:

1. Infrastructure component: consists of sub-component water infrastructure and sub-component energy infrastructure (section 2.2);
2. Operation options component (section 2.3);
3. Policy drivers component (section 2.4);
4. Scenarios component (section 2.5).

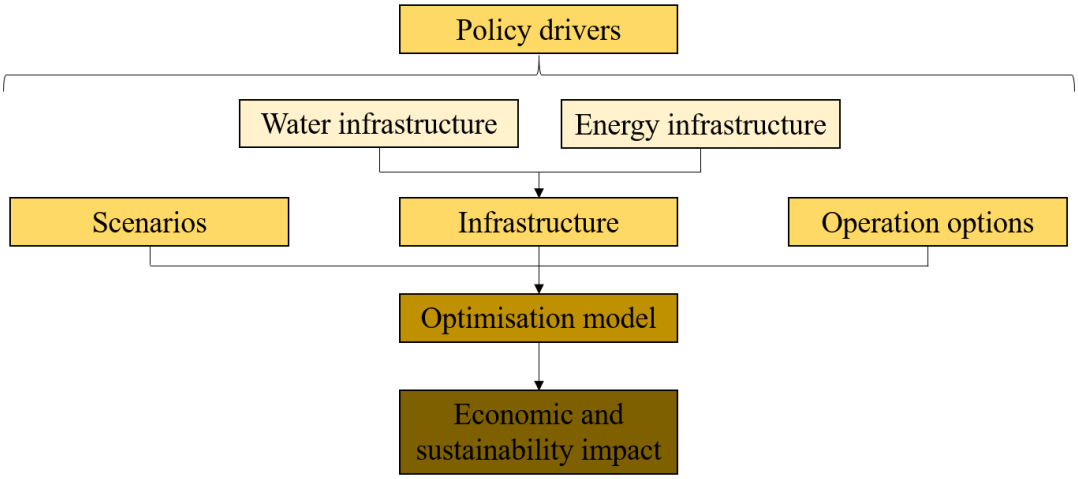

Figure 2.1: Theoretical framework of this research, derived from Stokes et al. (2014).

2.2. Infrastructure component

In order to optimise the operation of a WTS, it is important to consider the real-world infrastructure of the WTS. Two infrastructure components are therefore important: the water infrastructure and the energy infrastructure.

2.2.1. Sub-component water infrastructure

The sub-component water infrastructure is used to represent the physical elements that allows the transport of water from the supply sources to the storage areas and finally to the customers. The sub-component is also used to illustrate the options related to the design of the network. These considerations include the selection of pipe sizes and materials, storage tanks/reservoirs sizes and the pumping station characteristics and pump types (fixed-speed pumps (FSPs) and variable speed pumps (VSPs)). These options can all significantly affect the economic costs and GHG emissions of the system.

Pipes

Energy losses occur due to friction in the pipelines, also called the friction head loss. The friction head loss is the loss of head caused by the pipe wall friction and the viscous dissipation[1] in the flowing water. The friction head loss can be determined by the use of the Darcy-Weisbach equation, where it is written in the form of a discharge and a resistance coefficient, and calculated with the following formulas:

$$dH = C \cdot Q^2 \tag{2.1}$$

$$C = \frac{f \cdot L}{2 \cdot g \cdot A^2 \cdot d} \tag{2.2}$$

Where C = resistance coefficient [s^2/m^5], Q = discharge [m^3/s], f = friction factor [-], L = length of pipeline [km], g = gravitational acceleration [9.81 m/s^2], A = cross sectional area of pipe [m^2] and d = diameter of pipe [mm]. To determine the friction factor, the Reynolds number (Re) and the relative roughness (k) are needed. These values are calculated with the following formulas:

$$Re = \frac{v \cdot d}{\vartheta} \tag{2.3}$$

$$k = \frac{\epsilon}{d} \tag{2.4}$$

Where Re = Reynolds number [-], v = speed of the flowing water [m/s], d = diameter of pipe [mm], k = relative roughness [-], ϑ = kinematic viscosity [m^2/s] and ϵ = pipe roughness [mm]. By knowing the Reynolds number and the relative roughness, the Moody diagram is used to determine the friction factor. Finally, the resistance coefficients of the pipelines are calculated with the use of formula 2.2.

Storage areas

Storages areas (tanks, reservoirs) in a WTS have four general purposes: 1) to meet a variable supply to a network with a constant water production, 2) to meet a variable demand to a network with a constant supply, 3) to maintain a stable pressure in the system, and 4) to provide a supply in emergency situations. Storage areas can be located at multiple parts of a WTS, for example at the source (treatment plants i.e. desalination plants), at the end of a pipeline, or at any other intermediate place in the distribution system. The selection for the optimal place for the storage areas depend on the following factors: the supply scheme, topographical conditions, economical aspects, climatic conditions, and the pressure situation in the system (Stokes et al., 2014). The relevant parameter for the storage areas is the reservoir volume, which is based on the cross sectional area and the minimum and maximum water elevation level of the storage areas.

Pumping stations

A pumping station consists of a set of pumps. The main function of pumps is to add energy to the water, and thus pumping water to the reservoirs and/or demand nodes. The water is transported from a downstream tank farm to an upstream tank farm through a pipeline. The pump must supply the static head (H_{stat}) and the dynamic head (H_{dyn}). The static head is the difference between the pressure level and the suction level. The pressure level is the head at the pressure side of the pump without a discharge through the pump. The suction level is the head at the suction side of the pump without a discharge through the pump. Besides the static head, the pump must also supply the hydraulic losses the water flow experiences, called the dynamic head. The formula for the total head is:

$$H_{total} = H_{stat} + H_{dyn} \tag{2.5}$$

[1] Viscous dissipation is the irreversible process in which the viscosity of the fluid takes energy from the motion of the fluid (i.e. kinetic energy) and transforms it into internal energy of the fluid (i.e. heating up of the fluid).

The dynamic head is generally proportional to the squared flow rate and thus to the squared discharge. Therefore, the formula can also be written as:

$$H_{total} = H_{stat} + CQ^2 \tag{2.6}$$

Figure 2.2 shows the definitions of pressure and suction levels, and the difference between static and dynamic head.

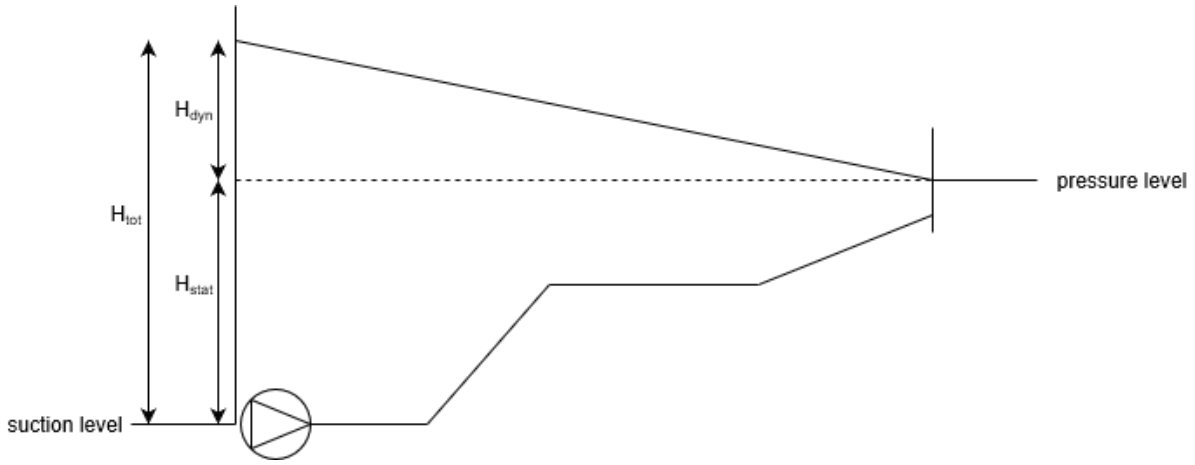

Figure 2.2: Definition of pressure level, suction level, static head and dynamic head.

The essential hydraulic properties of pumps are defined by four basic pump characteristics (see Figure 2.3), which are (Deltares, 2015a):

- The $Q-H$ characteristic (= capacity curve): shows the relationship between the discharge (Q) and the head (H) of the pumps at a fixed speed. The $Q-H$ curve shows the possible operating points of the pump. The system in which the pump is installed determines at which operating point the pump operates. The operating point of the pump is the intersection of the system characteristic (the energy that is needed to transport a certain discharge through the system) and the $Q-H$ curve of the pump.
- The $Q-\eta$ characteristic (= efficiency curve): shows the relationship between the discharge (Q) and the hydraulic efficiency (η) of the pumps at a fixed speed. The hydraulic efficiency is the ratio between the hydraulic energy absorbed by the water and the mechanical energy supplied by the motor of the pump via the drive shaft. The formula for the efficiency of the pumps is:

$$\eta = \frac{\rho \cdot g \cdot Q \cdot H}{M \cdot \omega} = \frac{\rho \cdot g \cdot Q \cdot H}{M \cdot \frac{2 \cdot \pi \cdot n}{60}} \tag{2.7}$$

  Where η = hydraulic efficiency [%], ρ = density of water [kg/m^3], g = gravitational acceleration [9.81 m/s^2], Q = discharge [m^3/s], H = head [m], M = torque in the drive shaft [Nm], ω = angular velocity [rad/s], and n = speed of the pump [rpm].

- The $Q-P$ characteristic (= power curve): shows the relationship between the discharge (Q) and the power supplied to the pump (P). The formula for the power supplied to the pump is:

$$P = \frac{\rho \cdot g \cdot Q \cdot H}{\eta} \tag{2.8}$$

  Where P = power [W], ρ = density of water [kg/m^3], g = gravitation acceleration [9.81 m/s^2], Q = discharge [m^3/s], H = head [m], and η = hydraulic efficiency [%].

- The NPSH (Net Positive Suction Head) characteristic (= cavitation curve): shows the relationship between the discharge (Q) and the required margin between the absolute energy level on the suction side of the pump and the vapor pressure level of the pumped liquid (water), so that a certain amount of (inadmissible) cavitation in the pump is not exceeded.

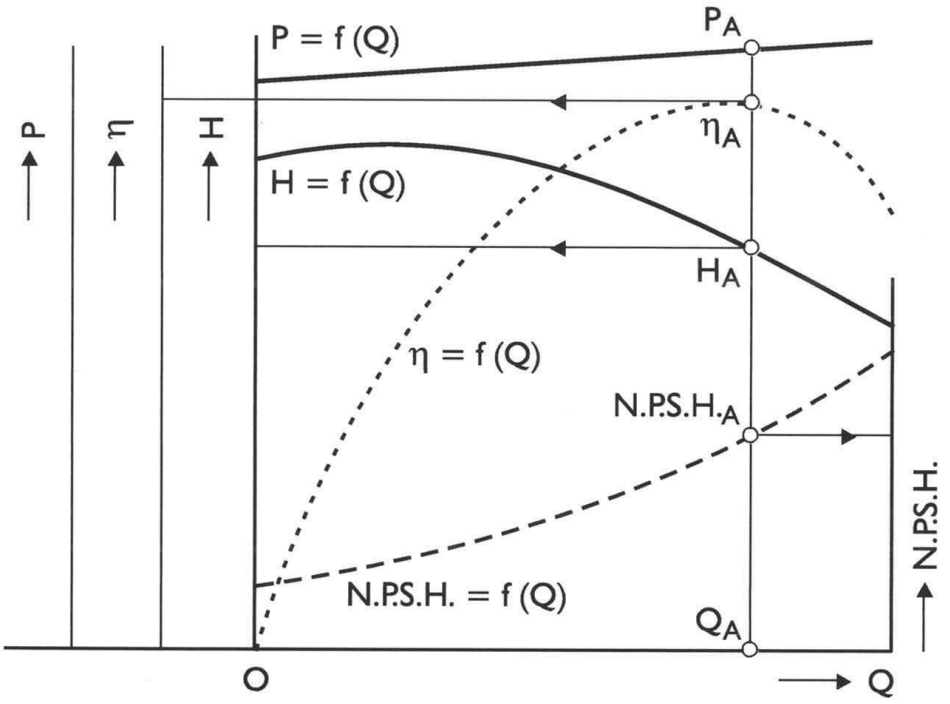

Figure 2.3: Pump characteristics (capacity, efficiency, power and cavitation curve) at a fixed speed.

Water demand

Including daily water demand patterns in the model, also called diurnal curves, increases the accuracy of modelling the time-dependency of water demands. Here, the pump scheduling is not only influenced by the cheapest electricity price or lowest GHG emissions factor, it must also provide the customer demand during each timestep (for example hourly).

Water leakages

WTSs can experience water leakages resulting in pressure, supply and financial losses. Leakages can occur in different parts of the system, such as the transmission and distribution mains, the connection lines and the valves. Multiple sources can originate leakages, for example aging materials and defect materials, but also water hammer (changes in water pressure), heavy traffic volumes, aggressive soil conditions, corrosion, etc. (Boulos & Schade, 2008). This research does not take into account the possible water leakages since software such as WANDA or EPANET are much better in detecting them. However, it should be mentioned.

2.2.2. Sub-component energy infrastructure

The sub-component energy infrastructure is used to represent the structure of UAEs energy infrastructure and to give an overview of the production, transmission and distribution networks of the area between Shuweihat and Mussafah (emirate Abu Dhabi). Next, electricity tariff and GHG emissions structures are discussed in general.

Overview electricity and water networks

The Abu Dhabi electricity (and water) sector is structured by a single buyer model, meaning that the production capacity (water and electricity) is purchased centrally by ADWEC (Abu Dhabi Water and Electricity Company). ADWEC is a wholly owned subsidiary of ADWEA (Abu Dhabi Water and Electricity Authority). The main responsibility of ADWEC is to secure the supply of water and electricity to customers in the emirate of Abu Dhabi through short- and long-term balancing of supply and demand, through long-term power and water purchase agreements with power and water producers, through bulk supply tariff (BST) sales agreements with distribution companies, and through fuel supply agreements with fuel suppliers (ADWEC, 2019a). ADWEC sells the water and electricity to distribution and supply companies through an annually adjusted bulk supply tariff (BST). The distribution and supply companies sell it eventually to the final customers. Next to this, the two distribution companies (AADC (Al Ain Distribution Company) and ADDC (Abu Dhabi Distribution Company)) also pay TRANSCO a so called 'transmission use of system (TUoS) tariff' for the use of its

transmission system for the transport of water and electricity from the production plants to their distribution systems. All the companies described before are monopolies in their service area and are regulated economically through price control reviews by the government (RSB, 2019b). The physical and financial structure of the water and electricity sector is found in Figure 2.4.

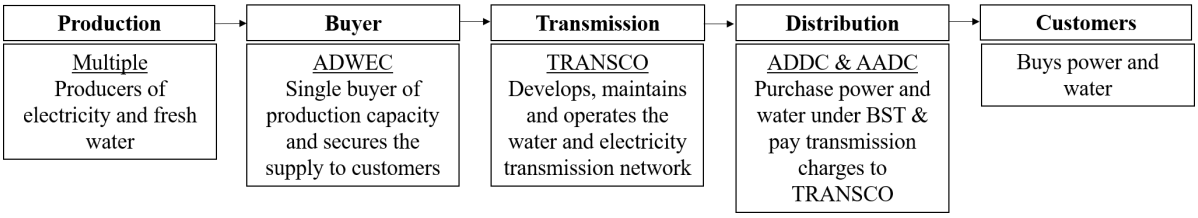

Figure 2.4: Physical and financial structure of the water and electricity sector of the Emirate Abu Dhabi.

Electricity tariffs structure

The electricity costs are the costs of electricity consumed by the pumps in the WTS during the optimisation period. These costs are strongly dependent on the electricity tariff structure within the area or country[2]. The electricity tariff structure depends on a list of factors, such as fuel prices, CO_2 prices, generating technologies and installed capacity, renewable energy and installed capacity, demand pattern and demand response, market design and capacity payments, adoption and learning rates of innovative demand and supply technologies, but also sudden events and catastrophes. The electricity tariff structure can have a flat rate tariff and thus having the same electricity price during the day, or Time of Use (ToU) rates, where the tariffs are fluctuating during the day. The electricity tariffs in UAE are dependent on sectors (residential, commercial, industrial) but also for example on the income and origin of residential customers. TRANSCO, which is a commercial customer and uses the power grid of ADDC for their electricity consumption (mainly consisting of gas)), pays currently a flat rate electricity price of 0.20 AED (Arab Emirates Dirham[3]) (ADDC, 2019).

GHG emissions structure

Although WTSs provide an essential service, they also contribute indirectly to the release of GHG emissions when using electricity from fossil fuel sources for pumping the water through their system. Therefore, investigating the optimal pump schedule to reduce GHG emissions is an important factor as well. Similar to electricity tariffs, emissions factors can vary during a specific time period as well. Also similar to the effect of time-dependent electricity tariffs on costs, time-dependent GHG emissions factors have the potential to affect the optimal operation schedule of pumps in a WTS when considering the minimisation of GHG emissions. A study in Australia for example investigated the results between the use of actual (time-varying) emissions factors for the South Australia electricity grid with a 5-min timestep, compared to the use of an average emissions factor, which does not consider the time dependency of the factors. The results show that actual emissions factors can drastically reduce GHG emissions by switching the pumping to low emissions moments (during sun and wind production) (Stokes et al., 2015). To properly account for the GHG emissions of a WTS, the sources of electricity of the country must be known, as each source has different GHG emissions per unit of energy produced.

2.3. Operation options component

The operation of pumps in a WTS can be controlled twofold. First, it can be controlled by the use of pump scheduling. Pump scheduling is used to control the on/off status and the speed of the pumps (time interval), providing an optimal arrangement between the storage filling and releasing phase and the off-peak and on-peak electricity time periods (Alvisi & Franchini, 2016). For an optimal pattern, the storages are filled during the off-peak electricity tariffs and are emptied during the on-peak electricity tariffs, while fulfilling to the demand of water. This requires algorithms than can periodically (e.g. hourly) identify the optimal schedule of the pumps. Second, the status of the pumps can also be switched on/off according to prefixed trigger values of the water level in the storages. Conventional systems use level based controllers, where the control action depends on the level of the tank and not on the time of the day. A research of Ertin et al. (2001) investigated the energy efficiency of both pump scheduling and trigger levels of a simple WTS. The results show that by

[2]The electricity tariff structure depends on the grid operator and the electricity supplier, which may vary inside a country.
[3]1.0 AED = 0.24 EUR.

the use of pump scheduling instead of storage trigger levels, a 12.5% energy saving is possible. Therefore, pump scheduling is used in this research. Next to electricity usage savings, the aforementioned operation options can also be used to reduce the operational GHG emissions by taking into account time-dependent emissions factors. This because emissions factors fluctuate with time and location due to the contribution of the different energy sources supplying to the electricity grid as explained in section 2.2.2.

2.4. Policy drivers component

Policy and governance drivers may have a significant effect on the operation of a WTS and the associated electricity usage, GHG emissions and economic costs, especially when calculated over longer time-periods. This section explains three government policy considerations: economic discounting, GHG emissions discounting, and carbon costing.

When looking at both the design and the operation phase of a WTS, economic and emissions discount rates are two important drivers to include since operating costs and emissions occur progressively over the design period. For example, a higher economic discount rate places less value on future (operating) costs compared to present (construction) costs. Also, a higher emissions discount rate means that the value of future emissions will be reduced due to for example the belief that future technologies can better abate the impact of GHG emissions than present technologies. With this present value analysis, costs occurring in the different years can be compared (Stokes et al., 2014). However, since the scope of this research only focuses on the operating phase of the system and not on the design or maintenance phase, the two aforementioned policy drivers are not included in this research.

The third and final policy driver is carbon costing, where taxes are implemented by adding monetary costs to each unit of GHG emissions produced. Carbon taxes can be implemented on GHG emissions produced during the construction phase (capital emissions), calculated from embodied energy (out of this research scope), and during the operation phase, calculated from electricity usage (Wu, 2009b). Capital emissions are due to the manufacturing and installation of the elements of the WTS (pumps, pipes, storages, etc.), where pipes represents the largest proportion of the total capital emissions (Filion et al., 2004). The operating GHG emissions depend on the electricity consumption related to the operation of the system (may vary over time and region), see also section 2.2.2. Although TRANSCO is a transmission operator which does not provide their own electricity for running the pumps, they are dependent on the power grid of UAE. Therefore, the policy driver carbon costing has indirectly an influence on the sustainability of TRANSCO, since such a policy will incentivize TRANSCO to pump when the most sustainable energy sources are producing during the day/night.

2.5. Scenarios component

Lots of uncertainties occur during decision making, for example due to changes in population growth (temporal and spatial), per-capita water use, government regulations, climatic conditions, etc. (Kang & Lansey, 2011). Therefore, one of the most powerful and convenient ways to represent these uncertainties is by the use of scenarios. Scenario planning is useful to gain insight in how the future water and energy infrastructure of UAE changes the operational costs and GHG emissions of the WTS of TRANSCO. Possible scenarios to include are for example different electricity prices, changes in the power source mix, policy decision and network changes. This will be further elaborated in Chapter 6.

II

Methodology

3

Base case (unoptimised) configuration

The Shuweihat water transmission scheme is designed to transport water from the Shuweihat tank farm, which comes from desalination plants, to Mirfa, Sila, Delma and Mussafah, see Figure 3.1. The Shuweihat pumping station consists of ten pumps supplying both Mirfa lines (six pumps + two pumps stand-by) and Delma lines (one pump + one pump stand-by), where the Delma pipeline is out of the research scope. The Mirfa pumping station consists of fifteen pumps supplying both Mussafah lines (seven pumps + one pump stand-by), Mirfa City lines (two pumps + one pump stand-by), and Madinat Zayet lines (three pumps + one pump stand-by), where the Mirfa City and Madinat Zayet pipelines are out of the research scope. Also at the Mirfa pumping station, there is an inflow of water coming from desalination plants. The transmission line between Shuweihat and Mirfa consists of two pipelines (one transmission line and one distribution line where the distribution line has seven tap-off stations) which are covering approximately 100 km and are passing several height differences. The highest point (33 m) is at approximately 63 km from the Shuweihat pumping station. The total water capacity through the two pipelines is 200 Million Imperial Gallons per Day (MIGD)[1]. At maximum flow rate, both pipelines are operating at the same time. The transmission line between Mirfa and Mussafah consists of two pipelines which are covering approximately 130 km. One pipeline (line A) transports water from the Mirfa tank farm to the Mussafah tank farm (approximately 130 km). This transmission line also delivers water 25 km further towards two tank farms in the direction of Abu Dhabi (Unit IV and Unit V), but this is out of the research scope. The second pipeline (line B) transports water from the Mirfa tank farm to the Mussafah tank farm, with five intermediate tap-off stations along the pipeline. The highest point of both lines is at an elevation of 10 m, which is located 43.7 km downstream of the Mirfa pumping station. The total water capacity through the two pipelines is 186 MIGD[2]. In Mirfa and in Mussafah, the water is delivered in a downstream tank farm area where control valves are maintaining the pressure at the end of the water transportation (Deltares, 2015b). Although the model made is explicitly for the Shuweihat to Mussafah scheme, the model can be expanded when optimising a larger part of the WTS of TRANSCO.

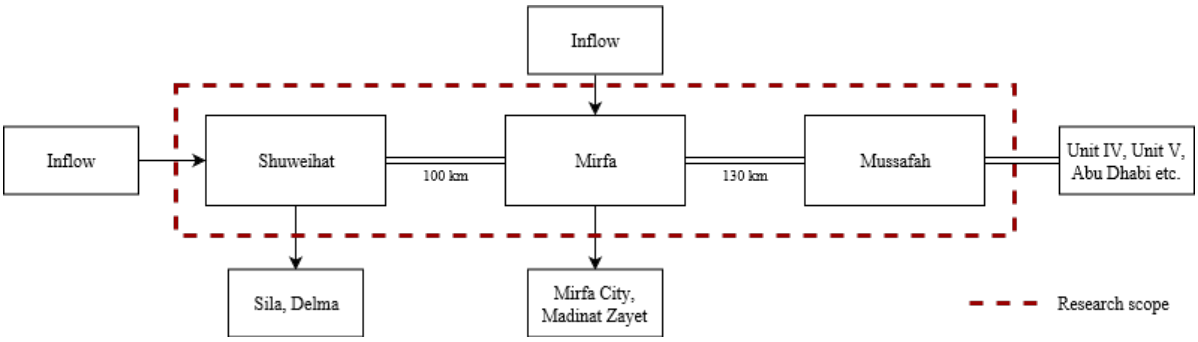

Figure 3.1: Simplified transmission scheme Shuweihat - Mirfa - Mussafah, retrieved from TRANSCO (scope of the research).

[1] 200 MIGD = 909.2 Million Liters per Day (MLD).
[2] 186 MIGD = 845.6 Million Liters per Day (MLD).

4

Internal model

This chapter describes the internal model of the optimisation problem. The internal model represents the water infrastructure component of the WTS of TRANSCO. It consists of the following elements (Figure 4.1):

- The inflows from the desalination plants (inflows Shuweihat and Mirfa), modelled as discharge boundary conditions (section 4.2);
- The (intermediate) demand nodes (outflows), modelled as discharge boundary conditions (section 4.3);
- The three storage areas (Shuweihat tank farm, Mirfa tank farm and Mussafah tank farm), modelled as linear storage elements (section 4.4);
- The two pumping stations (Shuweihat pumping station and Mirfa pumping station), consisting of multiple pumps (section 4.5);
- The pipelines between Shuweihat, Mirfa and Mussafah, modelled as discharge boundary conditions (section 4.6);
- The control valves at the end of the pipelines, modelled as discharge boundary conditions (section 4.7).

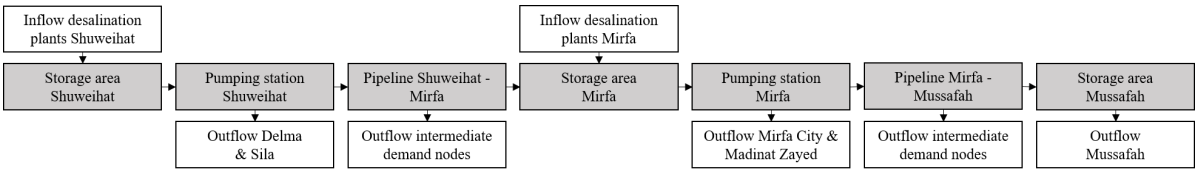

Figure 4.1: Simplified internal model of WTS of TRANSCO between Shuweihat, Mirfa and Mussafah.

The characteristics and parameters of the different elements, and the software used (section 4.1), are further explained in the following sections.

4.1. Software

The internal model, the water infrastructure of the WTS of TRANSCO, is built within the software OpenModelica[1]. OpenModelica is a modelling language for physical problems. It has a Python interface and with this software, complex systems such as a WTS can be modelled, simulated, optimised and analysed, both in textual and graphical modes. Deltares developed their own library in OpenModelica, consisting of routing and reservoir models. The packages of this library are used for modelling the water infrastructure component of the WTS of TRANSCO. By placing the folder 'model' of the water infrastructure component, also called internal model, in the same main folder as the optimisation script (placed in folder 'src'), RTC-Tools (the optimisation software) will automatically read and implement the internal model script into the optimisation script.

[1] Source: https://openmodelica.org/.

4.2. Inflow desalination plants

The fresh water flowing into the WTS of TRANSCO is coming from desalination plants. At Shuweihat, two co-generation plants (SHU1 and SHU2) are producing the water inflow. At Mirfa, one co-generation plant (MIR1) and one reverse osmosis plant (MIR2) are producing the water inflow. For simplicity, the inflows of the two plants at Shuweihat and at Mirfa are modelled together, same as for Mirfa. Consequently, there is one inflow into the Shuweihat tank farm (inflow SHU) and one inflow into the Mirfa tank farm (inflow MIR). The production patterns of the desalination plants of one specific day (July 21, 2018) are provided by TRANSCO and are found in Figure 4.2. A more detailed description of the inflow patterns is found in Appendix A.

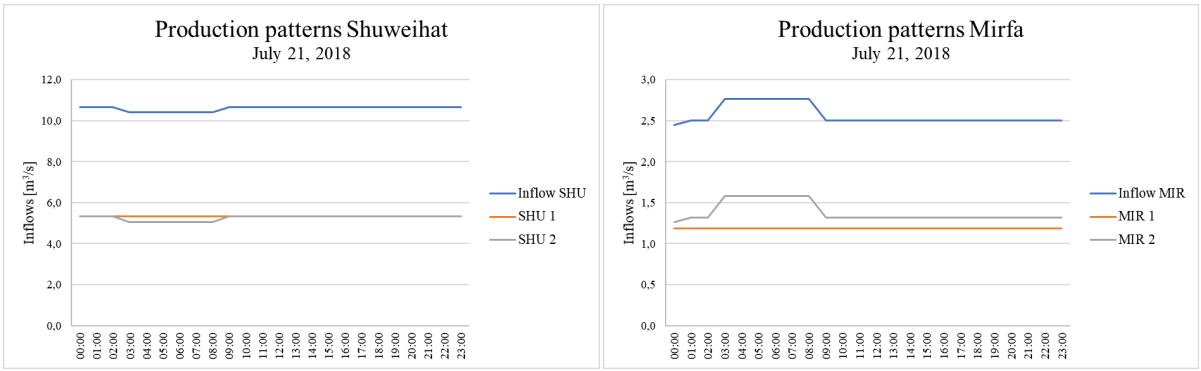

(a) Shuweihat (b) Mirfa

Figure 4.2: Production patterns of desalination plants at Shuweihat (SHU1 & SHU2) and Mirfa (MIR1 & MIR2) and total inflow of July 21, 2018.

4.3. Demand nodes

Although the optimised part of the WTS does not deliver the water directly to the customers, there is a variation in the water demand. Therefore, to obtain the most optimal pump schedule, the peak demands of water are taken into account. However, the data availability is limited. No customer demand pattern is provided by TRANSCO or available online. There is however data available of the water flows through the system at specific locations, such as a limited amount of intermediate demand nodes and the inflow into the Mirfa storage coming from Shuweihat. Since the maximum flow scenario through the system is known (Deltares, 2015b), assumptions are made of the outflows of the model (see Figure 4.1). The calculated outflows of the model of July 21, 2018 are found in Figure 4.3. A detailed description of the flow patterns through and out of the system is found in Appendix A. Note that the peak water flows at Mussafah are during the night. This is due to the fact that most of the water is used for irrigation which is done during the night when the sun does not shine. The flows at Shuweihat and Mirfa are more constant throughout the day, except for the intermediate demand nodes between Shuweihat and Mirfa. This is possibly due to the fact that this water is not used for irrigation, but rather residential water use.

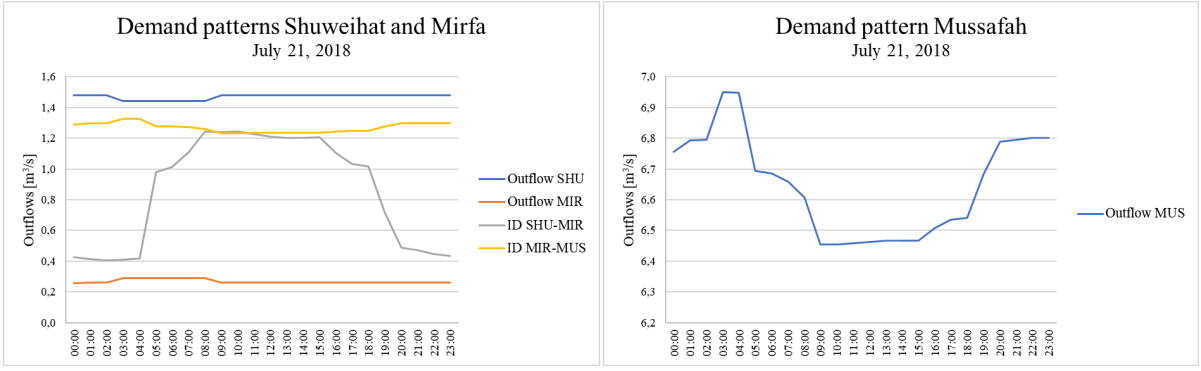

(a) Shuweihat and Mirfa (b) Mussafah

Figure 4.3: Demand patterns and intermediate demand (ID) nodes (outflows of model) between Shuweihat, Mirfa and Mussafah of July 21, 2018.

4.4. Storage areas

The available data retrieved from TRANSCO of the three storage areas between Shuweihat and Mussafah have different characteristics and parameters, which are the amount of tanks in the farm ($\#_{tanks}$), the volume of the individual tanks (V_{tank}), the minimum and maximum water elevation which is the minimum or maximum level of water in the individual tanks compared to sea level ($HQ.H_{min}$ and $HQ.H_{max}$), and the level of the bottom of the individual tanks compared to sea level (H_b). All three storages are assumed to have a cylinder shape. The parameters of the three storages are retrieved from TRANSCO and are found in Table 4.1.

However, two adjustments are made to the input parameters. First, to simplify the model, each storage farm is modelled as one large tank instead of multiple individual smaller tanks since there is no need to know the water levels of the multiple smaller tanks individually. Second, the parameters needed as input for the element 'storage' in the library of Deltares in OpenModelica are the cross-section areas of the tanks (A_{total}), H_b, $HQ.H_{min}$ and $HQ.H_{max}$. The last three parameters are known. The cross-section areas of the storages are calculated with the following formulas:

$$h_{tank} = HQ.H_{max} - H_b \tag{4.1}$$

$$V_{total} = V_{tank} \cdot \#_{tanks} \tag{4.2}$$

$$r_{tank} = \sqrt{\frac{V_{total}}{\pi \cdot h_{tanks}}} \tag{4.3}$$

$$A_{total} = \pi \cdot r_{tank}^2 \tag{4.4}$$

Where h_{tank} = height of the tank [m] and r_{tank} = radius of the tank [m]. The calculated cross-section areas of the storages are found in Table 4.1. The values, especially compared to the height of the tanks, are large due to the multiple tanks modelled together as one large tank.

Table 4.1: Characteristics and calculated input parameters of storage areas between Shuweihat, Mirfa and Mussafah, retrieved from TRANSCO.

Storage name	$\#_{tanks}$ [-]	V_{tank} [m^3]	H_b [m]	$HQ.H_{min}$ [m]	$HQ.H_{max}$ [m]	A_{total} [m^2]
Shuweihat tank farm	12	75,720	4.52	6.25	22.25	51,248.73
Mirfa tank farm	4	45,450	4.09	6.85	21.36	10,526.93
Mussafah tank farm	6	45,450	5.28	7.60	22.49	15,854.44

Note, a surge tank area is located at the discharge side of the Shuweihat pumping station. It consists of 2x5 non-vented surge tanks, each with a volume of 120 m^3. Non-vented surge tanks can quickly provide extra water during a brief drop in pressure, and also absorb sudden rises in pressure. In a short time after the disruption (less than one hour), the surge tanks will be restored to their average water level. Since the timeframe of the model consists of timesteps of one hour (see section 5.2), it is assumed that the surge tanks have a constant water level. Therefore, the non-vented surge tanks are left out of the analysis.

4.5. Pumping stations

As mentioned before in Chapter 3, the Shuweihat transmission scheme consists of two pumping stations: the Shuweihat pumping station and the Mirfa pumping station. This section describes the characteristics of the two pumping stations and explains how these characteristics are implemented into the model.

4.5.1. Shuweihat pumping station

The part of the Shuweihat pumping station supplying the Mirfa lines consists of six pumps and two pumps stand-by. The Shuweihat pumping station consists of only variable speed pumps, with the pumps having an operational rated speed of 995 rpm. Only the six operating pumps are included in the model, since the two pumps stand-by are only used when the operating pumps are defect. However, the Shuweihat pumping station has two different types of pumps (called existing pumps and new pumps), both with their own characteristics (Q, H, ρ, P). This is caused by the enlargement of the piping system between Shuweihat and Mirfa (extension from one pipeline to two pipelines) due to the growing water demand in UAE and therefore the

need of the instalment of new pumps to allow the transport of the higher amount of water through the system.

The characteristics of the two types of pumps are found in Figure 4.4 (performance curves) and Figure 4.5 (power curves). As seen, the characteristics of the two types of pumps are almost identical. Therefore, the pump characteristics are combined into new pump characteristics, so that all the pumps in the Shuweihat pumping station have equal characteristics. Consequently, the stand-by pumps can now easily replace the defect operating pumps and are therefore not included in the model as back-up pumps. The exact values of the pump characteristics are found in Appendix B.

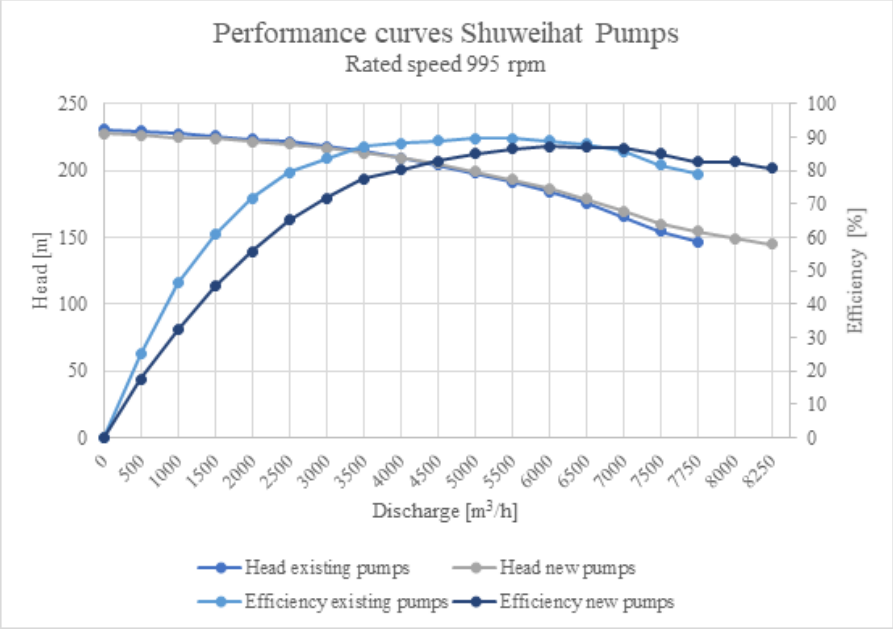

Figure 4.4: Characteristics of Shuweihat to Mirfa pumps at a rated speed of 995 rpm.

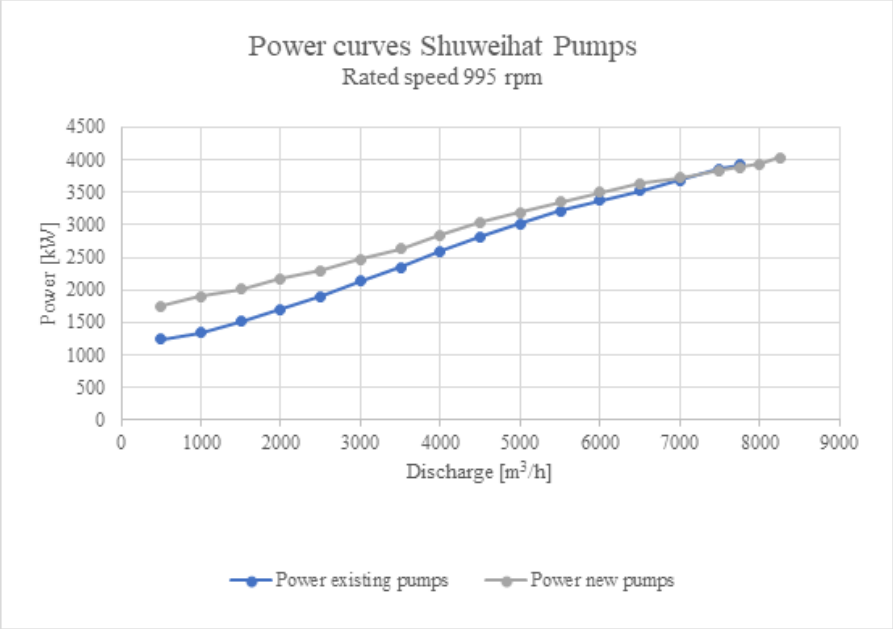

Figure 4.5: Power curves of Shuweihat to Mirfa pumps at a rated speed of 995 rpm.

4.5.2. Mirfa pumping station

The part of the Mirfa pumping station supplying the Mussafah lines consists of seven pumps and one pump stand-by. The Mirfa pumping station consists of only variable speed pumps, with the pumps having an operational rated speed of 994 rpm. Same as for the Shuweihat pumping station, only the seven operating pumps are included in the model, since the one pump stand-by is only used when the operating pumps are defect. However, also the Mirfa pumping station has two different types of pumps due to the growing water demand and therefore the instalment of new pumps to allow the transport of the higher amount of water through the system (also called existing pumps and new pumps). The characteristics of the two types of pumps are found in Figures 4.6 and 4.7. Since the Mirfa pump characteristics are almost identical as well, the characteristics are combined into new pump characteristics, so that all pumps have equal characteristics. Consequently, the stand-by pump can now easily replace the defect operating pumps and is therefore not included in the model. The exact values of the pump characteristics are found in Appendix B.

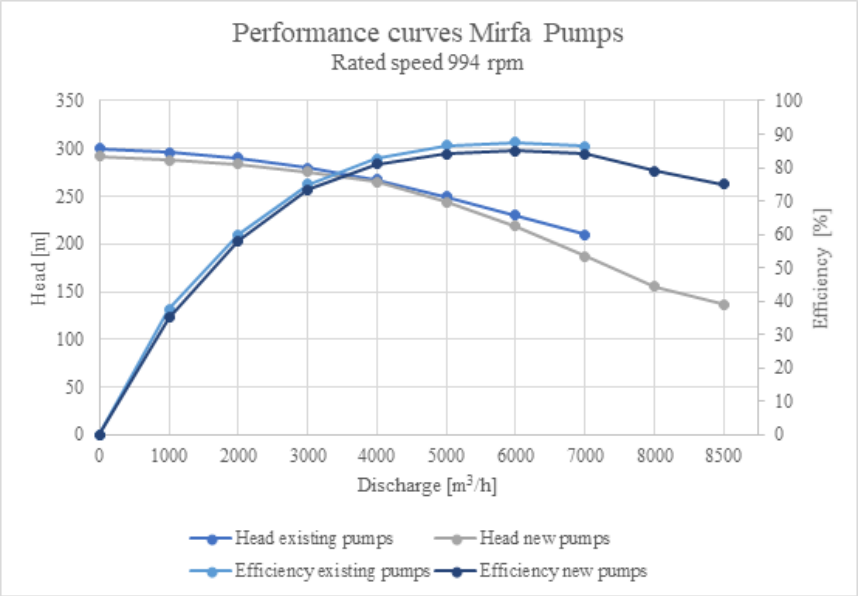

Figure 4.6: Characteristics of Mirfa to Mussafah pumps at a rated speed of 994 rpm.

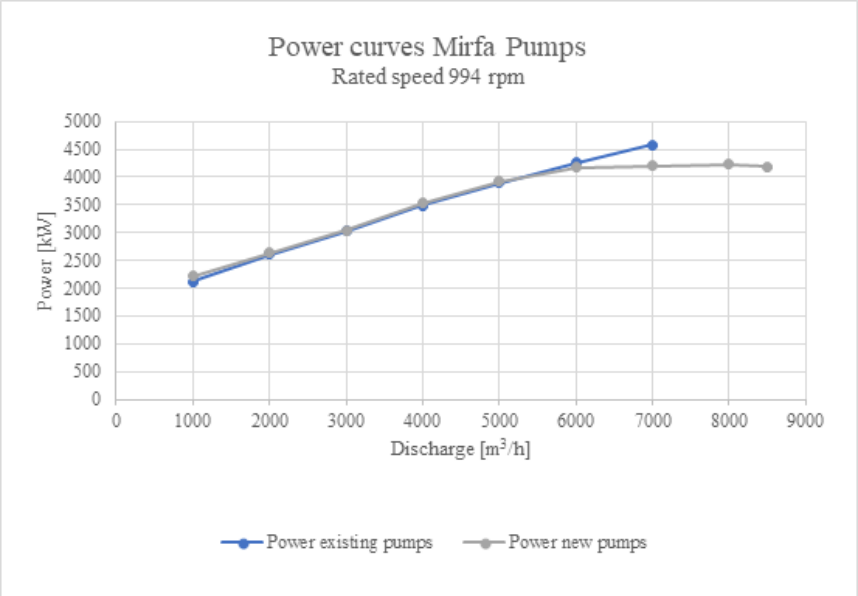

Figure 4.7: Power curves of Mirfa to Mussafah pumps at a rated speed of 994 rpm.

4.5.3. Input parameters

As mentioned before, the element 'pumping station' consists of multiple pumps (six for Shuweihat and seven for Mirfa). The pumps are modelled into the pumping station as a nested model which represents the multiple pump objects. The parameters needed as input in the library of Deltares in OpenModelica are the following: the power coefficients of the pumps, the working area of the pumps, the working area direction of the pumps, the speed coefficients of the pumps, and the minimum and maximum amount of time the pumps need to be on or off before aloud to switch off or on again. The characteristics of the input data for the pumps are explained below:

- Power coefficients: the power coefficients describe the relationship between the discharge, the head and the power of the pumps. The following equation is the fit of the pump power:

$$P = C_{1,1} + C_{1,2}Q + C_{2,1}H + C_{2,2}QH + C_{1,3}Q^2 + ... \tag{4.5}$$

  Out of this equation, a matrix of the power coefficients follows, where the power coefficients matrix corresponds to the coefficients C in equation 4.5. The optimisation should find a good and stable solution. Therefore, RTC-Tools automatically requires the coefficients of this polynomial equation to be chosen such that the polynomial is convex over the entire domain. The specific power coefficients of the Shuweihat and Mirfa pumps are found in Appendix B.
- Working area: the working area describes the boundaries of the polynomials of the convex set of allowed $Q-H$ coordinates, retrieved from the $Q-H$ curve at rated pump speed. The specific working areas of the Shuweihat and Mirfa pumps are found in Appendix B.
- Working area direction: the polynomials in the working area describe the boundaries of the polynomials, but do not yet indicate on which side of the polynomial the $Q-H$ combination should be. Therefore, for each of the polynomials in the working area there is specified whether the expression should evaluate to a positive expression (= 1) or to a negative expression (= -1). The specific working area directions for the Shuweihat and Mirfa pumps are found in Appendix B.
- Speed coefficients: the speed coefficients are based on the minimum and rated speed of the pumps (for Shuweihat pumps for example: minimum speed = 500 rpm and rated speed = 995 rpm). The specific speed coefficients for the Shuweihat and Mirfa pumps are found in Appendix B.
- Minimum time on: the minimum amount of time in seconds a pump needs to be on before allowed to switch off again.
- Minimum time off: the minimum amount of time in seconds a pump needs to be off before allowed to switch on again.

Note, the element 'pumping station' also consists of a resistance object, which represents the head loss of the pumps related to the discharge. However, since this resistance is negligible compared to the resistance in the pipelines, the resistance of the two pumping stations is set at zero.

4.6. Pipelines

There are two pipelines connecting the Shuweihat and Mirfa storages and there are two pipeline connecting the Mirfa and Mussafah storages. The two pipelines connecting the Shuweihat and Mirfa storages have the same characteristics and are retrieved from TRANSCO. This also counts for the two pipelines between Mirfa and Mussafah. Since the characteristics of the two pipelines are the same, the model is simplified by only modelling one pipeline between Shuweihat and Mirfa, and one pipeline between Mirfa and Mussafah. Therefore, a new diameter (d) of the pipelines is calculated while keeping the length (L) of the pipelines the same and where the volume (V) of the single pipelines doubles. The new diameter is calculated with the following formulas:

$$V_{single} = \pi \cdot \left(\frac{d}{2}\right)^2 \cdot L \tag{4.6}$$

$$V_{alternative} = 2 \cdot V_{single} \tag{4.7}$$

$$d_{alternative} = 2 \cdot \left(\sqrt{\frac{V_{alternative}}{\pi \cdot L}}\right) \tag{4.8}$$

Where V_{single} = the volume of a single pipeline [m^3], $V_{alternative}$ = the volume of the two pipeline modelled together [m^3] and thus two times the volume of V_{single}, and $d_{alternative}$ = the diameter of the two pipelines modelled pipeline [mm]. The characteristics of the single pipeline and the alternative pipeline for both Shuweihat to Mirfa and for Mirfa to Mussafah are found in Table 4.2.

Table 4.2: Characteristics of the pipelines between Shuweihat, Mirfa and Mussafah.

Pipeline	Length [km]	Volume [m^3]	Diameter [mm]
Single Shuweihat - Mirfa	97.15	195,331.50	1,600.00
Modelled Shuweihat - Mirfa	97.15	390,663.00	2,262.74
Single Mirfa - Mussafah	127.79	256,936.82	1,600.00
Modelled Mirfa - Mussafah	127.79	513,873.65	2,262.74

However, as explained in section 4.3, the pipelines have multiple intermediate demand nodes (seven for the area Shuweihat - Mirfa and five for the area Mirfa - Mussafah). To simplify the model, the demand nodes for the area Shuweihat - Mirfa are modelled together as one demand node. The same is done for the area Mirfa - Mussafah. The intermediate demand nodes are placed exactly in between the cities (Figure 4.8), and therefore, four pipeline elements are implemented into the model. Consequently, the length of the modelled pipelines is divided by two (Shuweihat - Mirfa = 48.58 km and Mirfa - Mussafah = 63.90 km) and the pipelines are implemented in a row, with the intermediate demands in between modelled as outflows of the system.

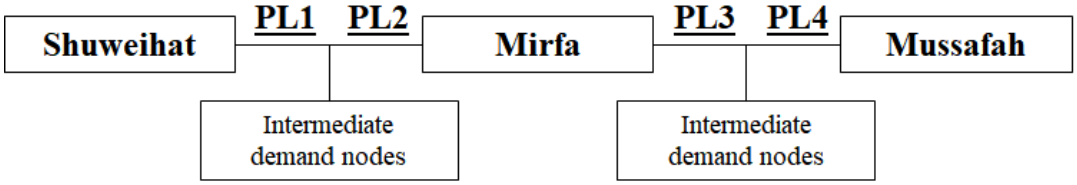

Figure 4.8: Simplified illustration of modelled pipelines between Shuweihat, Mirfa and Mussafah (PL = pipeline).

4.7. Control valves

The water flow entering the downstream boundary conditions (i.e. the storage farms) from the pipelines is controlled by control valves. These control valves have a minimum pressure (P) override setting of 2.5 bar. Therefore, a counter pressure from the downstream farms (Mirfa and Mussafah), expressed in head (H_{cp}), is necessary. This counter pressure is calculated with the following formula:

$$H_{cp} = \frac{P}{\rho_{water} \cdot g} \tag{4.9}$$

Where P = minimum pressure override setting of control valves [2.5 bar = 2.5 $\cdot 10^5$ Pa = 2.5 $\cdot 10^5$ kg/(m $\cdot s^2$)], ρ_{water} = density of water at 45 °C [990.2 kg/m^3], and g = gravitational acceleration [9.81 m/s^2]. The density of water at 45 °C is chosen since this is the average temperature of water in the pipelines in UAE (Deltares, 2015b).

The result of a minimum pressure override setting of 2.5 bar is equal to a head of 25.74 m, meaning that the minimum and maximum actual head of the downstream storage farm is 25.74 m higher than the water elevations of the downstream storage farm retrieved from TRANSCO. To account for this in the model, control valves at the end of the pipelines are included as discharge boundary conditions, meaning that is must take into account this extra counter pressure.

5
Optimisation model

This chapter describes the model that is used to optimise the operation phase of the WTS of TRANSCO. Section 5.1 describes the software and the solver that is used for the optimisation model. Section 5.2 describes the decision variables of this model. Section 5.3 describes the two objectives of the optimisation model. Section 5.4 describes the multiple constraints that are implemented in the model and finally section 5.5 gives the full optimisation model written in formulas.

5.1. Software

The software that is used for the optimisation of the WTS is called RTC-Tools[1] (Real Time Control). RTC-Tools, developed by Deltares, is an open-source toolbox for control and optimisation of environmental systems and can be used as a Python package. The tool has a focus on resolving conflicting constraints and optimisation goals. The tool offers two approaches for a multi-objective optimisation:

1. Weighting method: the goals are traded off against each other;
2. Lexicographic goal programming: goals are arranged into an ordered list, which are worked down step by step. This ensures that when optimising the goal, the previously optimised goals are not forgotten. This is especially important when goals have clearly defined priorities, such as that safety concerns are more important than economic optimisation.

In general, pumping costs (or GHG emissions) minimisation is a mixed integer nonlinear programming problem (MINLP) due to the binary nature of some of the variables and the quadratic functions involved (for example, $dH = C \cdot Q^2$). Additionally, the size of the solution space makes the problem difficult to solve. To simplify the model and to reduce the computational time, the formulas of the optimisation model (objectives and constraints) are made linear and a solver (Gurobi) is included. This makes it a mixed integer linear programming (MILP) problem.

The optimisation problem is solved by the use of the software library of Gurobi. Since the optimisation problem consists of many decision variables and binary integers (pump on/off), and because Gurobi includes features such as support for multiple objectives and for models with convex, piecewise-linear objective functions, Gurobi is chosen as a suitable solver. However, the fact that Gurobi is only available for free for academic licences and so commercial licences are really expensive, the research is harder to reproduce when using a different solver.

5.2. Decision variables

The decision variables consist of the operational setting for each individual pump for each timestep during the total operating time chosen. The decision variables are based on the pump status which can be either on or off and are therefore 0/1 binary decisions. Since WTSs generally operate on a daily basis, the operating horizon is chosen to be 24 h. Each timestep is chosen to be 1 h. These values are chosen since then the computational time of the model is minimised, but the accuracy of the real life model is still included. This is because a simulation of 24 h takes into account the diurnal variation in demand, the fluctuations in the water storage areas, and the variations of the pump operating points during the day.

[1] Source: https://www.deltares.nl/en/software/rtc-tools/.

5.3. Objectives

The three following sections describe the objective functions for the optimisation problem. Section 5.3.1 describes the objective function for the minimisation of the total costs of the system without the implementation of carbon taxes, section 5.3.2 describes the objective function for the minimisation of the total GHG emissions of the system, and section 5.3.3 describes the objective function for the minimisation of the total costs of the system with the implementation of carbon taxes. All three functions are calculated over a time period of one day, with timesteps of one hour, as explained in section 5.2.

5.3.1. Total costs without carbon tax

The minimisation objective for the total costs without the implementation of carbon taxes is expressed as follow:

$$\min \sum_{t=i}^{N} C_{tot}(t) \tag{5.1}$$

Where $C_{tot}(t)$ = total costs of the system without the implementation of carbon taxes at timestep t [AED] and the range of N is from 0 till 24 [h]. $C_{tot}(t)$ is calculated with the following formula:

$$C_{tot}(t) = P(t) \cdot p_{elec}(t) \tag{5.2}$$

Where $P(t)$ = power of the system at timestep t [kWh] and $p_{elec}(t)$ = electricity price at timestep t [AED/kWh]. $P(t)$ is calculated with the following formula:

$$P(t) = \Big(\sum_{i=1}^{6} P_{pump,shu} + \sum_{i=1}^{7} P_{pump,mir} \Big)(t) \tag{5.3}$$

Where $\sum_{i=1}^{6} P_{pump,shu}(t)$ = total power of the pumping station of Shuweihat ($n_{pumps} = 6$) at timestep t [kWh] and $\sum_{i=1}^{7} P_{pump,mir}(t)$ = total power of the pumping station of Mirfa ($n_{pumps} = 7$) at timestep t [kWh].

5.3.2. Total GHG emissions

The minimisation objective for the total GHG emissions is expressed as follow:

$$\min \sum_{t=i}^{N} E_{tot}(t) \tag{5.4}$$

Where $E_{tot}(t)$ = total GHG emissions of the system at timestep t [kg CO_2-eq] and the range of N is from 0 till 24 [h]. $E_{tot}(t)$ is calculated with the following formula:

$$E_{tot}(t) = P(t) \cdot f_{GHG}(t) \tag{5.5}$$

Where $P(t)$ = power of the system at timestep t [kWh] and $f_{GHG}(t)$ = GHG emissions factor at timestep t [kg CO_2-eq/kWh]. $P(t)$ is calculated with the following formula:

$$P_{tot}(t) = \Big(\sum_{i=1}^{6} P_{pump,shu} + \sum_{i=1}^{7} P_{pump,mir} \Big)(t) \tag{5.6}$$

Where $\sum_{i=1}^{6} P_{pump,shu}(t)$ = total power of the pumping station of Shuweihat ($n_{pumps} = 6$) at timestep t [kWh] and $\sum_{i=1}^{7} P_{pump,mir}(t)$ = total power of the pumping station of Mirfa ($n_{pumps} = 7$) at timestep t [kWh].

5.3.3. Total costs with carbon tax

When taking into account both electricity costs and the costs related to GHG emissions due to the implementation of carbon taxes, the minimisation objective for the total costs is expressed as follows:

$$\min \sum_{t=i}^{N} K_{tot}(t) \tag{5.7}$$

Where $K_{tot}(t)$ = total costs of the system with the implementation of carbon taxes at timestep t [AED] and the range of N is from 0 till 24 [h]. $K_{tot}(t)$ is calculated with the following formula:

$$K_{tot}(t) = P(t) \cdot p_{elec+carbon}(t) \tag{5.8}$$

Where $P(t)$ = power of the system at timestep t [kWh] and $p_{elec+carbon}(t)$ = total price (electricity + carbon tax) at timestep t [AED/kWh]. $P(t)$ is calculated with the following formula:

$$P(t) = \Big(\sum_{i=1}^{6} P_{pump,shu} + \sum_{i=1}^{7} P_{pump,mir} \Big)(t) \tag{5.9}$$

Where $\sum_{i=1}^{6} P_{pump,shu}(t)$ = total power of the pumping station of Shuweihat (n_{pumps} = 6) at timestep t [kWh] and $\sum_{i=1}^{7} P_{pump,mir}(t)$ = total power of the pumping station of Mirfa (n_{pumps} = 7) at timestep t [kWh].

5.4. Constraints

Multiple constraints, conditions that the solution of the model must satisfy, are implemented in the model. These constraints include the water level constraint, the pump switching constraint, the pump power constraint, the pipeline flow constraint, and the control valve constraint. The following sections discuss the constraints.

5.4.1. Water level constraint

The water in the three storage areas (Shuweihat, Mirfa and Mussafah) must stay within their lower and upper limit during each timestep of the optimisation. Therefore, the following constraint is included in the model for the storage area at Shuweihat:

$$WL_{shu,min}(t) \leq WL_{shu}(t) \leq WL_{shu,max}(t) \tag{5.10}$$

For the storage area at Mirfa, the following constraint is included in the model:

$$WL_{mir,min}(t) \leq WL_{mir}(t) \leq WL_{mir,max}(t) \tag{5.11}$$

For the storage area at Mussafah, the following constraint is included in the model:

$$WL_{mus,min}(t) \leq mus(t) \leq WL_{mus,max}(t) \tag{5.12}$$

Where WL_{shu}, WL_{mir} and WL_{mus} = water level at the storage areas of Shuweihat, Mirfa and Mussafah [m], $WL_{shu,min}$, $WL_{mir,min}$ and $WL_{mus,min}$ = minimum water level at the storage areas of Shuweihat, Mirfa and Mussafah [m], $WL_{shu,max}$, $WL_{mir,max}$ and $WL_{mus,max}$ = maximum water level at the storage areas of Shuweihat, Mirfa and Mussafah [m], and t = timestep number [h].

5.4.2. Pump switching constraint

To minimise the computational calculation time of the optimisation problem, a constraint is included which describes which pumps are allowed to be switched on at the same time. Here, a matrix is included that implies that the second pump can only be switched on when the first pump is on, the third pump can only be switched on when the second pump is on, etc. The following formula shows the matrix multiplication form:

$$b[:,1] \leq A \cdot x \leq b[:,2] \tag{5.13}$$

Where A = the pump switching matrix, b = the pump switching constraint, and x = the vector of the pump statuses. The values for A, b and x are found below.

$$\text{A} = \begin{bmatrix} 0 & 0 & 0 \\ 1 & -1 & 0 \\ 1 & 1 & -2 \end{bmatrix} \quad \text{b} = \begin{bmatrix} 0 & 0 \\ 1 & 1 \\ 1 & 2 \end{bmatrix} \quad \text{x} = \begin{bmatrix} S_1 \\ S_2 \\ S_3 \\ \dots \end{bmatrix}$$

Where, S_n is the status of pump n (on = 1, off = 0).

5.4.3. Pump power constraint

The power of the pumps of the pumping stations in Shuweihat and Mirfa is a non-linear function of the discharge and head. Since this is not solvable in a linear model, the power equation specified by the power coefficients is made linear and turned into a set of inequality constraints:

$$P \geq P_{min} \cdot S \tag{5.14}$$

$$P \leq P_{max} \cdot S \tag{5.15}$$

$$P \geq C_{1,1} + C_{1,2}Q + ... - P_{max} \cdot (1 - S) \tag{5.16}$$

Where S = the pump status (on = 1, off = 0), C = power coefficients [-] and P_{min} and P_{max} = the minimum and maximum possible power [kW] when the pump is on. With minimisation of the costs (or GHG emissions) of the pumps (goal of this study), the optimisation results in RTC-Tools will automatically satisfy the inequality constraint as if it was an equality constraint at its boundary[2].

5.4.4. Pipeline flow constraint

As explained in section 2.2.1, energy losses occur due to friction in the pipelines, also called the friction head loss. Therefore, a constraint is included which calculates this head loss. To calculate the friction head loss, the resistance coefficient (C) is needed. The resistance coefficient is calculated using the Darcy-Weisbach equation (formulas are found in section 2.2.1). Table 5.1 shows the parameters which are used to calculate the Reynolds number and the relative roughness for the pipelines between Shuweihat and Mirfa. Table 5.2 shows the parameters which are used to calculate these numbers for the pipelines between Mirfa and Mussafah. The water flow speed through the system is not known. Therefore, the assumption[3] is made that this speed is 1.0 m/s. Also, as described in section 4.6, the length of the pipelines is divided by two to implement the intermediate demand nodes into the model. Therefore, the length given in the tables below is half the length of the total pipeline. The final calculated values of the same pipelines are equal (because the intermediate demand node is exactly in the middle of the pipeline) and are used twice in the optimisation model.

Table 5.1: Input parameters for the calculation of the Reynolds number and the relative roughness for the water flow of the pipelines between Shuweihat and intermediate demand node, and between intermediate demand node and Mirfa.

Parameter	Input	Unit	Comment
Length (L)	48.58	[km]	Retrieved from TRANSCO
Diameter (d)	2262.74	[mm]	Retrieved from TRANSCO
Cross sectional area (A)	4.02	[m^2]	Calculated based on information from TRANSCO
Kinematic viscosity (ϑ)	$0.6 \cdot 10^{-6}$	[m^2/s]	Value based on temperature of 45 °C
Pipe roughness (ϵ)	0.15	[mm]	Roughness of pipe material
Water flow speed (v)	1.0	[m/s]	Assumption

Table 5.2: Input parameters for the calculation of the Reynolds number and the relative roughness for the water flow of the pipelines between Mirfa and intermediate demand node, and intermediate demand node and Mussafah.

Parameter	Input	Unit	Comment
Length (L)	63.90	[km]	Retrieved from TRANSCO
Diameter (d)	2262.74	[mm]	Retrieved from TRANSCO
Cross sectional area (A)	4.02	[m^2]	Calculated based on information from TRANSCO
Kinematic viscosity (ϑ)	$0.6 \cdot 10^{-6}$	[m^2/s]	Value based on temperature of 45 °C
Pipe roughness (ϵ)	0.15	[mm]	Roughness of pipe material
Water flow speed (v)	1.0	[m/s]	Assumption

By knowing the Reynolds number and the relative roughness, the Moody diagram is used to determine the friction factors. The final values for the friction factors and the resistance coefficients of the pipelines between Shuweihat, Mirfa and Mussafah are found in Table 5.3.

[2] Equation 5.16 is the linear expression of the non-linear function stated in equation 4.5.
[3] The assumption is based on knowledge of supervisor Deltares.

Table 5.3: Friction factors and resistance coefficients for pipelines between Shuweihat, Mirfa and Mussafah.

Pipeline	Friction factor (f) [-]	Resistance coefficient (C) [s^2/m^5]
Shuweihat - Mirfa	0.01172	0.793
Mirfa - Mussafah	0.01172	1.043

The friction head loss would normally be calculated by the use of equation 2.1. However, this equation is quadratic (non-linear) and thus not possible to implement into the linear optimisation model. Therefore, the quadratic function is subdivided into fifty linear pieces to approach the quadratic function (see Figure 5.1 for an example of linear approaching).

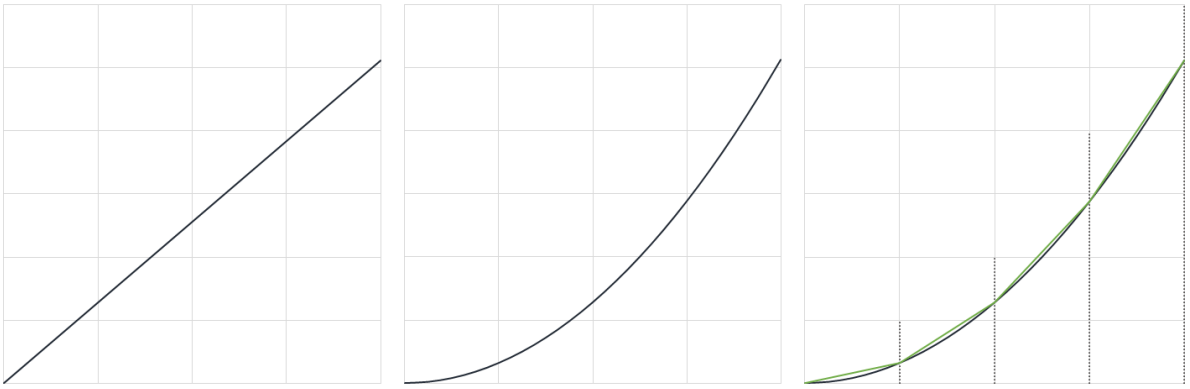

Figure 5.1: Example of order 1 linear (left figure), order 2 polynomial (middle figure) and linear approach of order 2 (subdivided into four pieces) (right figure).

The following formula shows the pipeline flow constraint, expressed in a linear formulation:

$$dH_{pipeline} \geq a_0 \cdot Q_{pipeline} + b_o \tag{5.17}$$

Where a and b are the fitted parameters for each linear line (n = 50). This constraint is added four times in the model (pl1, pl2, pl3 and pl4), since the pipelines are divided into four pieces due to the intermediate demand nodes.

Note, this optimisation model does not take into consideration the amount of time the water stays in the pipeline before it enters the downstream storage farm. The assumption is made that the amount of water flowing into the pipes from the upstream farm automatically results in the same amount of water flowing out of the pipes into the downstream farm. This approach is justified since this study does not take the quality of the drinking water into discussion. The amount of time the water stays in the pipes would have been important when researching the chlorine concentration in the water.

5.4.5. Valve constraint

As explained in section 4.7, the water flow entering the downstream boundary conditions is controlled by control valves which have a minimum pressure override setting of 2.5 bar. When expressed in head, this is equal to a counter pressure (H_{cp}) of 25.74 m. Therefore, the following constraint is added into the optimisation model:

$$V_{downstreamfarm}.HQUp.H = H_{cp} + H_{valve} \tag{5.18}$$

Where $V_{downstreamfarm}$ = name of the control valve at the specific downstream farm [-], H_{cp} = 25.74 m as explained above, and H_{valve} = height at which the specific valve is located [m]. For both the valves, they are located at the top of the inflow of the storage area. Table 5.4 shows the specific values.

Table 5.4: Counter pressures of water flow at entrance storage farms due to control valves.

Downstream tank farm	H_{cp} [m]	H_{valve} [m]	Total head [m]
Mirfa	25.74	21.36	47.10
Mussafah	25.74	22.49	48.23

5.5. Full optimisation problem

The full optimisation problem (objectives and constraints), only expressed in formulas, is found below.

$$\min \sum_{t=i}^{N} \Big(\sum_{i=1}^{6} P_{pump,shu} + \sum_{i=1}^{7} P_{pump,mir} \Big)(t) \cdot p_{elec}(t) \tag{5.19}$$

$$\min \sum_{t=i}^{N} \Big(\sum_{i=1}^{6} P_{pump,shu} + \sum_{i=1}^{7} P_{pump,mir} \Big)(t) \cdot f_{GHG}(t) \tag{5.20}$$

$$\min \sum_{t=i}^{N} \Big(\sum_{i=1}^{6} P_{pump,shu} + \sum_{i=1}^{7} P_{pump,mir} \Big)(t) \cdot p_{elec+carbon}(t) \tag{5.21}$$

Subject to:

$$WL_{shu,min}(t) \leq WL_{shu}(t) \leq WL_{shu,max}(t) \tag{5.22}$$

$$WL_{mir,min}(t) \leq WL_{mir}(t) \leq WL_{mir,max}(t) \tag{5.23}$$

$$WL_{mus,min}(t) \leq WL_{mus}(t) \leq WL_{mus,max}(t) \tag{5.24}$$

$$b[:,1] \leq A \cdot x \leq b[:,2] \tag{5.25}$$

$$P_{shu} \geq P_{shu,min} \cdot S_n \tag{5.26}$$

$$P_{shu} \leq P_{shu,max} \cdot S_n \tag{5.27}$$

$$P_{shu} \geq C_{1,1} + C_{1,2}Q + ... - P_{shu,max} \cdot (1 - S_n) \tag{5.28}$$

$$P_{mir} \geq P_{mir,min} \cdot S_n \tag{5.29}$$

$$P_{mir} \leq P_{mir,max} \cdot S_n \tag{5.30}$$

$$P_{mir} \geq C_{1,1} + C_{1,2}Q + ... - P_{mir,max} \cdot (1 - S_n) \tag{5.31}$$

$$dH_{pl1} \geq a_0 \cdot Q_{pl1} + b_o \tag{5.32}$$

$$dH_{pl2} \geq a_0 \cdot Q_{pl2} + b_o \tag{5.33}$$

$$dH_{pl3} \geq a_0 \cdot Q_{pl3} + b_o \tag{5.34}$$

$$dH_{pl4} \geq a_0 \cdot Q_{pl4} + b_o \tag{5.35}$$

$$V_{mir}.HQUp.H = H_{cp} + H_{mir} \tag{5.36}$$

$$V_{mus}.HQUp.H = H_{cp} + H_{mus} \tag{5.37}$$

6 Scenarios

Scenario planning is useful to gain insight in how the future water and energy infrastructure of UAE affects the pump schedule of the WTS of TRANSCO and thus their total operating costs and GHG emissions. The following sections explain the different scenarios included in this research.

6.1. Electricity tariffs

Nowadays, the UAE has a flat electricity tariff rate of 0.20 AED/kWh. However, the UAE is investigating whether they should implement ToU rates in the coming years. Therefore, the effect of varying tariffs on the pump schedule is researched. To investigate the effect of ToU rates compared to flat rates, three scenarios are researched. All three scenarios have a blended rate of 0.20 AED/kWh and are based on a low, medium and extreme difference between the off-peak tariff and the on-peak tariff. In UAE, day time (on-peak) is identified between 10 am and 10 pm. Night time (off-peak) is identified between 10 pm and 10 am. Therefore, the investigated ToU rates are based on these times. The tariffs of the different scenarios are found in Figure 6.1 and are used as inputs in equation 5.2 (p_{elec})[1].

From	To	Base case (now)	Scenario 1 (low)	Scenario 2 (medium)	Scenario 3 (extreme)
00:00	01:00	Flat rate tariff 0.20 AED/kWh	Off-peak tariff 0.18 AED/kWh	Off-peak tariff 0.15 AED/kWh	Off-peak tariff 0.10 AED/kWh
01:00	02:00				
02:00	03:00				
03:00	04:00				
04:00	05:00				
05:00	06:00				
06:00	07:00				
07:00	08:00				
08:00	09:00				
09:00	10:00				
10:00	11:00		On-peak tariff 0.22 AED/kWh	On-peak tariff 0.25 AED/kWh	On-peak tariff 0.30 AED/kWh
11:00	12:00				
12:00	13:00				
13:00	14:00				
14:00	15:00				
15:00	16:00				
16:00	17:00				
17:00	18:00				
18:00	19:00				
19:00	20:00				
20:00	21:00				
21:00	22:00				
22:00	23:00		Off-peak tariff 0.18 AED/kWh	Off-peak tariff 0.15 AED/kWh	Off-peak tariff 0.10 AED/kWh
23:00	00:00				

Figure 6.1: Base case electricity tariff structure and included three scenarios (low, medium and extreme).

[1]The assumption is made that the electricity tariffs will stay the same in the future. Chapter 12: 'Discussion' further elaborates on this.

6.2. GHG emissions factors

Nowadays (last available data is from 2017), the power source mix of UAE consists of mainly natural gas. In the emirate Abu Dhabi, the power source mix consisted of 99.75% natural gas and 0.25% gas oil in 2017 (ADWEC, 2019b). The UAE aims towards a more sustainable but also towards a more diversified power source mix in order to have a reliable network and to sustain the progress of it (AE, 2019). Therefore, coal power plants, nuclear power plants and solar power will be implemented in the coming years. To investigate the effect of the new power source mixes on the pump schedule, average GHG emissions factors are compared with time-dependent GHG emissions factors for three different years: 2017, 2030 and 2050, where 2030 and 2050 are the 'Energy Strategy' deadlines years of UAE (AE, 2019). The average GHG emissions factors per year are used as base case scenarios. Table 6.1 below shows the power source mixes of the three years.

Table 6.1: Power source mix UAE now (2017) and 'Energy Strategy' deadline years (2030 & 2050).

Energy source	'Now' (2017)	Goal 2030	Goal 2050
Natural Gas	99.75 %	71 %	38 %
Gas Oil	0.25 %	0 %	0 %
Coal	0 %	12 %	12 %
Nuclear	0 %	12 %	6 %
Solar	0 %	5 %	44 %

6.2.1. Breakdown of the system

To calculate the average and time-dependent GHG emissions factors for the three years, calculations are made based on the principle of a merit order. A merit order is a way of ranking the available power sources based on an ascending order of their marginal costs together with the amount of energy generated. The power sources with the lowest ranking (cheapest sources) are the first ones used to meet the demand. The sources with the highest marginal costs are the last sources used to meet the demand. Dispatching generation therefore minimises the costs of electricity production. Implementing renewable sources into the system results in a decreasing average price of electricity, since renewable sources have very low marginal costs (no fuel costs, only operation and maintenance costs) compared to traditional sources such as natural gas and oil, called the merit order effect (Sensfub et al., 2009). Figure 6.2 below illustrates the electricity price fluctuations due to the merit order effect.

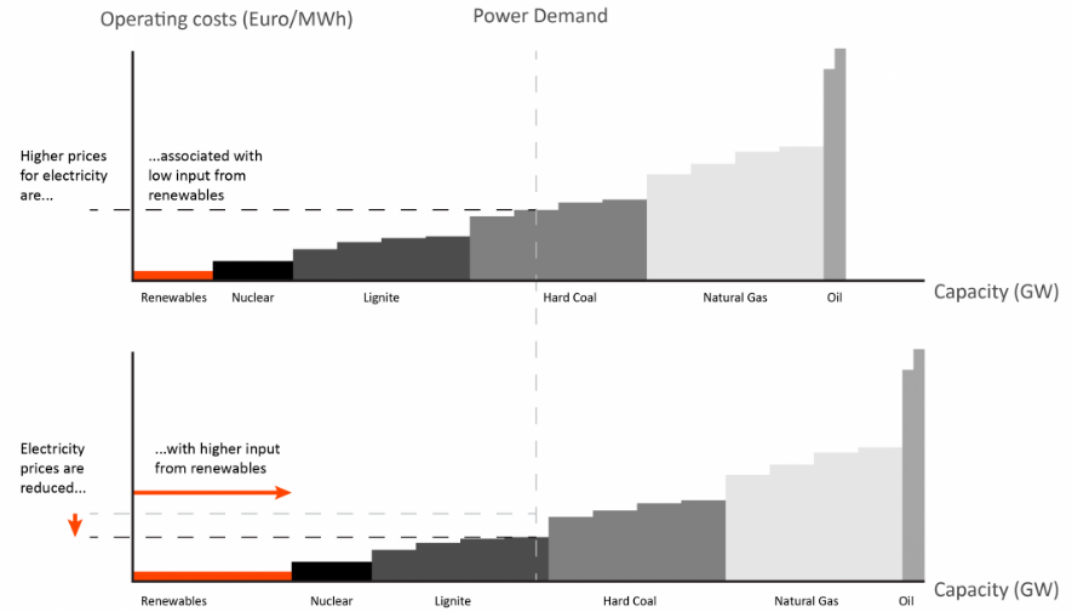

Figure 6.2: Illustrating electricity price fluctuations due to the merit order effect.

The principle of the merit order is used to make a breakdown of the different power sources during the day and with that the calculation of the GHG emissions factors. To calculate the GHG emissions factors, the fol-

lowing steps are done. First, a 24 h electricity demand profile of the system is needed. Two average electricity demand profiles of 2017 are available, one for the month February and one for the month August (ADWEC, 2019b). The average demand profile of August is used for the calculation since this profile is more similar to the profile of July than for February (and the water flow patterns retrieved from TRANSCO are from the end of July). A figure of the demand profile is found in Appendix C (Figure C.1). The demand profile is then filled up with the available sources found in Table 6.1. The order of the sources is the following: nuclear - solar - coal - natural gas - gas oil. A description of the different sources is found in the following sections. Note, the expected growth in electricity demand up till 2050 is not taken into account. This is chosen since the electricity demand is only used to know the demand pattern variation (electricity peaks) during the day. Since the assumption is made that the pattern during the day stays the same over the years, the absolute number of electricity demand is not relevant since the division in percentage of the different sources stays the same.

Nuclear
Although nuclear power has higher marginal costs than solar power and would therefore normally be ordered after solar power in a merit order, nuclear power is used as the baseload generator due to their long start up and shutdown times. The steady hourly nuclear power generation for a full day is calculated as follows. First, the total power demand for the whole day is summed up. Then, the part fulfilled by nuclear power (12% for 2030 and 6% for 2050) is calculated. Finally, this is divided equally over the day, so that every timestep of one hour generates the same amount of nuclear power. The exact values for the different years are found in Tables C.2 and C.3 in Appendix C.

Solar
There is no 24 h solar intensity profile of UAE available (only monthly profiles). Therefore, a daily sun profile is made based on the sunrise (05:36h) and sunset (19:01h) of July 21, 2018 and a prediction of the sun intensity within the available sun hours. The daily sun profile and thus the sun intensities during the day are found in Appendix C (Figure C.2). The sun intensity percentages are then used to calculate the solar power generation during the day for the years 2030 and 2050 (not for 2017 since the emirate Abu Dhabi does not use solar power generation yet). The hourly solar power generation for a full day is calculated as follows. First, the total power demand for the whole day is summed up. Then, the part fulfilled by solar power (5% for 2030 and 44% for 2050) is calculated. Finally, this is divided over the available hours taking into account the solar intensities shown in Figure C.2. The exact values for the different years are found in Tables C.2 and C.3 in Appendix C.

Coal
The power source coal provides 12% of the demand at every timestep (for both 2030 and 2050), except for a few hours during the day in 2050 when there is an excess of solar power and therefore no coal plants are needed for electricity generation. The exact values for the different years are found in Tables C.2 and C.3 in Appendix C.

Natural gas
Natural gas plants are used as peak power plants since they can quickly provide electricity due to their fast start up and shutdown times. Therefore, the remaining electricity demand at every timestep not generated by the other power sources is generated by natural gas plants. The exact values for the different years are found in Tables C.1, C.2 and C.3 in Appendix C.

Gas oil
A small amount of gas oil is still used at the moment (0.25% in 2017). In 2030 and 2050, there will be no electricity generated anymore by this source. The power source gas oil therefore only provides 0.25% of the demand at every timestep in 2017. The exact values are found in Table C.1 in Appendix C.

Out of this division, three breakdowns are made (2017, 2030 and 2050) which show the amount of electricity generated by each source and the demand profile during the day. The breakdowns are found in Figures 6.3, 6.4 and 6.5. As seen, there is a surplus of solar power between 11:00 and 15:00 in 2050. This surplus is out of the research scope and is therefore not relevant.

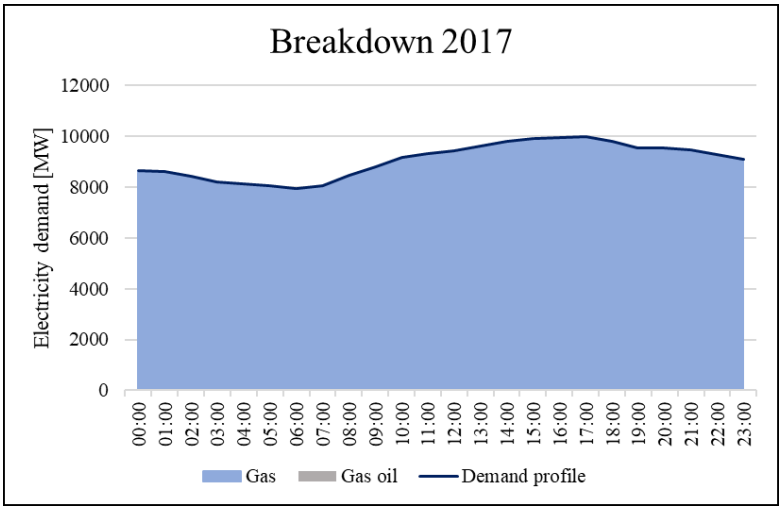

Figure 6.3: Hourly average breakdown of total production by power source in 2017.

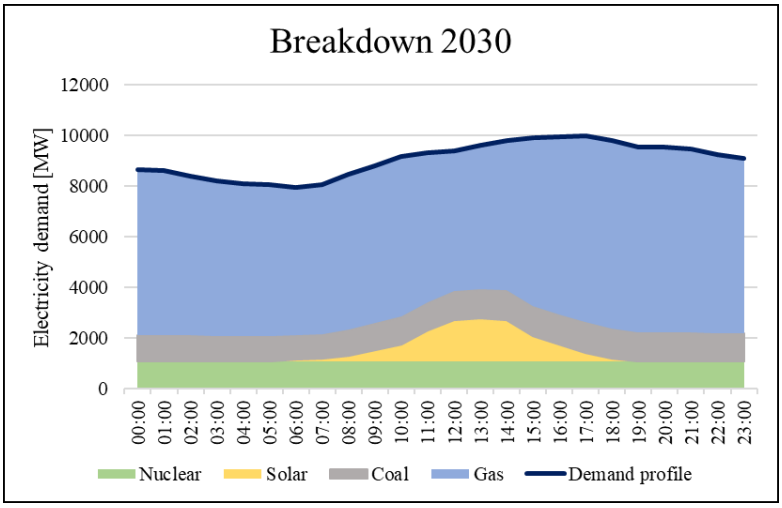

Figure 6.4: Hourly average breakdown of total production by power source in 2030.

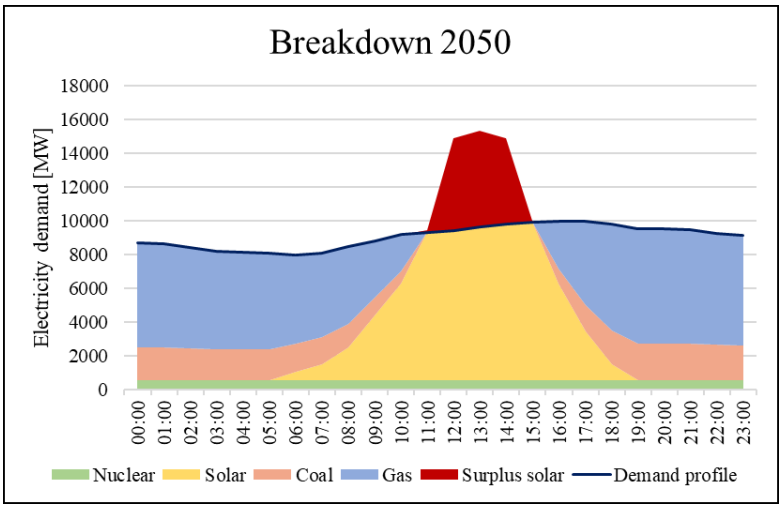

Figure 6.5: Hourly average breakdown of total production by power source in 2050.

6.2.2. Average and time-dependent GHG emissions factors

By knowing the breakdown per year, the distribution of the power sources [%] for each timestep are calculated with the following formula:

$$Distr_{source}(t) = \frac{P_{source}(t)}{P_{demand}(t)} \tag{6.1}$$

Where $Distr_{source}$ = distribution per source [%], P_{source} = amount of electricity generated by the different sources (nuclear, solar, natural gas, coal and gas oil) [MW], P_{demand} = demand profile of the system [MW], and t = time [h]. The distributions are found in Tables C.1, C.2 and C.3 in Appendix C. To calculate the GHG emissions factors, GHG emission intensities per source are needed. Table 6.2 below shows the GHG emissions intensities used in this research (EI mean). These numbers are life cycle intensities and are a compilation of multiple sources which needed to meet the following requirements: 1) coming from a credible source (only studies published by governments and universities), 2) clearly defined life cycle in the assessment, and 3) expressed GHG emissions as a function of electricity production. Per power source there are at least five different sources and a maximum of fourteen sources used to calculate the GHG emissions intensities (IPCC, 2014; WNA, 2011). A factor that has for example an influence on the ranges of the GHG emissions intensities is the definition of life cycle (including or excluding waste management and treatment in the scope).

Table 6.2: GHG emissions intensities (EI) per power source based on life cycle assessment values [kg CO_2-eq/kWh].

Energy source	**EI mean**	EI low	EI high	Unit
Natural Gas	**0.499**	0.362	0.891	[kg CO_2-eq/kWh]
Gas Oil	**0.733**	0.547	0.935	[kg CO_2-eq/kWh]
Coal	**0.888**	0.756	1.310	[kg CO_2-eq/kWh]
Nuclear	**0.029**	0.002	0.130	[kg CO_2-eq/kWh]
Solar	**0.085**	0.013	0.170	[kg CO_2-eq/kWh]

Finally, to calculate the average and time-dependent GHG emissions factors, the following formulas are used:

$$AV_{factor} = \left(PS_{gas} \cdot EI_{gas}\right) + \left(PS_{oil} \cdot EI_{oil}\right) + ... \tag{6.2}$$

$$TD_{factor}(t) = \left(Distr_{gas}(t) \cdot EI_{gas}(t)\right) + \left(Distr_{oil}(t) \cdot EI_{oil}(t)\right) + ... \tag{6.3}$$

Where AV_{factor}[2] = average GHG emissions factor [kg CO_2-eq/kWh], PS_{gas}, PS_{oil}, etc = power source mix percentages for 2017, 2030 and 2050 [%] as seen in Table 6.1, EI_{gas}, EI_{oil}, etc = GHG emissions intensity [kg CO_2-eq/kWh], TD_{factor} = time-dependent GHG emissions factors [kg CO_2-eq/kWh], $Distr_{gas}$, $Distr_{oil}$, etc = distribution per source [%] as seen in Tables C.1, C.2 and C.3, and t = time [h].

The average GHG emissions factors are 0.500, 0.469, and 0.405 for years 2017, 2030 and 2050 respectively. Figure 6.6 shows the time-dependent GHG emissions factors per hours. As the figure shows, there is no difference in GHG emissions factors per timestep for the year 2017 since no renewable sources are included in the power source mix. For 2030 and 2050, there are periods during the day with lower GHG emissions factors due to the inclusion of renewable sources. For 2030, this period is between 09:00 and 16:00 (green area) and for 2050 this period is between 08:00 and 17:00 (yellow area). Especially in 2050, the time dependent factors compared to the average factors are significant.

[2]The average GHG emissions factor of 2050 is 0.303. However, due to the surplus of solar in the merit order (see Figure 6.5), part of the available solar power is out of the research scope and is therefore not used. The average GHG emissions factor for 2050 is calculated by only taking into account the sources below the demand profile line. Therefore, the average GHG emissions factor for 2050 used in this research is higher than UAE's goal for 2050.

From	To	2017	2030	2050
00:00	01:00	0.500	0.487	0.557
01:00	02:00	0.500	0.486	0.557
02:00	03:00	0.500	0.485	0.556
03:00	04:00	0.500	0.483	0.555
04:00	05:00	0.500	0.483	0.555
05:00	06:00	0.500	0.481	0.554
06:00	07:00	0.500	0.476	0.493
07:00	08:00	0.500	0.471	0.434
08:00	09:00	0.500	0.469	0.384
09:00	10:00	0.500	0.467	0.337
10:00	11:00	0.500	0.461	0.241
11:00	12:00	0.500	0.438	0.082
12:00	13:00	0.500	0.415	0.082
13:00	14:00	0.500	0.408	0.082
14:00	15:00	0.500	0.411	0.082
15:00	16:00	0.500	0.435	0.082
16:00	17:00	0.500	0.472	0.318
17:00	18:00	0.500	0.486	0.465
18:00	19:00	0.500	0.489	0.512
19:00	20:00	0.500	0.492	0.560
20:00	21:00	0.500	0.492	0.560
21:00	22:00	0.500	0.492	0.560
22:00	23:00	0.500	0.491	0.559
23:00	00:00	0.500	0.490	0.559

Figure 6.6: Average (AV) and Time-Dependent (TD) GHG emissions factors for 2017, 2030 and 2050. All emissions factors have the unit [kg CO_2-eq/kWh].

6.3. Policy driver carbon tax

As explained in section 2.4, carbon taxes can be implemented into the model by adding a monetary costs per unit of GHG emissions produced. Carbon taxes provide countries with a low cost tool to effectively reduce their emissions (OECD, 2016). The UAE has currently no carbon taxes related to electricity usage in their policy. However, since the UAE is aiming to a more sustainable power source mix, it is possible that the government will implement this policy driver in the future. Therefore, the effect of the implementation of carbon taxes on the system are investigated. As no carbon taxes are currently implemented in the policy of UAE and no future numbers are known, the report of OECD (2016) is used which provides a comprehensive analysis of the integrated carbon price resulted from taxes and emissions trading systems. This report covers 41 OECD and G20 economies, which are together responsible for 80% of the global energy use and CO_2-eq emissions. For example, the Netherlands has a average price carbon tax for the sector industry of 44.2 EUR/t CO_2-eq (which is equal to 0.184 AED/kg CO_2-eq). The carbon tax numbers stated in this report are used to provide an overview of the range of the carbon taxes. To calculate the carbon price, the following formula is used:

$$CP_{y,f}(t) = CT_{y,f}(t) \cdot EI_{y,f}(t) \tag{6.4}$$

Where CP = carbon price [AED/kWh], CT = carbon tax [AED/kg CO_2-eq], EI = emissions intensity [kg CO_2-eq/kWh], y = year [-], f = average (AV) or time-dependent (TD) factor [-], and t = time [h]. Since the UAE

already uses an electricity price (currently flat rate of 0.20 AED/kWh), the carbon price is added up as extra costs. The total price at timestep t is then:

$$TP_{y,f,r}(t) = EP_r(t) + CP_{y,f}(t) \tag{6.5}$$

Where TP = total price [AED/kWh], EP = electricity price [AED/kWh] and r = flat tariff rate or ToU rate (see Figure 6.1). Since the carbon price is added up on the electricity price, the following will happen. When the carbon tax is low, the influence on the system is small since the electricity price is dominating. The effect on the pump schedule will therefore be small. However, when the carbon tax reaches a certain value, the optimal pump schedule will be during daytime when the availability of solar power is used due to the low GHG emissions and thus the low carbon price. However, this is during the on-peak electricity tariffs (daytime). Eventually, a trade-off will occur between the electricity price and the carbon price. This trade-off is investigated for the four electricity tariff scenarios (see Figure 6.1 for the exact values), and for the three different years and thus the different GHG emissions factor scenarios (average and time-dependent, see Figure 6.6 for the exact values). This makes it a total of 24 scenarios.

Note, a different approach is possible in which the carbon price is not added to the electricity price, but a new total price per timestep during the day is calculated based on the increasing supply of renewable sources and thereby the addition of sources with lower marginal costs (electricity price forecasting). However, no historical data of the electricity prices in UAE is available and research into electricity price forecasting in UAE is limited. Therefore, the aforementioned method is chosen in favor of electricity price forecasting.

6.4. Infrastructure influence

The effect of the infrastructure of the WTS of TRANSCO on the pump schedule and thus the corresponding costs / GHG emissions is investigated by changing different parameters of the system. Only the parts of the WTS that can easily be expanded are investigated, since TRANSCO will not replace their whole infrastructure. Also, only an increase of the parameters is investigated, since in the future the water use in UAE will only further increase due to the growing water demand. Two parameters are investigated: the storage area size and the pipeline size.

Storage area size

By changing the storage area size, more water can be stored in the system during the same time period. The parameter that is changed is the cross sectional area of the storages (A). An increase of 10% and 20% is investigated for both the electricity tariff scenarios as well as the GHG emissions scenarios. Table 6.3 below shows the values of the investigated storage area sizes.

Table 6.3: Investigated storage area sizes [m^2] for the effect of the infrastructure influence on the system.

Storage area	Original	+10%	+20%	Unit
Shuweihat	51,249	56,374	61,498	[m^2]
Mirfa	10,527	11,580	12,632	[m^2]
Mussafah	15,845	17,430	19,015	[m^2]

Pipeline size

By changing the pipeline size, more water can flow through the system during the same time period. The parameter that is changed is the diameter of the pipes (d) which results in different resistance coefficients (see sections 2.2.1 and 5.4.4 for the formulas). An increase of 10% and 20% is investigated for both the electricity tariff scenarios as well as the GHG emissions scenarios. Table 6.4 below shows the values of the investigated pipe sizes.

Table 6.4: Investigated pipeline sizes [mm] and corresponding resistance coefficients [s^2/m^5] for the effect of the infrastructure influence on the system.

Pipeline	Original (d)	+10% (d)	+20% (d)	Unit	Original (C)	+10% (C)	20% (C)	Unit
SHU - MIR	2.263	2.489	2.715	[mm]	0.793	0.490	0.316	[s^2/m^5]
MIR - MUS	2.263	2.489	2.715	[mm]	1.043	0.645	0.416	[s^2/m^5]

6.5. Sensitivity analysis

A sensitivity analysis is performed to test the robustness of the model through the identification of uncertain parameters. The two following uncertain parameters are tested: 1) GHG emissions intensities (section 6.5.1), and 2) speed of water flow (section 6.5.2).

6.5.1. GHG emissions intensities

The GHG emissions intensities per power source used in this research are the mean values of a compilation of multiple sources. However, lower and higher GHG emissions intensities are also possible due to the calculation approach, such as the definition of life cycle (include or exclude waste management and treatment in the scope). Therefore, to test this uncertain parameter, the effect of different GHG emissions intensities per power source on the system are modelled. Table 6.2 in section 6.2.2 shows the low and high EI. With the use of formulas 6.2 and 6.3, new GHG emissions factors per hour are calculated. Figure 6.7 shows the time-dependent GHG emissions factors when using low EI. The average GHG emissions factors are here 0.363, 0.349 and 0.295 for the years 2017, 2030 and 2050 respectively. Figure 6.8 shows the time-dependent GHG emissions factors when using high EI. The average GHG emissions factors are here 0.891, 0.814 and 0.692 for the years 2017, 2030 and 2050 respectively. The green (2030) and yellow (2050) areas show the periods during the day when the time-dependent GHG emissions factors are smaller than the average GHG emissions factors due to the inclusion of renewable sources.

From	To	2017	2030	2050
00:00	01:00	0.363	0.364	0.428
01:00	02:00	0.363	0.364	0.428
02:00	03:00	0.363	0.363	0.427
03:00	04:00	0.363	0.362	0.426
04:00	05:00	0.363	0.361	0.426
05:00	06:00	0.363	0.361	0.426
06:00	07:00	0.363	0.355	0.372
07:00	08:00	0.363	0.351	0.321
08:00	09:00	0.363	0.350	0.277
09:00	10:00	0.363	0.348	0.236
10:00	11:00	0.363	0.342	0.152
11:00	12:00	0.363	0.323	0.012
12:00	13:00	0.363	0.303	0.012
13:00	14:00	0.363	0.298	0.012
14:00	15:00	0.363	0.300	0.012
15:00	16:00	0.363	0.320	0.012
16:00	17:00	0.363	0.351	0.219
17:00	18:00	0.363	0.363	0.347
18:00	19:00	0.363	0.366	0.388
19:00	20:00	0.363	0.368	0.431
20:00	21:00	0.363	0.368	0.431
21:00	22:00	0.363	0.368	0.430
22:00	23:00	0.363	0.367	0.430
23:00	00:00	0.363	0.366	0.429

Figure 6.7: Average (AV) versus Time-Dependent (TD) GHG emissions factors for 2017, 2030 and 2050 with low emissions intensities per source, see Table 6.2. All emissions factors have the unit [kg CO_2-eq/kWh].

From	To	2017	2030	2050
00:00	01:00	0.891	0.846	0.938
01:00	02:00	0.891	0.845	0.937
02:00	03:00	0.891	0.843	0.936
03:00	04:00	0.891	0.841	0.935
04:00	05:00	0.891	0.839	0.934
05:00	06:00	0.891	0.839	0.934
06:00	07:00	0.891	0.828	0.834
07:00	08:00	0.891	0.819	0.739
08:00	09:00	0.891	0.816	0.658
09:00	10:00	0.891	0.812	0.582
10:00	11:00	0.891	0.800	0.426
11:00	12:00	0.891	0.760	0.168
12:00	13:00	0.891	0.720	0.168
13:00	14:00	0.891	0.709	0.168
14:00	15:00	0.891	0.713	0.168
15:00	16:00	0.891	0.755	0.168
16:00	17:00	0.891	0.819	0.550
17:00	18:00	0.891	0.843	0.787
18:00	19:00	0.891	0.849	0.864
19:00	20:00	0.891	0.855	0.942
20:00	21:00	0.891	0.855	0.942
21:00	22:00	0.891	0.854	0.942
22:00	23:00	0.891	0.852	0.941
23:00	00:00	0.891	0.851	0.940

Figure 6.8: Average (AV) versus Time-Dependent (TD) GHG emissions factors for 2017, 2030 and 2050 with high emissions intensities per source, see Table 6.2. All emissions factors have the unit [kg CO_2-eq/kWh].

6.5.2. Speed of water flow

The water flow speed through the system is not known and the assumption is made to set this speed at 1.0 m/s as explained in section 5.4.4. The water flow speed has an effect on the resistance coefficient of the pipeline, which has an effect on the head loss. To test this uncertain parameter, the effect of different water flow speeds (0.5 and 1.5 m/s) on the system is modelled. The calculated resistance coefficients for the different water flow speeds (0.5 and 1.5 m/s) per pipeline are found in Table 6.5.

Table 6.5: Resistance coefficients for pipelines between Shuweihat, Mirfa and Mussafah for different water flow speeds.

Pipeline	Water flow speed (v) [m/s]	Resistance coefficient (C) [s^2/m^5]
Shuweihat - Mirfa	0.5	0.827
Shuweihat - Mirfa	1.5	0.781
Mirfa - Mussafah	0.5	1.088
Mirfa - Mussafah	1.5	1.026

III

Results

7

Electricity tariffs

This chapter shows the results of the effect of ToU electricity rates on the pump schedule of the WTS of TRANSCO. It first shows the different scenarios that are researched as explained in section 6.1, followed by the results of these scenarios. Section 7.6 presents the conclusion of the effect of ToU rates on the pump schedule. The start values of the storages are all defined at 14 m, which is the rounded average of the storage areas.

7.1. Overview

Figure 7.1 shows the profiles of the flat rate tariffs and ToU tariffs over a period of 24 hours for the following three scenarios compared to the base case scenario: low, medium and extreme.

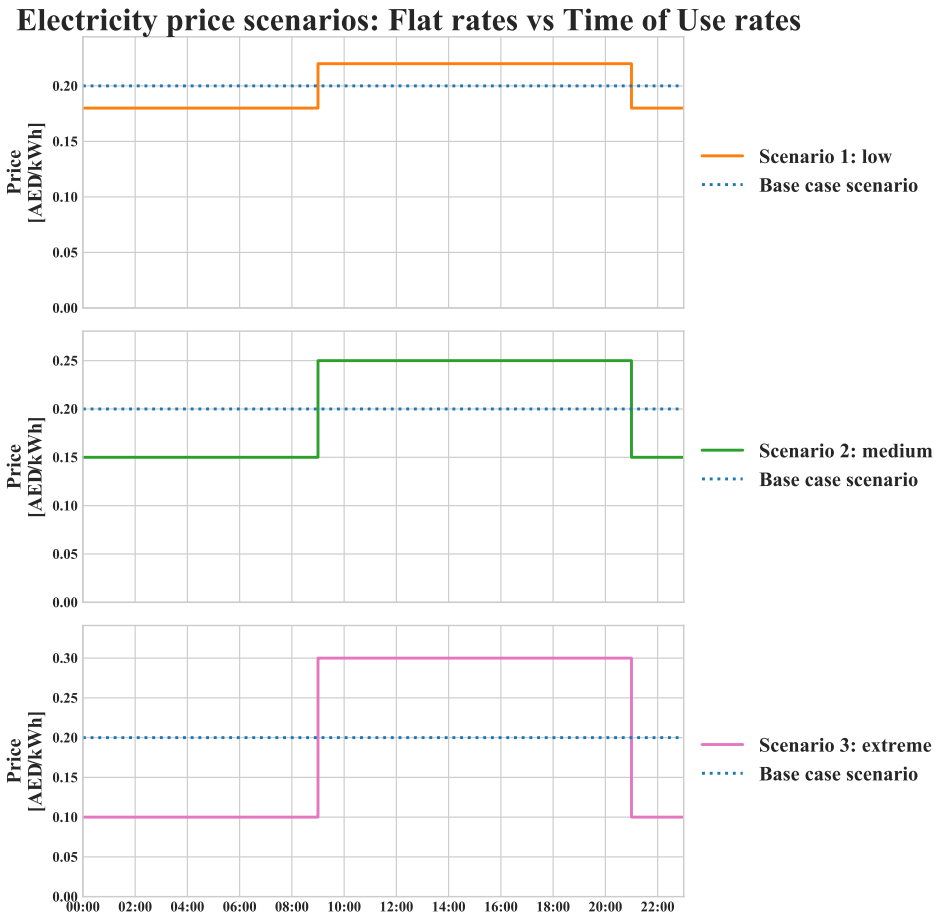

Figure 7.1: Base case electricity tariff structure and included three scenarios (low, medium and extreme).

7.2. Base case scenario

Figure 7.2 shows the results of the base case electricity tariff scenario of July 21, 2018. The total power of the 24 hour profile is 339.7 MW, and with a flat rate tariff of 0.20 AED/kWh, this results in a total costs of 67,948 AED. As seen in the figure, the pumps needed to fulfill to the water demand in UAE pump almost gradually during the day, meaning that the pumps do not have much capacity fluctuations and are thus pumping steady during the day. Figure 7.2b shows the exact profiles per pump.

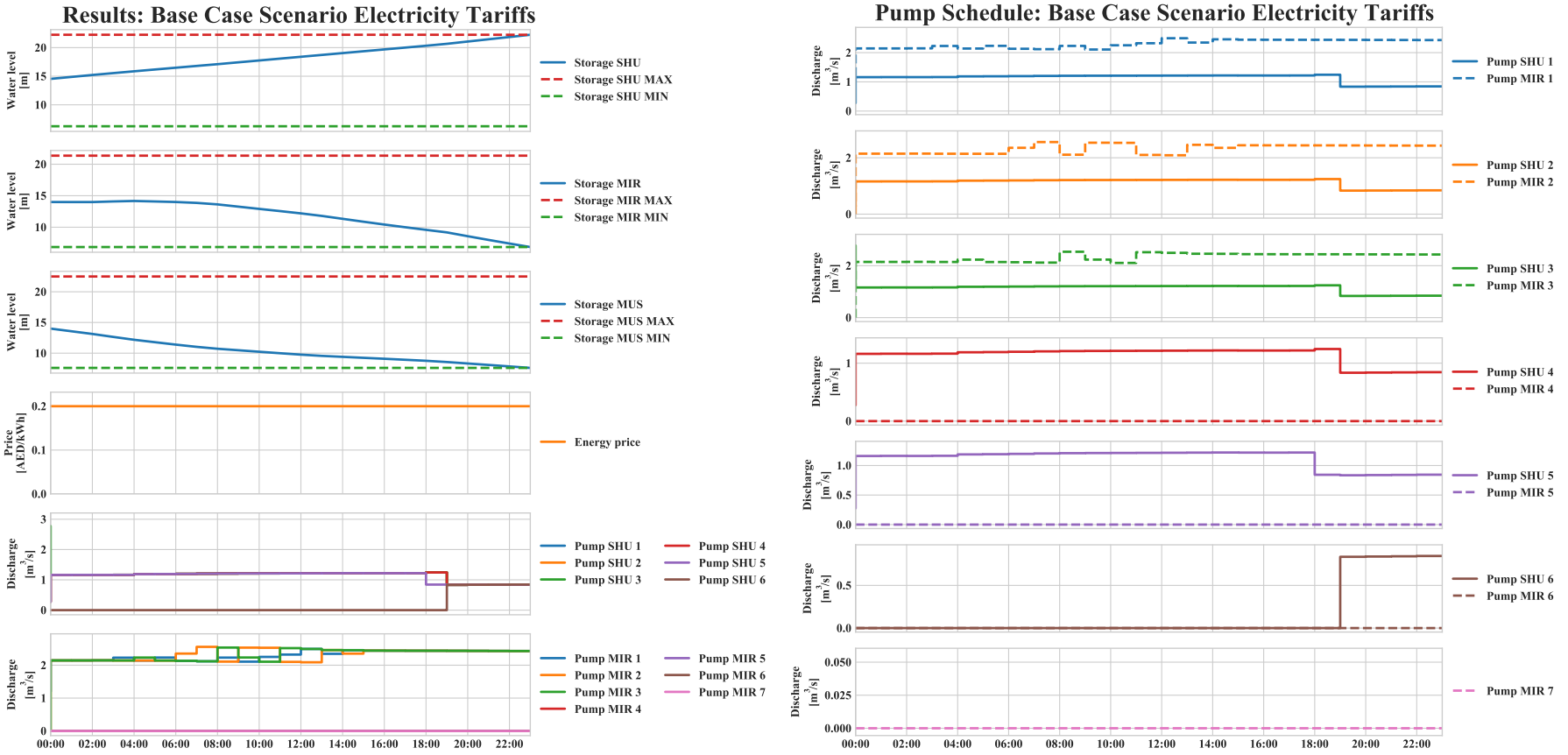

(a) Results base case scenario

(b) Pump schedule base case scenario

Figure 7.2: Results of electricity tariffs (base case scenario) on the pump schedule of the WTS of TRANSCO of July 21, 2018.

7.3. Low scenario

Figure 7.3 shows the results of scenario 1 (low) of July 21, 2018. The total power of the 24 hour profile is 342.1 MW, and with a ToU rate of 0.18 AED/kWh off-peak (10 pm - 10 am) and 0.22 AED/kWh on-peak (10 am - 10 pm), this results in a total costs of 67,688 AED. Now, more pump fluctuations occur during the day, especially at the beginning of a new electricity price. Also, the water decrease in the storage areas is faster by higher electricity tariffs, which is logical since less pumping is done in those hours.

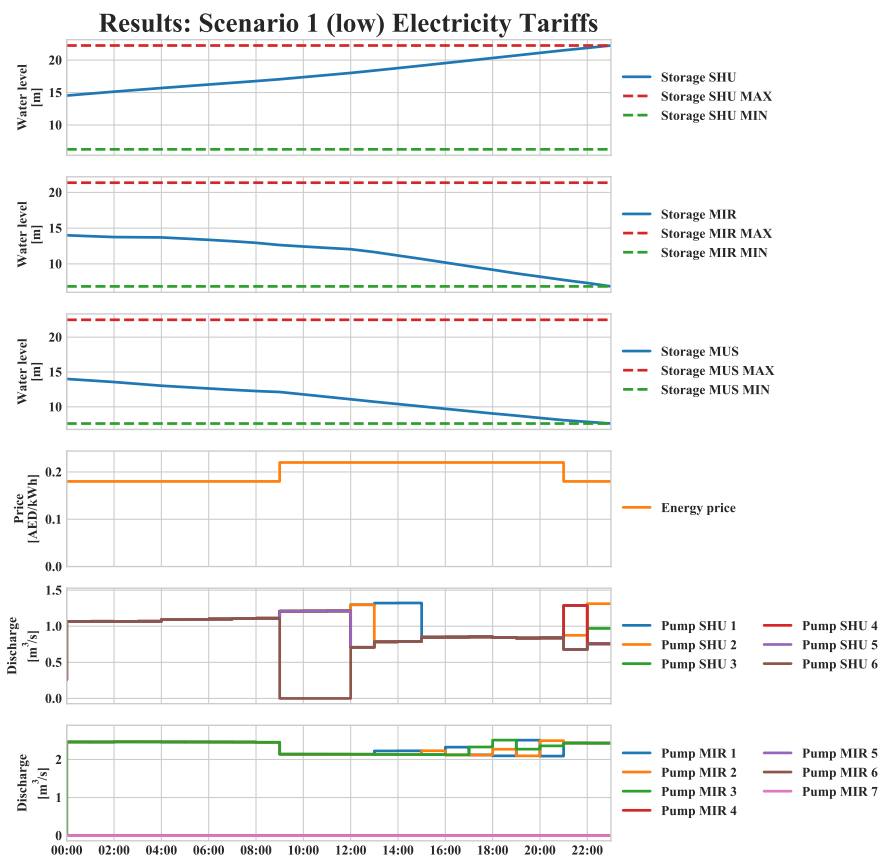

(a) Result scenario 1: low

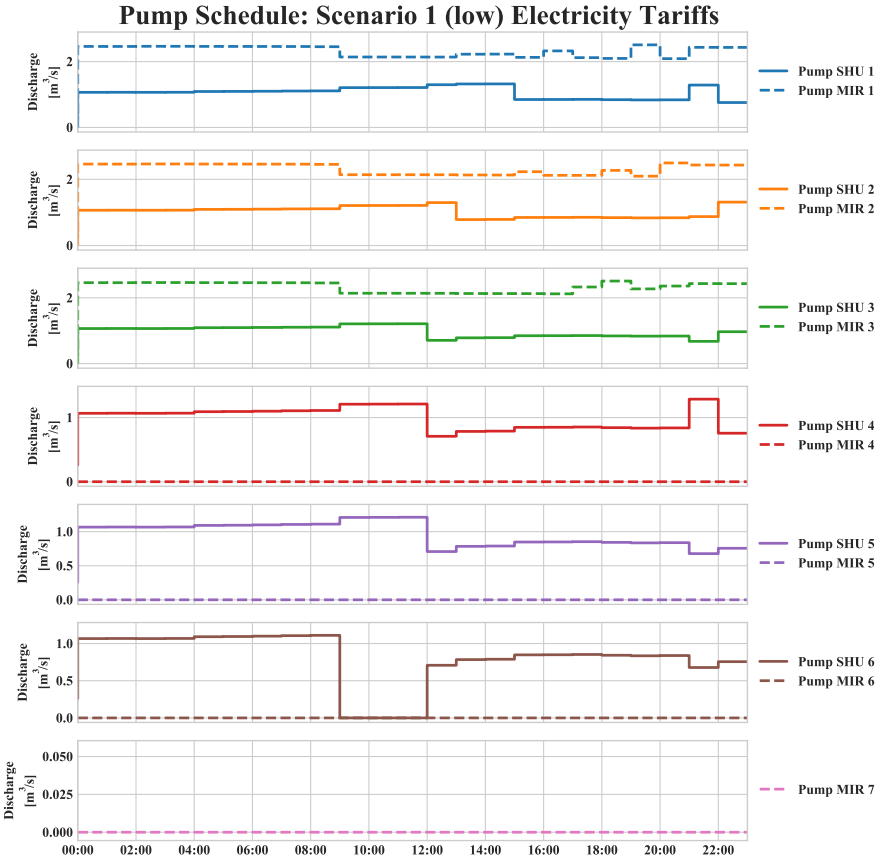

(b) Pump schedule scenario 1: low

Figure 7.3: Results of electricity tariffs (scenario 1: low) on the pump schedule of the WTS of TRANSCO of July 21, 2018.

7.4. Medium scenario

Figure 7.4 shows the results of scenario 2 (medium) of July 21, 2018. The total power of the 24 hour profile is 343.9 MW, and with a ToU rate of 0.15 AED/kWh off-peak (10 pm - 10 am) and 0.25 AED/kWh on-peak (10 am - 10 pm), this results in a total costs of 66,472 AED. This scenario acts similar to scenario 1 (low), where the storage areas faster decrease during high electricity tariffs, and where the pump capacity is higher during low electricity tariffs.

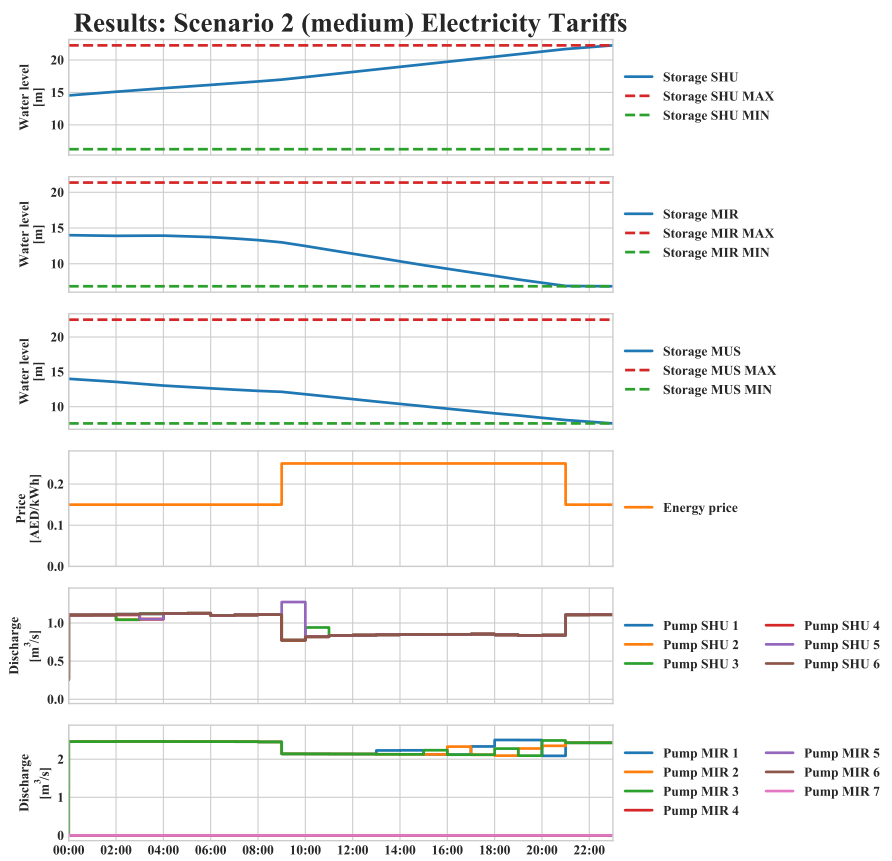

(a) Results scenario 2: medium

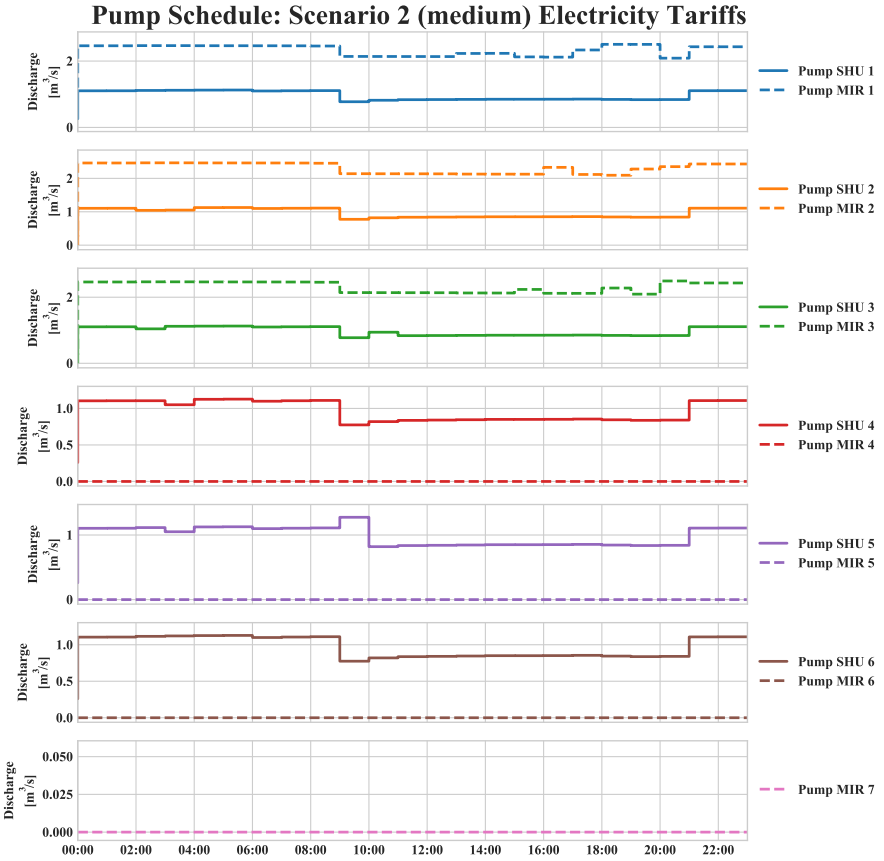

(b) Pump schedule scenario 2: medium

Figure 7.4: Results of electricity tariffs (scenario 2: medium) on the pump schedule of the WTS of TRANSCO of July 21, 2018.

7.5. Extreme scenario

Figure 7.5 shows the results of scenario 3 (extreme) of July 21, 2018. The total power of the 24 hour profile is 354.2 MW, and with a ToU rate of 0.10 AED/kWh off-peak (10 pm - 10 am) and 0.30 AED/kWh on-peak (10 am - 10 pm), this results in a total costs of 63,696 AED. This scenario, where the tariffs differ drastically between on-peak and off-peak hours, has the largest influence on the pump schedule compared to the base case scenario. During off-peak electricity tariffs, the storage area at Mirfa is filling up, followed by a large decrease during on-peak electricity tariffs. Also, less pumps are on during on-peak electricity tariffs.

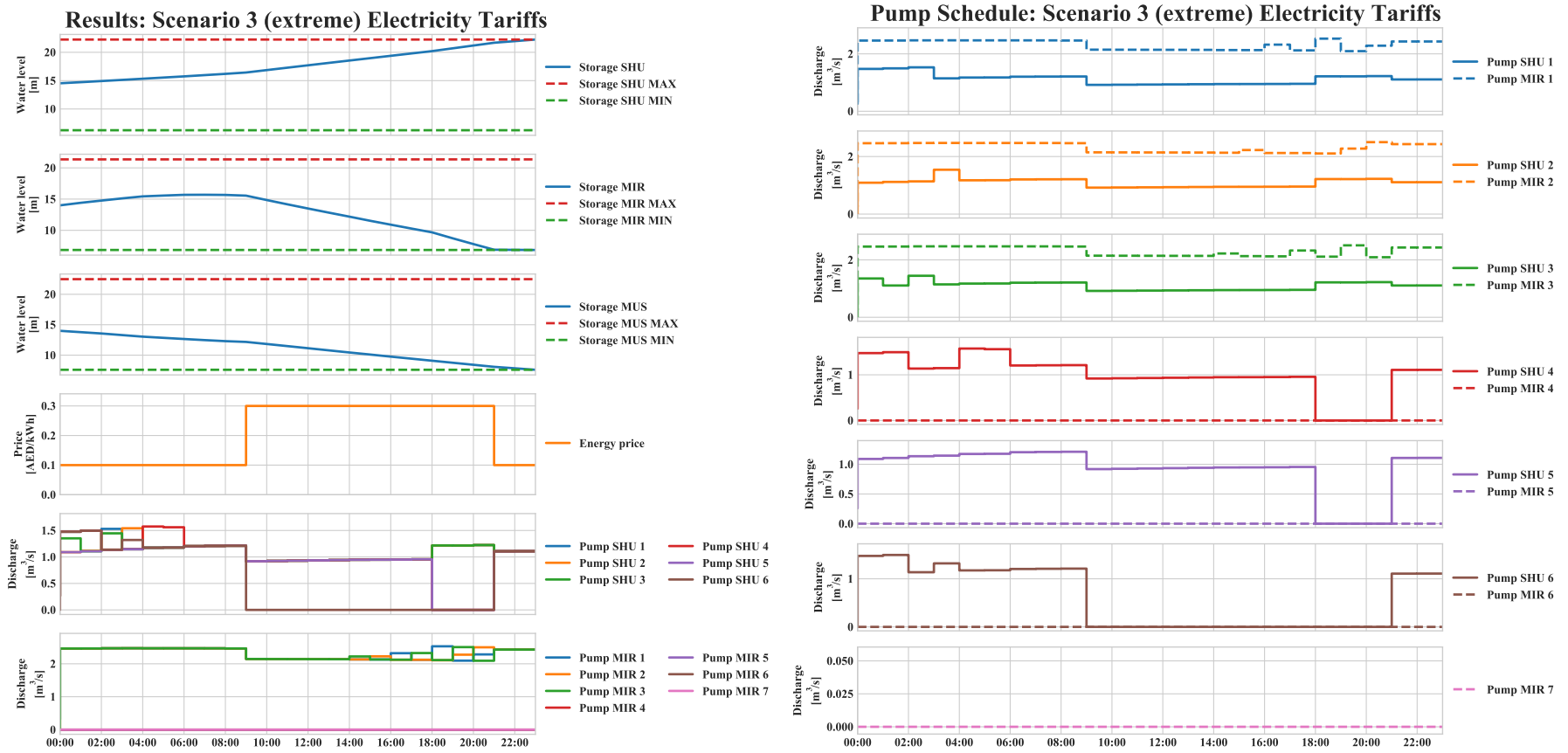

(a) Results scenario 3: extreme

(b) Pump schedule scenario 3: extreme

Figure 7.5: Results of electricity tariffs (scenario 3: extreme) on the pump schedule of the WTS of TRANSCO of July 21, 2018.

7.6. Conclusion

The effect of ToU electricity tariffs on the pump schedule of the WTS of TRANSCO for one full day (July 21, 2018) is investigated for three different scenarios compared to the base case scenario: low, medium and extreme. Figure 7.6 shows the absolute power usage and costs for the different electricity tariff scenarios compared to the base case scenario (flat rate tariff). As seen, the total costs over the whole time period reduces when taking into account ToU rates. The larger the difference between on-peak and off-peak rates, the larger the costs reduction is. When implementing scenario 1 (low), a costs savings of -0.38% is possible. For scenario 2 (medium) the savings are -2.17% and for scenario 3 (extreme) the savings are -6.26%. However, an increase in power usage is necessary to achieve this costs savings (scenario 1 (low) = 0.70%, scenario 2 (medium) = 1.21% and scenario 3 (extreme) = 4.23%). This is possibly due to the fact that during off-peak electricity tariffs, more pumps are on and they operate closer to their maximum capacity compared to on-peak electricity tariffs. This results in a higher power usage compared to the pump scheduling according to flat rates tariffs where the pumps operate more gradually during the day.

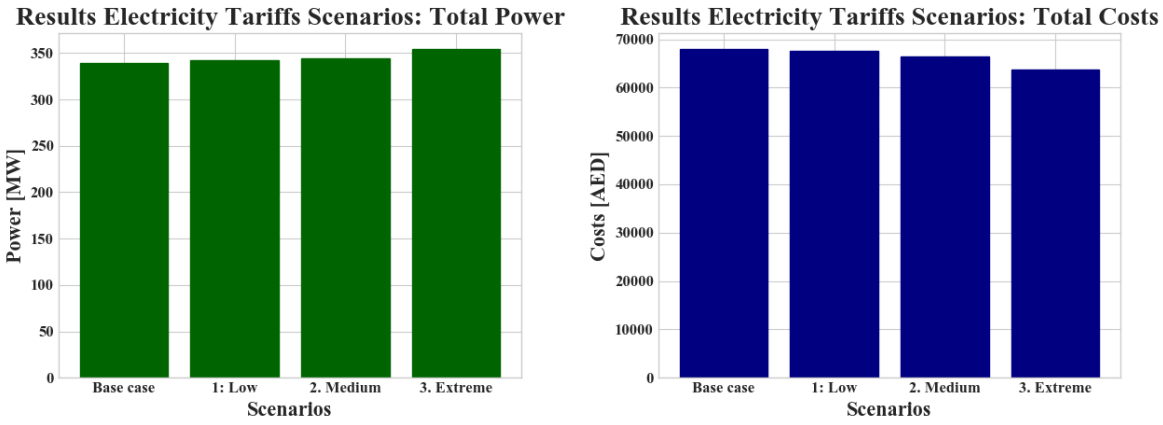

(a) Total power [MW]

(b) Total costs [AED]

Figure 7.6: Overall results of the three ToU tariffs scenarios compared to the base case scenario: total power [MW] and total costs [AED].

8

GHG emissions factors

This chapter shows the results of the effect of time-dependent versus average GHG emissions factors on the pump schedule of the WTS of TRANSCO. It first shows the different scenarios that are researched as explained in section 6.2, followed by the results of these scenarios. Section 8.5 presents the conclusion of the effect of time-dependent GHG emissions factors on the pump schedule. The start values of the storages are all defined at 14 m, which is the rounded average of the storage areas.

8.1. Overview

Figure 8.1 shows the profiles of the AV and TD GHG emissions factor over a period of 24 hours for the following three years: 2017, 2030 and 2050.

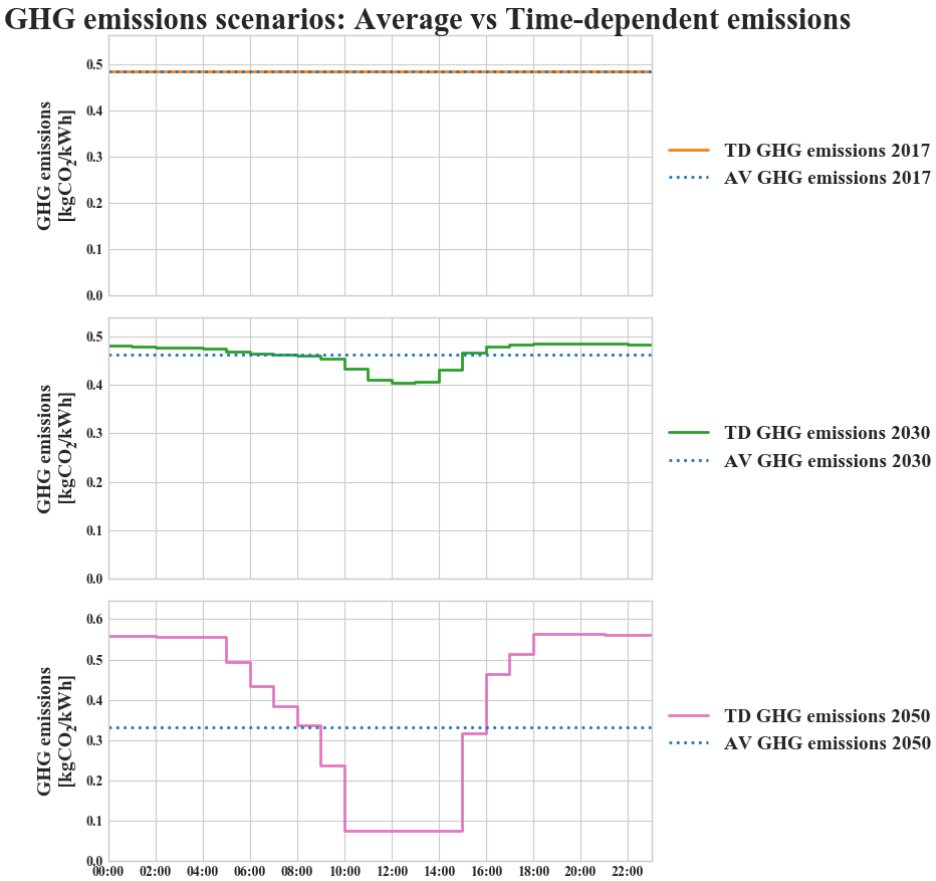

Figure 8.1: Profiles of the average and time-dependent GHG emissions factor for three years: 2017, 2030 and 2050.

8.2. Average vs time-dependent GHG emissions 2017

Figure 8.2 shows the results of the AV versus the TD GHG emissions factors of 2017. The total power for the AV and the TD GHG emissions factor is equal (339.7 MW) because there is no fluctuation in the GHG emissions factor during the day since the power mix consists mainly of natural gas (99.75%). The total emissions for both the AV and the TD factors are equal as well (169.9 t CO_2-eq). Therefore, the pump schedule for both AV and TD is the same.

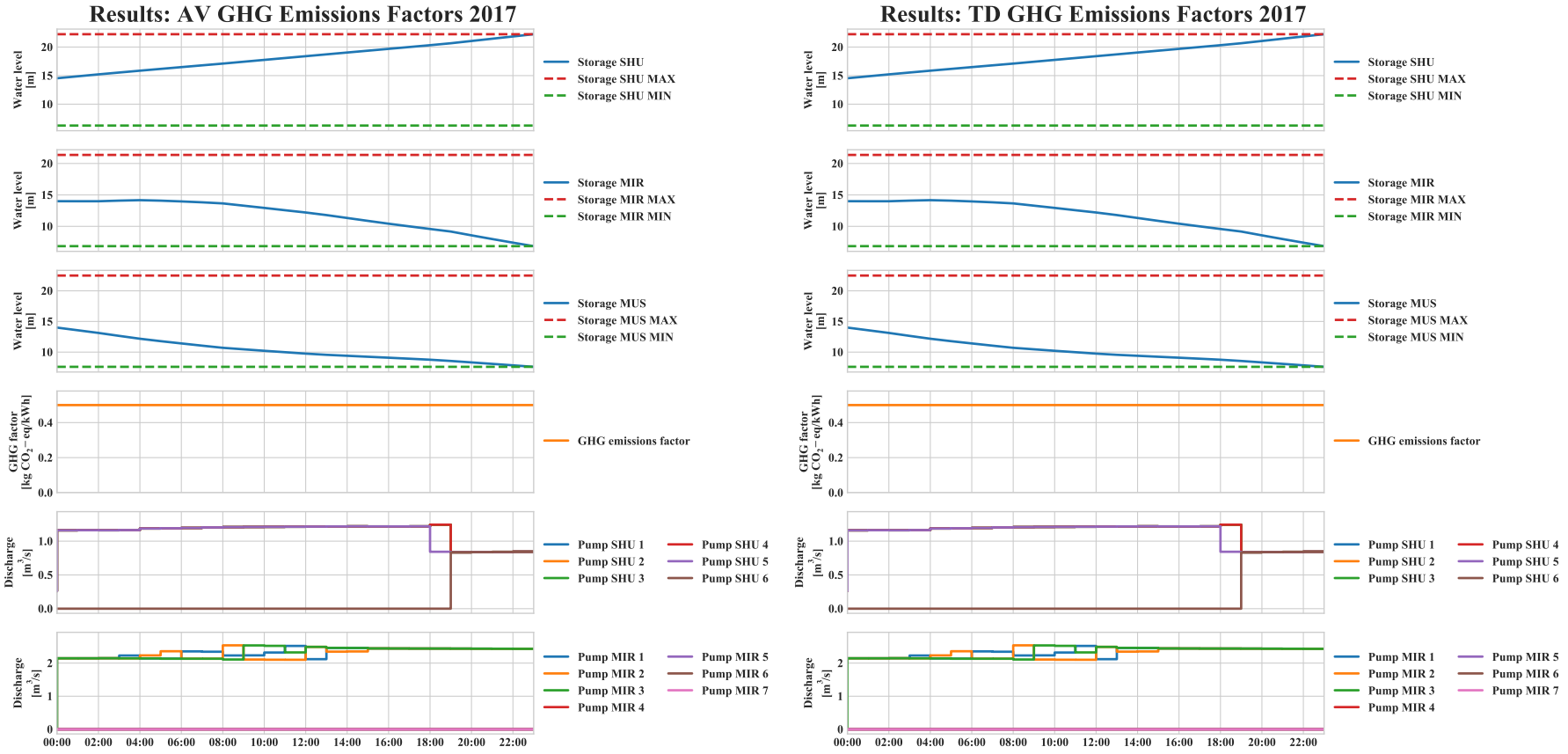

(a) AV 2017

(b) TD 2017

Figure 8.2: Results of AV vs TD GHG emissions factors on the pump schedule of the WTS of TRANSCO in 2017.

8.3. Average vs time-dependent GHG emissions 2030

Figure 8.3 shows the results of the AV versus the TD GHG emissions factors of 2030. The total power usage for the AV and the TD scenario is almost similar (339.7 MW for AV and 340.3 MW for TD). A slight decrease of GHG emissions is possible when using TD factors in 2030 (159.3 t CO_2-eq for AV compared to 158.6 t CO_2-eq for TD). As seen, all pumps at Shuweihat are on during the lowest GHG emissions factors (12:00 - 15:00). Also, the water in the storage areas is decreasing less during the hours with low factors. During hours with high factors, the water in the storage areas is used resulting in less pumping at those timesteps.

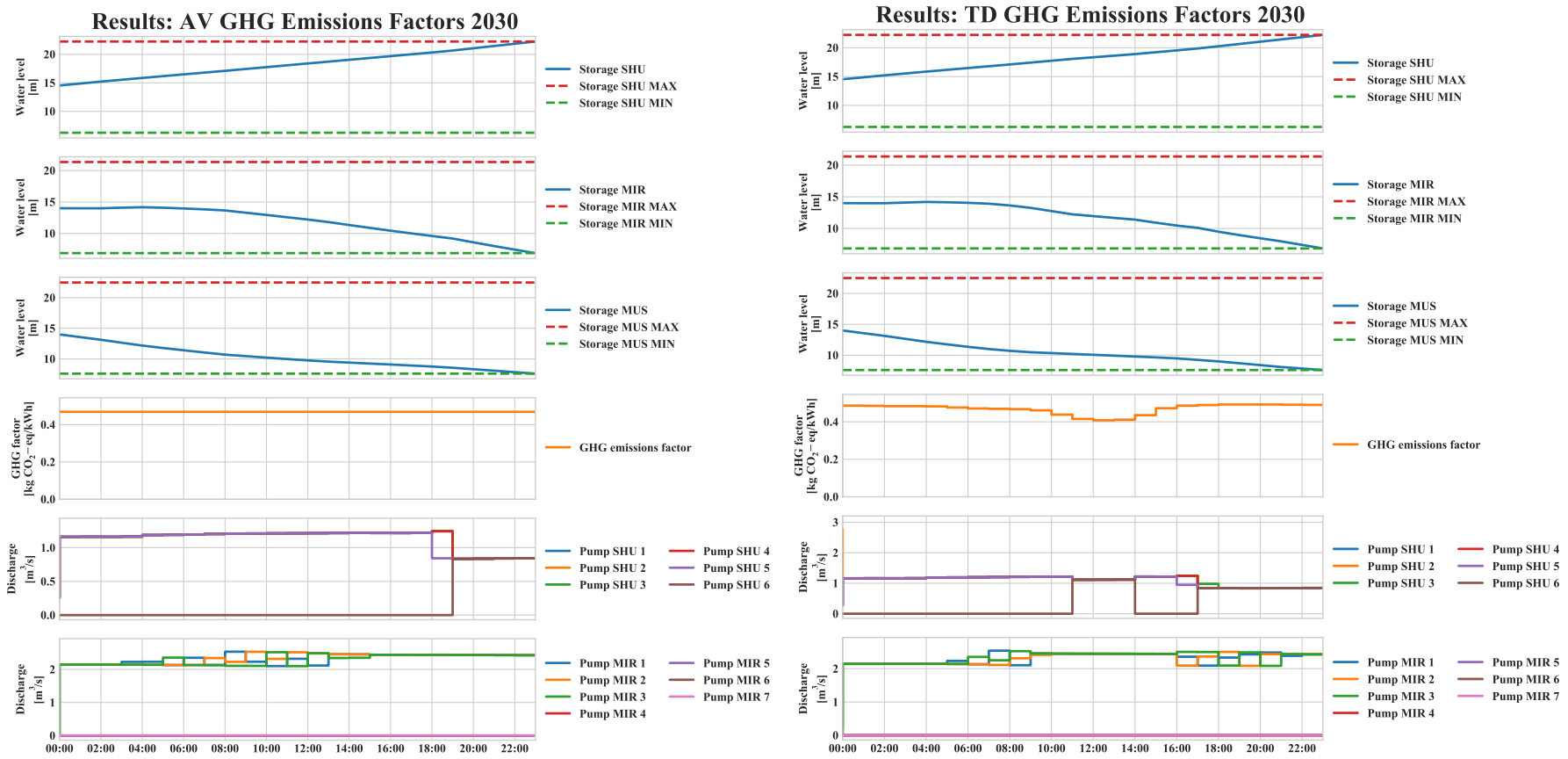

(a) AV 2030

(b) TD 2030

Figure 8.3: Results of AV vs TD GHG emissions factors on the pump schedule of the WTS of TRANSCO in 2030.

8.4. Average vs time-dependent GHG emissions 2050

Figure 8.4 shows the results of the AV versus the TD GHG emissions factors of 2050. There is an increase of power usage when using TD factors (378.5 MW compared to 339.7 MW for AV factors). A saving of 13.7 t CO_2-eq is possible when using TD factors in 2050 (137.6 t CO_2-eq for AV compared to 123.9 t CO_2-eq for TD). As seen, the storage areas of Shuweihat and Mussafah are steady during the high GHG emissions factors, the storage area in Mirfa is filling up rapidly. Also, all pumps at Shuweihat are on during the lowest GHG emissions factors.

(a) AV 2050

(b) TD 2050

Figure 8.4: Results of AV vs TD GHG emissions factors on the pump schedule of the WTS of TRANSCO in 2050.

8.5. Conclusion

The effect of time-dependent versus average GHG emissions factors on the pump schedule of the WTS of TRANSCO is investigated for three different years: 2017, 2030 and 2050. Figure 8.5 shows the absolute power usage and GHG emissions for the AV and TD scenarios for the different years. In the 2017 scenario, no savings are possible since no renewable sources are implemented and therefore, the AV and TD GHG emissions factors are equal. In the 2030 scenario, a small savings of GHG emissions is possible (-0.46%) by pumping according to TD GHG emissions factors. However, a small increase of power usage is necessary (0.16%). In the 2050 scenario, a remarkable saving of -9.99% is possible by pumping according to TD GHG emissions factors due to the low GHG emissions factors during daytime (lowest value is 0.082 kg CO_2-eq/kWh compared to the average value of 0.405 kg CO_2-eq/kWh). However, an increase in power usage (11.48%) is necessary to achieve this GHG emissions savings compared to the AV GHG emissions factors pump schedule where the pumps operate more gradually during the day. This is possibly due to the fact that during low GHG emissions factors, more pumps are on and they operate close to their maximum capacity compared to high GHG emissions factors. For example, the pumps at the Shuweihat pumping station have a discharge of around 1.0 m/s during high GHG emissions factors and a discharge of around 1.8 m/s during low GHG emissions factors, where a higher discharge results in a higher power usage as seen in Figure 4.5 in Chapter 4.

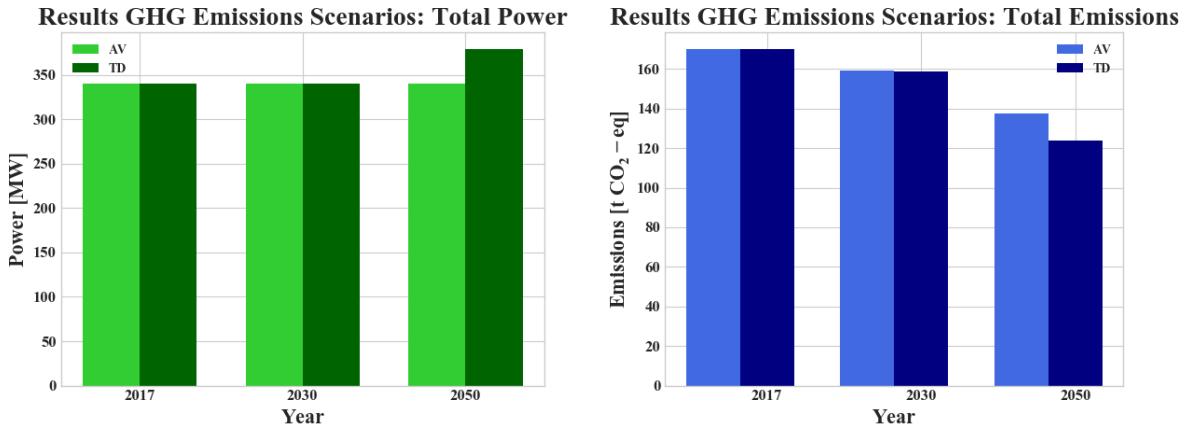

(a) Total power [MW]

(b) Total emissions [t CO_2-eq]

Figure 8.5: Overall results of average versus the time-dependent GHG emissions factors for the three different years (2017, 2030, 2050): total power [MW] and total emissions [t CO_2-eq].

9

Policy driver carbon tax

This chapter shows the results of the effect of implementing the policy driver carbon tax into the system. Here, an extra monetary cost is added on the electricity costs based on the amount of CO_2-eq emitted per timestep. For each year (2017, 2030 2050), the minimum carbon tax for shifting the pump schedule to daytime (solar availability) is investigated for each electricity tariff scenario combined with the GHG emissions factors scenarios (AV and TD). The first three sections show the results per year (sections 9.1, 9.2 & 9.3), followed by the conclusion in section 9.4.

9.1. Effect in 2017

Figure 9.1 shows the effect of including a carbon tax on the total price per timestep for the four electricity tariff scenarios in the year 2017. In this year, implementing a carbon tax has no influence on the pump schedule since no renewable sources are included in the system. The only change the system experiences is the fact that a higher price must be paid to pump at each timestep compared to the situation where no carbon taxes are included. Thus, the total price during daytime is always higher than the total price during nighttime, since the on-peak electricity hours are during daytime (10 am - 10 pm). This counts however only for the three ToU electricity tariff scenarios. For the base case scenario, which has a flat rate tariff of 0.20 AED/kWh, there is no total price fluctuation during the day. Thus, adding a carbon tax in the year 2017 has no influence on the pumping hours. The only effect is the higher price that must be paid, where the increase in price is equal at every timestep as seen in Figure 9.1.

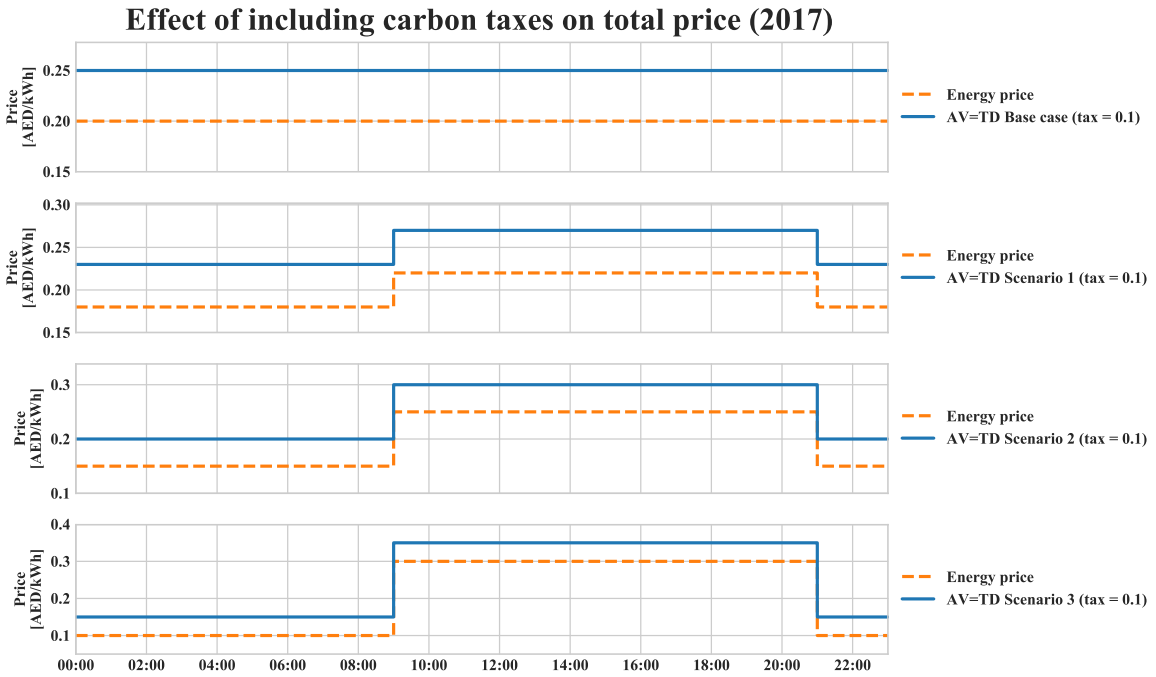

Figure 9.1: The effect of including a carbon tax on the total price per timestep in 2017.

Figure 9.2 shows the absolute power usage and costs for the AV and TD GHG emissions scenarios together with the four electricity tariff scenarios in 2017. As seen, there is no difference in costs and power usage between the AV and TD scenarios since yet no renewable sources are included. When compared with the original power usage and costs (no carbon tax included, see Figure 7.6), the power usage stays equal. The total costs however increases due to the higher total price that must be paid. When adding a carbon tax of 0.1 AED/kg CO_2-eq into the system in 2017, the total costs increases between 25.05% and 27.51%. Note that the carbon tax of 0.1 AED/kg CO_2-eq is only chosen as an illustration. Since including a carbon tax in 2017 has no influence on the pumping schedule, even a small carbon tax of 0.01 AED/kg CO_2-eq automatically results in higher total costs.

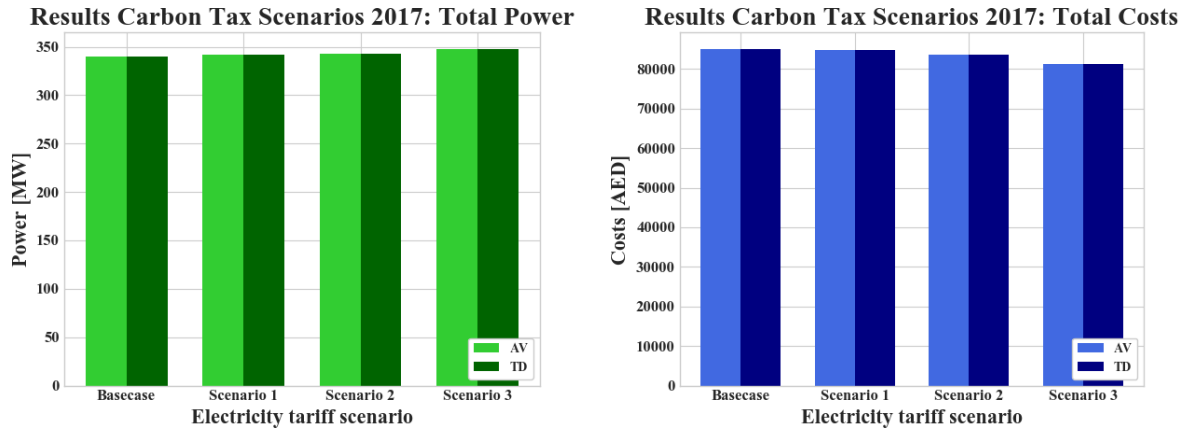

(a) Total power [MW]

(b) Total costs [AED]

Figure 9.2: Overall results of average versus time-dependent GHG emissions factors together with the four electricity tariff scenarios in 2017: total power [MW] and total costs [AED].

9.2. Effect in 2030

Figure 9.3 shows the effect of including a carbon tax on the total price per timestep for the four electricity tariff scenarios in the year 2030. In this year, there is a fluctuation of GHG emissions factors during the day due to the implementation of renewable sources. Therefore, implementing carbon taxes will eventually shift the pump schedule to daytime. However, since the implementation of renewable sources is limited in 2030 (5% solar), high carbon taxes are necessary to provide this shift to day pumping. For the base case electricity scenario, a minimum carbon tax of 0.3 AED/kg CO_2-eq is needed to switch to day pumping. Day pumping is here defined as 9 am till 4 pm. Those are also the hours the TD factors are lower than the AV factors, as seen in Figure 6.6. For electricity tariff scenario 1, which has a small variation between on-peak and off-peak tariffs (0.04 AED/kWh), a minimum carbon tax of 0.9 AED/kg CO_2-eq is needed. For electricity tariff scenarios 2 and 3, where the on-peak and off-peak tariff variation keeps increasing (0.10 AED/kWh and 0.20 AED/kWh), the minimum carbon taxes to shift to day pumping are 2.1 AED/kg CO_2-eq and 3.5 AED/kg CO_2-eq respectively. However, for all three scenarios, the hours with the lowest costs are only between 12 pm and 3 pm. Therefore, by including those carbon taxes, only three hours are optimal to pump. To pump during the full optimal hours (TD < AV GHG emissions factors, which is between 9 am and 4 pm), even higher carbon taxes are necessary (1.3 AED/kg CO_2-eq, 3.2 AED/kg CO_2-eq and 6.4 AED/kg CO_2-eq for scenarios 1, 2 and 3 respectively). Compared to the electricity prices (range between 0.1 and 0.3 AED/kWh), the carbon taxes are disproportional high. For example, the total price per timestep for the electricity tariff scenario 3 (extreme) will be between 2.91 and 3.45 AED/kWh when including a carbon tax of 6.4 AED/kg CO_2-eq.

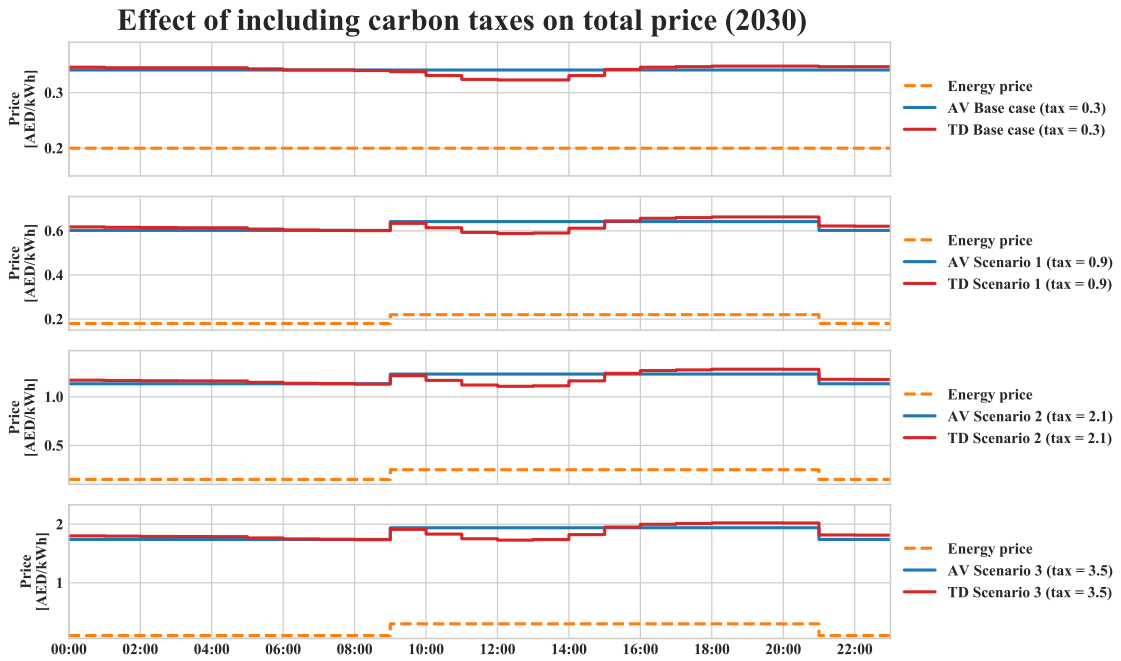

Figure 9.3: The effect of including a carbon tax on the total price per timestep in 2030.

Figure 9.4 shows the absolute power usage and costs for the AV and TD GHG emissions scenarios together with the four electricity tariff scenarios in 2030. As seen, there is only a small variation between the AV and TD scenarios for the total power usage (between -0.06% and 0.04%) and total costs (between -0.45% and -0.58%). Also, including carbon taxes has only a small effect on the total power usage compared to the situation with no carbon taxes (between -3.62% and 0.05%). However, including carbon taxes has a remarkable effect on the total costs compared with the total costs without carbon taxes as shown in Figure 7.6. The base case electricity scenario experiences an increase of 70.59% (AV) and 70.14% (TD). For electricity tariff scenario 1, an increase of 212.93% (AV) and 212.26% (TD) is necessary to shift the pumping to daytime. For scenario 2 this increase rises to 506.14% (AV) and 505.08% (TD) and for scenario 3 to 882.14% (AV) and 880.99% (TD). The results illustrate that how larger the difference is between the ToU rates, more money must be paid for CO_2 emissions to pump during daytime. Since the on-peak (daytime) rates are increasing with the scenarios, the ToU rates during daytime are only more dominating which shifts the pumping automatically to nighttime. Only a really high carbon tax will therefore have an impact, since the implementation of renewable sources in 2030 is still limited (5% solar).

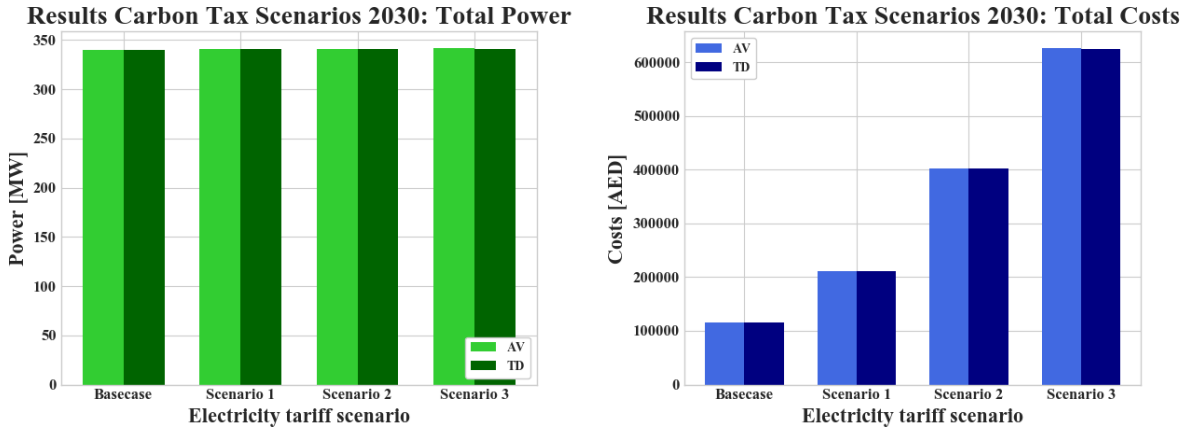

(a) Total power [MW]

(b) Total costs [AED]

Figure 9.4: Overall results of average versus time-dependent GHG emissions factors together with the four electricity tariff scenarios in 2030: total power [MW] and total costs [AED].

9.3. Effect in 2050

Figure 9.5 shows the effect of including a carbon tax on the total price per timestep for the four electricity tariff scenarios in the year 2050. In this year, there is a large fluctuation of GHG emissions during the day due to the implementation of renewable sources (44% solar power). Therefore, implementing carbon taxes will shift the pump schedule to daytime, especially during the hours with the highest solar intensities. For the base case electricity scenario, a small carbon tax of 0.1 AED/kg CO_2-eq is needed to shift to day pumping. Day pumping is for this scenario defined as 8 am till 5 pm. Those are also the hours the TD factors are lower than the AV factors, as seen in Figure 6.6. For the three ToU scenarios, the carbon taxes must increase to ensure that the shift to day pumping will occur. The minimum carbon taxes are 0.2 AED/kg CO_2-eq, 0.3 AED/kg CO_2-eq and 0.5 AED/kg CO_2-eq for scenarios 1, 2 and 3 respectively. The hours with the lowest total costs are between 8 am and 4 pm. Therefore, by including those carbon taxes, only eight hours are optimal to pump instead of the nine hours where the TD factors are lower than the AV factors. Comparing the taxes to shift to day pumping in 2050 with 2030, the taxes are more affordable due to the higher implementation of renewable sources.

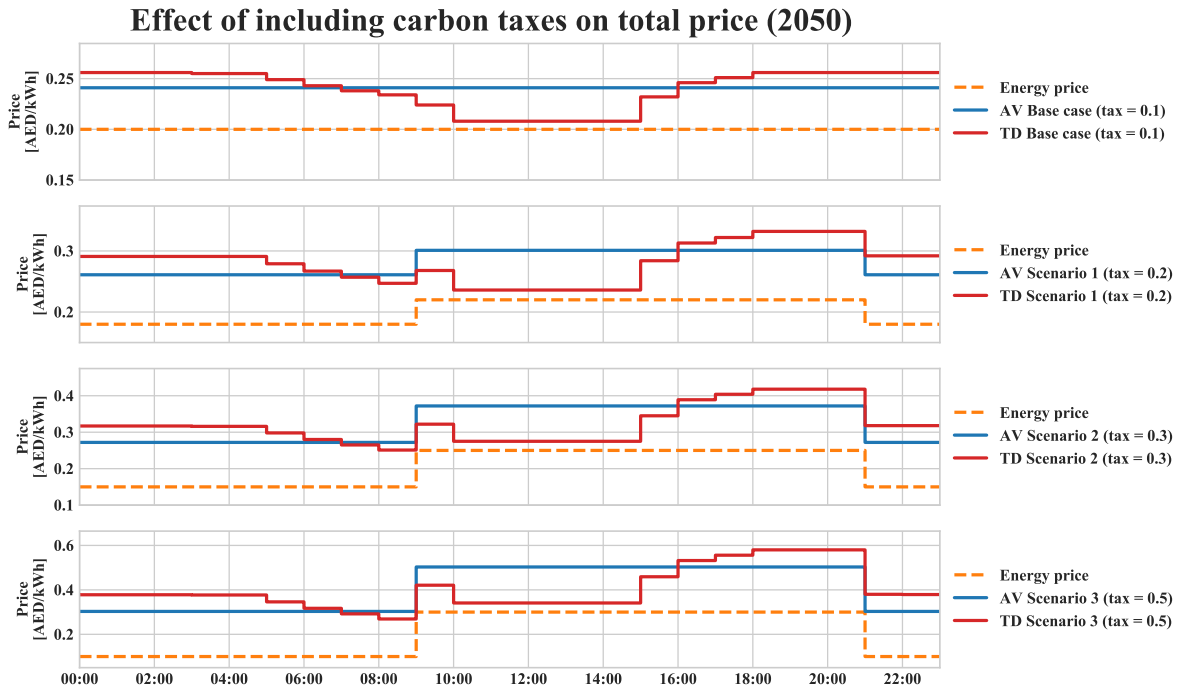

Figure 9.5: The effect of including a carbon tax on the total price per timestep in 2050.

Figure 9.6 shows the absolute power usage and costs for the AV and TD GHG emissions scenarios together with the four electricity tariff scenarios in 2050. As seen, there is a small variation between the AV and TD scenarios for the total power usage (between -0.19% and 0.41%) and total costs (between -1.23% and -0.78%). Also, including carbon taxes has only a small effect on the total power usage compared to the situation with no carbon taxes (between -2.93% and 0.25%). However, including carbon taxes has a remarkable effect on the total costs compared to the total costs without carbon taxes as shown in Figure 7.6. The base case electricity scenario experiences an increase of 20.52% (AV) and 19.13% (TD). For electricity tariff scenario 1, an increase of 40.95% (AV) and 39.21% (TD) is necessary to shift the pumping to daytime. For scenario 2 this increase rises to 62.91% (AV) and 61.64% (TD) and for scenario 3 to 110.33% (AV) and 108.69% (TD). Also for 2050 the results illustrate that how larger the difference is between the ToU rates, more costs must be paid to pump during daytime due to the dominating on-peak electricity hours. However, compared to the situation in 2030, the extra costs are lower due to the higher implementation of renewable sources (44% solar).

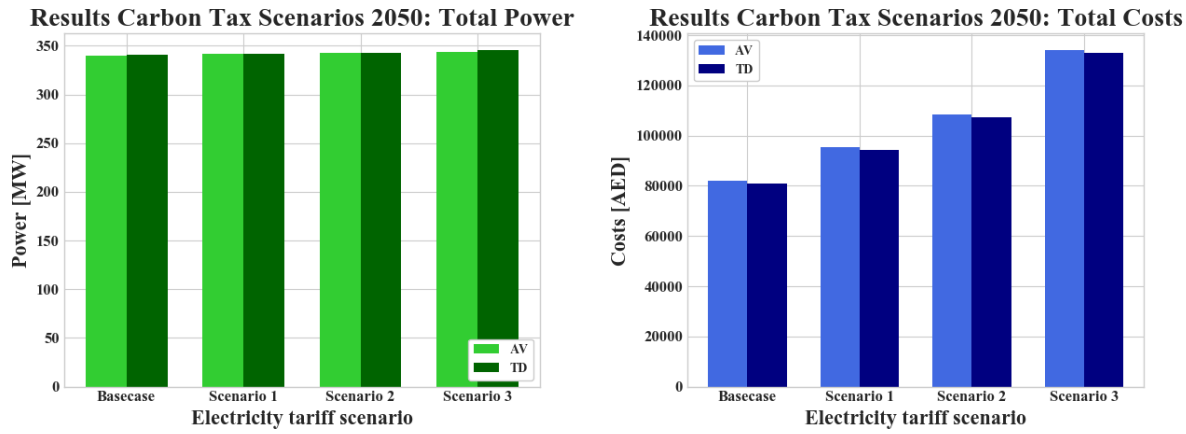

(a) Total power [MW]

(b) Total costs [AED]

Figure 9.6: Overall results of average versus time-dependent GHG emissions factors together with the four electricity tariff scenarios in 2050: total power [MW] and total costs [AED].

9.4. Conclusion

This chapter showed the results of the effect of implementing the policy driver carbon tax into the system and explained which carbon taxes are necessary per year and per electricity tariff scenario to make the shift to day pumping. The carbon taxes explained in sections 9.1, 9.2 and 9.3 are the minimum carbon taxes needed to shift to day pumping. That means that with those carbon taxes, around the same GHG emissions reductions are made as the GHG emissions scenarios in Chapter 8 when there was no influence of prices. In 2017, implementing carbon taxes has no influence on the pump schedule since no renewable sources are included. The only effect is the higher price that must be paid compared with no carbon taxes. In 2030 and 2050, when there are fluctuations of GHG emissions factors during the day, implementing carbon taxes will eventually shift the pump schedule to daytime. However, high carbon taxes are necessary which results in disproportionately extra total costs. This counts especially for 2030 when the implementation of renewable sources is still limited. The results also show that how larger the difference is between the ToU rates, more costs must be paid to pump during daytime due to the increasing dominant on-peak rate. Table 9.1 shows a summary of the minimum carbon taxes needed to shift to day pumping per year per electricity tariff scenario.

Table 9.1: Minimum carbon tax needed to shift to day pumping per year per electricity tariff scenario.

Year	Base case	Scenario 1	Scenario 2	Scenario 3	Unit
2017	0.1	0.1	0.1	0.1	AED/kg CO_2-eq
2030	0.3	0.9	2.1	3.5	AED/kg CO_2-eq
2050	0.1	0.2	0.3	0.5	AED/kg CO_2-eq

10 Infrastructure influence

This chapter shows the results of the effect of the infrastructure components of the WTS of TRANSCO on the pump schedule and thus on the corresponding costs, GHG emissions and power usage. The parameters that are investigated are the storage area sizes and the pipeline sizes. The results are investigated for all four electricity tariff scenarios and for AV and TD GHG emissions factors scenarios for the three different years, resulting in exactly 100 runs. The start values of the storages are all defined at 14 m, which is the rounded average of the storage areas.

10.1. Storage area sizes

By changing the storage area sizes, more water can be stored during the same time period. Each of the storage areas is increased with 10% and 20%. Section 10.1.1 shows the results of the increase of the storage areas on the total costs and power of the system. Section 10.1.2 shows the results of the increase of the storage areas on the total emissions and power of the system.

10.1.1. Electricity tariffs

Figure 10.1 shows the results of the increased storage area sizes on the total costs and power of the system for all the electricity scenarios. As seen, increasing the Shuweihat storage area has a small effect on the total costs and power usage (costs savings of -0.06% up till -0.25% and power savings of -0.06% up till -0.37% compared to original storage area sizes). The same count for the storage area at Mirfa, although the savings are a bit higher (costs savings of -0.68% up till -1.46% and power savings of -0.63% up till -1.63% compared to original storage area sizes). Increasing the storage area at Mussafah on the other hand results in remarkable costs savings of -4.45% up till -11.22% and power savings of -4.28% up till -8.92% compared to original storage area sizes. Table D.1 in Appendix D shows the exact costs and power savings by increasing the different storage area sizes with 10% and 20%.

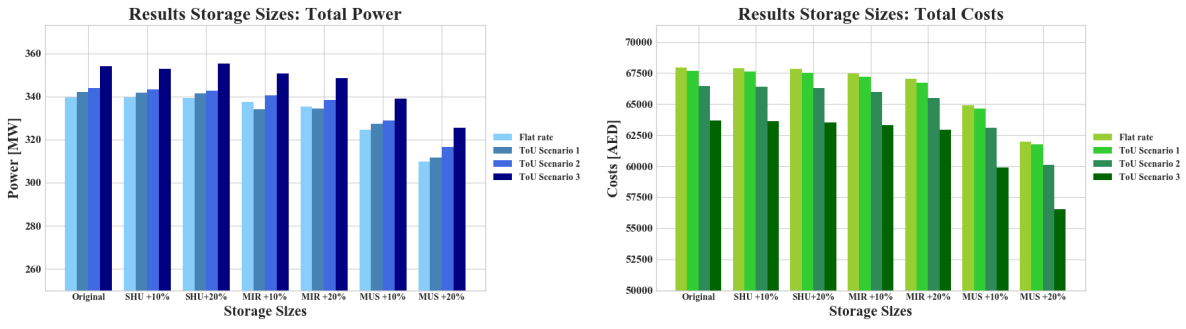

(a) Total power [MW]

(b) Total costs [AED]

Figure 10.1: Effect of increased storage areas sizes on the power [MW] and costs [AED] of the system.

10.1.2. GHG emissions factors

Figure 10.2 shows the results of the increased storage area sizes on the total GHG emissions and power of the system. The different color bars represent the different investigated scenario years (red = 2017, green =

2030 and blue = 2050). The differences between the years are large due to the implementation of renewable sources into the future and therefore lower GHG emissions, as explained in Chapter 8. However, the calculated changes are compared to the original storage sizes of the specific year. Results and conclusions about the GHG emissions savings and power usage between the different years due to the implementation of renewable sources (for example why so much power is required for the TD scenario for 2050) are found in Chapter 8.

Increasing the Shuweihat storage area sizes had a small effect on the total GHG emissions and power usage of the system (GHG emissions savings of -0.07% up till -0.21% and power savings of 0.95% (extra power usage) up till -0.20% compared to the original storage area sizes). Changing the storage area sizes at Mirfa also has a small effect on the system (GHG emissions savings of -0.68% up till -1.37% and power savings of -0.08% up till -0.20% compared to the original storage area sizes). Increasing the storage area sizes at Mussafah has a larger effect, where GHG emissions savings can be made of -2.49% up till -10.79% and power savings of -3.43% up till -8.81%. Table D.2 in Appendix D shows the exact GHG emissions and power savings by increasing the different storage area sizes with 10% and 20%.

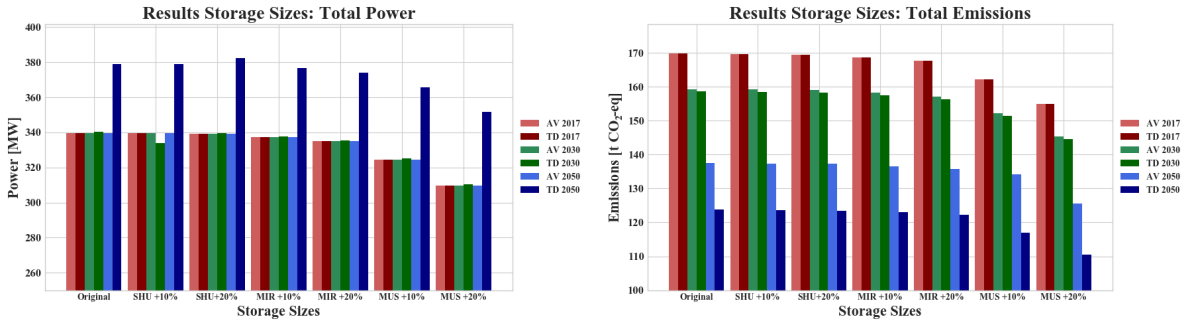

(a) Total power [MW]

(b) Total emissions [t CO_2-eq]

Figure 10.2: Effect of increased storage areas sizes on the total power [MW] and GHG emissions [t CO_2-eq] of the system.

10.2. Pipelines sizes

By changing the pipeline sizes, more water can flow through the system during the same time period. Each of the pipelines is increased with 10% and 20%. Section 10.2.1 shows the results of the increase of the pipelines on the total costs and power of the system. Section 10.2.2 shows the results of the increase of the pipelines on the total emissions and power of the system.

10.2.1. Electricity tariffs

Figure 10.3 shows the results of the increased pipe sizes on the total costs and power of the system for all the electricity scenarios. As seen, increasing the Shuweihat - Mirfa pipeline has an effect on the total costs and power savings compared to the original pipe size (cost savings of -3.07% up till -5.73% and power savings of -0.21% up till -4.69%). However, increasing the Mirfa - Mussafah pipeline has a larger effect. Here, cost savings can be made of -11.57% up till -23.02% and power savings can be made of -10.06% up till -18.38%. Table D.3 in Appendix D shows the exact costs and power savings by increasing the different pipe sizes with 10% and 20%.

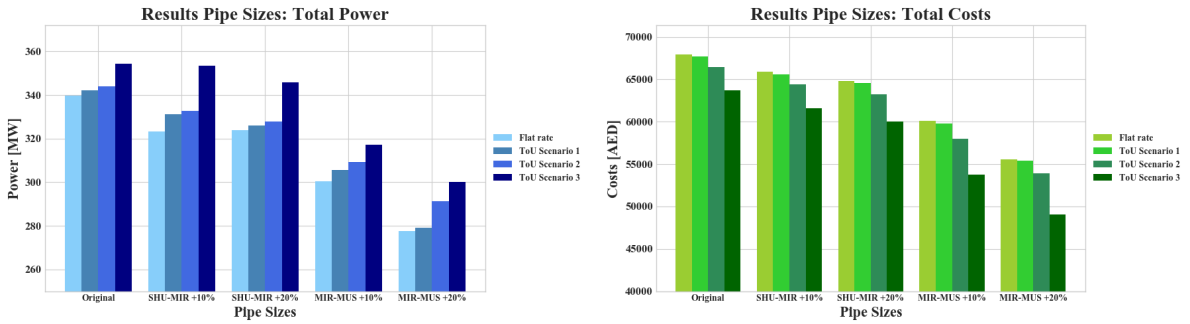

(a) Total power [MW]

(b) Total costs [AED]

Figure 10.3: Effect of increased pipe areas sizes on the total power [MW] and costs [AED] of the system.

10.2.2. GHG emissions factors

Figure 10.4 shows the results of the increased pipe sizes on the total GHG emissions and power of the system. Also here, the different color bars represent the different investigated scenarios years (red = 2017, green = 2030 and blue = 2050). The bars show the differences in GHG emissions and power usage between the years due to the implementation of renewable sources (see Chapter 8 for those results). In this section, the results of the calculated changes of increasing the pipe sizes compared to the original pipe sizes of the specific year are shown. Increasing the Shuweihat - Mirfa pipeline has an effect on the total GHG emissions and power savings compared to the original pipe sizes (GHG emissions savings of -2.96% up to -5.29% and power savings of 0.02% (increase of power usage) up till -4.72%). However, increasing the Mirfa - Mussafah pipeline has a larger effect. Here, GHG emissions savings can be made of -11.57% up till -23.17%. Power savings can be made of -9.22% up till -18.28%. Table D.4 in Appendix D shows the exact costs and power savings by increasing the different pipe sizes with 10% and 20%.

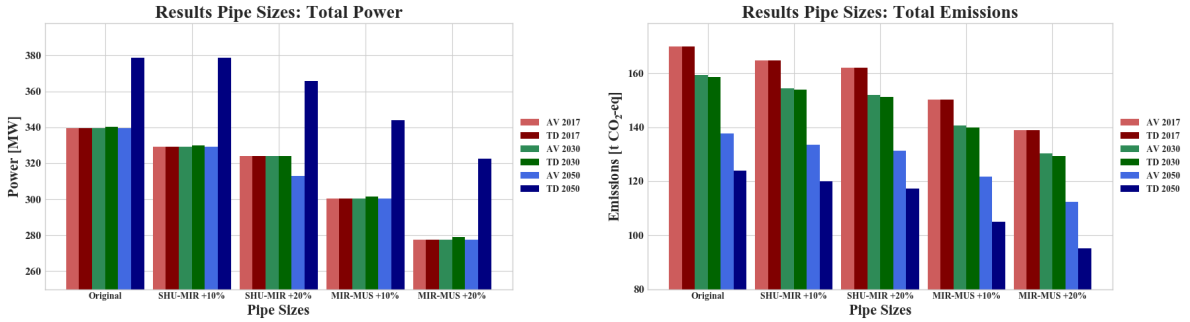

(a) Total power [MW]

(b) Total emissions [t CO_2-eq]

Figure 10.4: Effect of increased pipe areas sizes on the total power [MW] and GHG emissions [t CO_2-eq] of the system.

10.3. Conclusion

This chapter showed the results of the effect of the infrastructure components of the WTS of TRANSCO on the pump schedule and the corresponding costs, GHG emissions and power usage. Two infrastructure components are researched: increasing the storage area sizes and increasing the pipeline sizes. Increasing the storage area sizes and pipeline sizes both results in total costs and GHG emissions savings. First, more savings are possible by increasing the pipe sizes compared to the storage sizes, meaning that increasing the amount of water flowing through the system has a larger effect on the system than increasing the water storage sizes over the same time period. Second, more savings are possible at the end of the system (storage area Mussafah, pipeline between Mirfa and Mussafah). This is possibly due to the fact that the demand of water at the end of the system is the highest (largest flow of water coming from Shuweihat flows further towards Abu Dhabi and has much higher flow rates than the intermediate demand nodes) resulting in the largest influence on the system.

11

Sensitivity analysis

This chapter shows the results of the sensitivity analysis. Two uncertain parameters are tested, which are 1) the GHG emissions intensities (section 11.1) and 2) the speed of the water flow (section 11.2). The GHG emissions intensities parameter is tested for the average and time-dependent GHG emissions factors scenarios for the three different years. The speed of the water flow parameter is tested for the four electricity tariff scenarios. Together this results in twenty runs. The start values of the storages are all defined at 14 m, which is the rounded average of the storage areas.

11.1. GHG emissions intensities

The GHG emissions intensities per power source used in this research are the mean values of a compilation of multiple sources. Lower and higher emissions intensities are also possible due to for example the calculation approach. Section 11.1.1 shows the effect of the use of lower emissions intensities on the total emissions and power of the system. Section 11.1.2 shows the effect of the use of higher emissions intensities on the total emissions and power of the system.

11.1.1. Low emissions intensities

Figure 11.1 shows the results of the use of low emissions intensities on the total emissions and power of the system for the AV and TD GHG emissions factor scenarios of the three different years. In the 2017 scenario, no savings are possible when using time-dependent GHG emissions factors since no renewable source are implemented. In the 2030 scenario, a small savings of GHG emissions is possible (-0.56%). However, a small increase of power usage is necessary to achieve this (0.15%). In the 2050 scenario, a remarkable savings of -15.95% is possible by pumping according to TD GHG emissions factors due to the low GHG emissions factor during daytime (lowest value is 0.012 kg CO_2-eq/kWh compared to the average value of 0.295 kg CO_2-eq/kWh). However, an increase in power usage (20.19%) is necessary to achieve this GHG emissions savings.

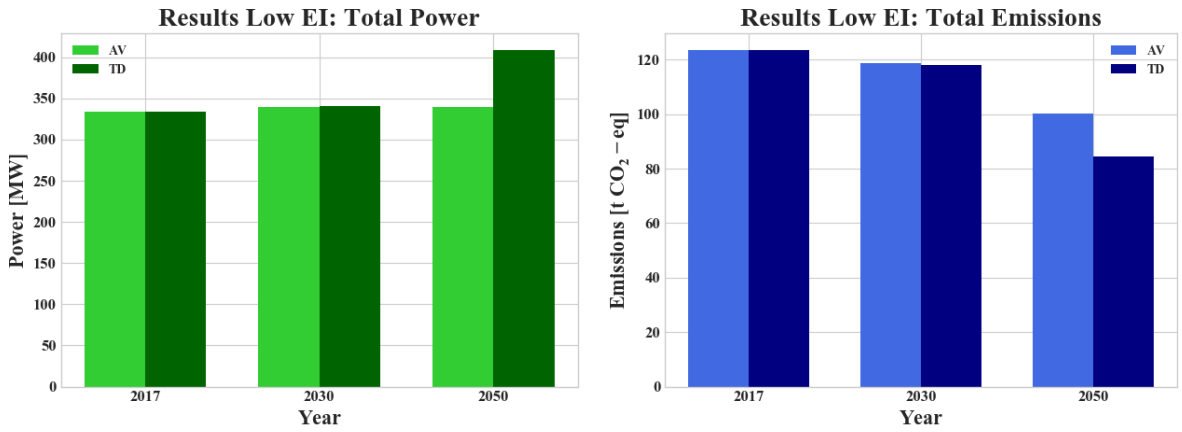

(a) Total power [MW]

(b) Total emissions [t CO_2-eq]

Figure 11.1: Results of using low emissions intensities for the average versus time-dependent GHG emissions factors for the three different years on the total power [MW] and GHG emissions [t CO_2-eq] of the system.

When comparing the results of the low emissions intensities with the original (mean) emissions intensities (Figure 8.5), GHG emissions savings between -25.63% and -31.97% are possible. Those savings are logic since lower GHG emissions factors per timestep are used when using lower emissions intensities. However, to test the robustness of the parameter, the increase/decrease in percentage between the AV and TD results are analysed. For the year 2017, applying a lower emissions intensity has no effect on the total power usage and emissions since no renewable sources are included and so the AV and TD results are equal. For the year 2030, applying a lower emissions intensity has no significant impact on the total power usage (mean EI: 0.15% and low EI: 0.16%) and emissions (mean EI: -0.46% and low EI: -0.56%) when switching to TD GHG emissions factors compared to the original emissions intensities values. For the year 2050, using low emissions intensities has a significant impact on the total power usage and emissions when switching to TD GHG emissions factors compared to the original emissions intensities values. A GHG emissions savings of 15.95% is possible when using low emissions intensities compared to the 9.99% savings when using the original emission intensities. Also a higher power usage is necessary to achieve this (20.19% for low EI compared to 11.48% for original EI). This is possibly due do the fact that when using low emissions intensities, the hours during day time (solar availability) have GHG emissions factors of almost zero (0.012 kg CO_2-eq/kWh), resulting in the fact that the pumps are even more triggered to work at maximum capacity and so more emissions savings are possible.

11.1.2. High emissions intensities

Figure 11.2 shows the results of the use of high emissions intensities on the total emissions and power of the system for the AV and TD GHG emissions factor scenarios of the three different years. In the 2017 scenario, no savings are possible when using time-dependent GHG emissions factors since no renewable source are implemented. In the 2030 scenario, a small savings of GHG emissions is possible (-0.38%). However, a small increase of power usage is necessary to achieve this (0.16%). In the 2050 scenario, a remarkable savings of -9.11% is possible by pumping according to TD GHG emissions factors due to the low GHG emissions factor during daytime (lowest value is 0.168 kg CO_2-eq/kWh compared to the average value of 0.692 kg CO_2-eq/kWh). However, an increase of power usage (9.10%) is necessary to achieve this GHG emissions savings.

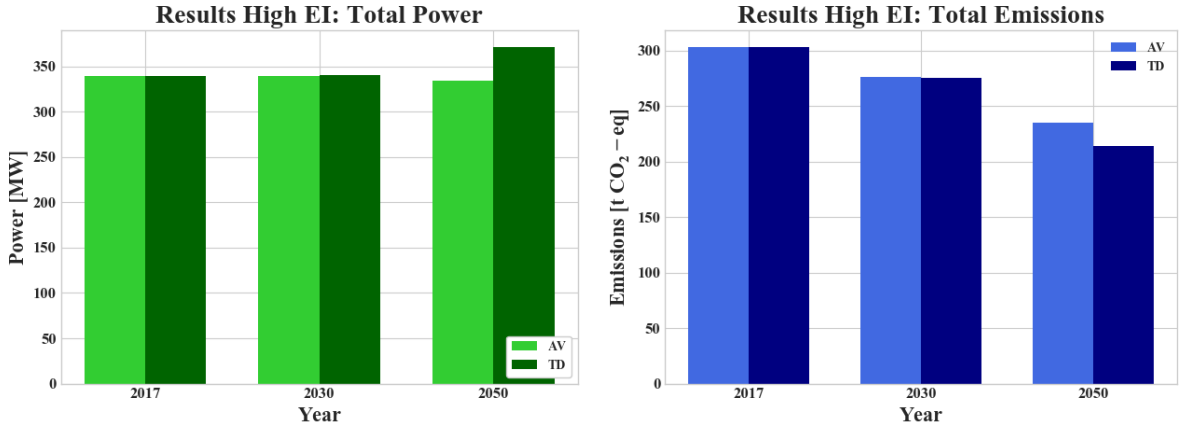

(a) Total power [MW]

(b) Total emissions [t CO_2-eq]

Figure 11.2: Results of using high emissions intensities for the average versus time-dependent GHG emissions factors for the three different years on the total power [MW] and GHG emissions [t CO_2-eq] of the system.

When comparing the results of the high emissions intensities with the original (mean) emissions intensities (Figure 8.5), more GHG emissions are emitted (between 70.93% and 78.23%). This increase is logic since higher GHG emissions factor per timestep are used when using high emissions intensities. However, to test the robustness of the parameter, the increase/decrease in percentage between the AV and TD results are analysed. For the year 2017, applying high emissions intensities has no effect on the total power usage and emissions since no renewable sources are included and so the AV and TD results are equal. For the year 2030, applying high emissions intensities has no significant impact on the total power usage (mean EI: 0.16% and high EI: 0.16%) and emissions (mean EI: -0.46% and high EI: -0.38%) when switching to TD GHG emissions factors compared to the original emissions intensities values. For the year 2050, applying high emissions intensities has only a small effect on the total power usage (mean EI: 11.48% and high EI: 9.10%) when switching

to TD GHG emissions factors compared to the original emissions intensities values. It has no significant impact on the emissions (mean EI: -9.99% and high EI: -9.11%).

11.2. Speed of water flow

The speed of the water flow in the pipes is not known and the assumption is made to set this speed at 1.0 m/s. Lower and higher water flow speeds are also possible. Section 11.2.1 shows the effect of the use of a lower water flow speed on the total costs and power of the system. Section 11.2.2 shows the effect of the use of a higher water flow speed on the total costs and power of the system.

11.2.1. Speed of 0.5 m/s

Figure 11.3 shows the absolute results of the use of a water flow speed of 0.5 m/s on the total costs and power of the system for the three ToU electricity tariff scenarios compared to the base case scenario (flat rate tariff). When implementing scenario 1 (low), a costs savings of -0.32% is possible. For scenario 2 (medium) the savings are -1.90% and for scenario 3 (extreme) the savings are -5.72%. However, an increase in power usage is necessary to achieve this costs savings (scenario 1 (low) = 0.68%, scenario 2 (medium) = 1.20% and scenario 3 (extreme) = 3.76%).

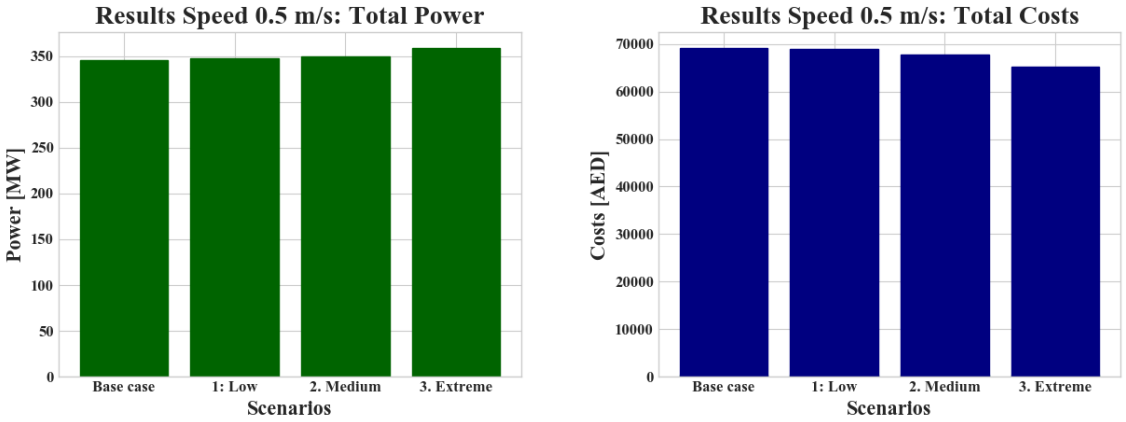

(a) Total power [MW]

(b) Total costs [AED]

Figure 11.3: Results of using a water flow speed of 0.5 m/s for the four electricity tariff scenarios on the total power [MW] and costs [AED] of the system.

When comparing the results of a water flow speed of 0.5 m/s with the original water flow speed (1.0 m/s) (Figure 7.6), the costs (between 1.70% and 2.29%) and power usage (between 1.21% and 1.70%) are increasing slightly due to the higher friction factor and thus the higher resistance coefficient. However, to test the robustness of the parameter, the savings (in %) when using ToU electricity tariffs instead of flat electricity tariffs are compared between the different water flow speeds. For scenario 1 (low), applying a water flow speed of 0.5 m/s instead of 1.0 m/s has no impact on the total power usage (1.0 m/s = 0.70% and 0.5 m/s = 0.68%) and costs (1.0 m/s = -0.38% and 0.5 m/s = -0.32%). This also counts for scenario 2 (medium) (power usage (1.0 m/s = 1.21% and 0.5 m/s = 1.20%) and costs (1.0 m/s = -2.17% and 0.5 m/s = -1.90%)) and scenario 3 (extreme) (power usage (1.0 m/s = 4.26% and 0.5 m/s = 3.76%) and costs (1.0 m/s = -6.26% and 0.5 m/s = -5.72%)).

11.2.2. Speed of 1.5 m/s

Figure 11.4 shows the absolute results of the use of a water flow speed of 1.5 m/s on the total costs and power of the system for the three ToU electricity tariff scenarios compared to the base case scenario (flat rate tariff). When implementing scenario 1 (low), a costs savings of -0.42% is possible. For scenario 2 (medium) the savings are -2.30% and for scenario 3 (extreme) the savings are -6.54%. However, an increase in power usage is necessary to achieve this costs savings (scenario 1 (low) = 0.79%, scenario 2 (medium) = 1.17% and scenario 3 (extreme) = 5.34%).

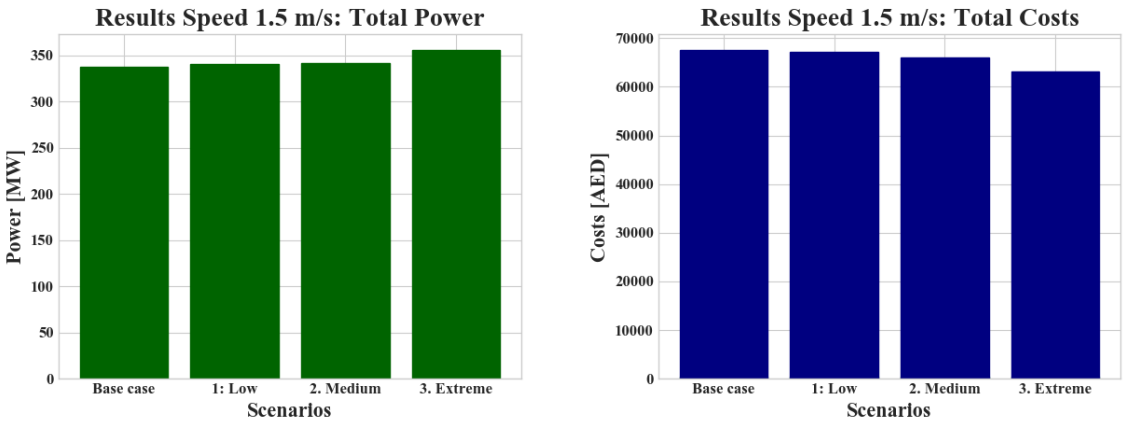

(a) Total power [MW]

(b) Total costs [AED]

Figure 11.4: Results of using a water flow speed of 1.5 m/s for the four electricity tariff scenarios on the total power [MW] and costs [AED] of the system.

When comparing the results of a water flow speed of 1.5 m/s with the original water flow speed (1.0 m/s) (Figure 7.6), the costs (between -0.63% and -0.92%) and power usage (between -0.54% and -0.67%) are decreasing slightly due to the lower friction factor and thus the lower resistance coefficient. However, to test the robustness of the parameter, the savings (in %) when using ToU electricity tariffs instead of flat electricity tariffs are compared between the different water flow speeds. For scenario 1 (low), applying a water flow speed of 1.5 m/s instead of 1.0 m/s has no impact on the total power usage (1.0 m/s = 0.70% and 1.5 m/s = 0.79%) and costs (1.0 m/s = -0.38% and 1.5 m/s = –0.42%). This also counts for scenario 2 (medium) (power usage (1.0 m/s = 1.21% and 1.5 m/s = 1.17%) and costs (1.0 m/s = -2.17% and 1.5 m/s = -2.30%)) and scenario 3 (extreme) (power usage (1.0 m/s = 4.26% and 1.5 m/s = 5.34%) and costs (1.0 m/s = -6.26% and 1.5 m/s = -6.54%)).

11.3. Conclusion

This chapter showed the results of the sensitivity analysis. Two uncertain parameters are tested: the GHG emissions intensity and the water flow speed through the pipelines. Increasing or decreasing the water flow speed has no significant effect on the difference between the ToU tariffs and the flat rate tariffs scenarios. Increasing or decreasing the GHG emissions intensities has no significant effect on the difference between the AV and TD GHG emissions for the years 2017 and 2030. For the year 2050, increasing the emissions intensities (high EI) has also no significant effect. Decreasing the emissions intensities (low EI) on the other hand has an effect, probably due to the fact that when using low emissions intensities, the hours during day time (solar availability) have GHG emissions factors of almost zero, resulting in the fact that the pumps are even more triggered to work at maximum capacity. Tables 11.1 (emissions intensities) and 11.2 (water flow speed) show a summary of the results of the sensitivity analysis that is performed.

Table 11.1: Overall results of sensitivity analysis for the parameters emissions intensities (% change between AV and TD factors).

Year	P (low EI)	P (mean EI)	P (high EI)	E (low EI)	E (mean EI)	E (high EI)
2017	0.00%	0.00%	0.00%	0.00%	0.00%	0.00%
2030	0.15%	0.16%	0.16%	-0.56%	-0.46%	-0.38%
2050	20.19%	11.48%	9.10%	-15.95%	-9.99%	-9.11%

Table 11.2: Overall results of sensitivity analysis for the parameter water flow speed (% change between ToU and base case scenario).

Scenario	P (0.5 m/s)	P (1.0 m/s)	P (1.5 m/s)	C (0.5 m/s)	C (1.0 m/s)	C (1.5 m/s)
Scenario 1	0.68%	0.79%	0.70%	-0.32%	-0.42%	-0.38%
Scenario 2	1.20%	1.17%	1.21%	-1.90%	-2.30%	-2.17%
Scenario 3	3.76%	5.34%	4.26%	-5.72%	-6.54%	-6.26%

IV

Remarks

---

12 Discussion

This chapter provide a trifold of information. First, the research limitations and uncertainties are given. Second, the contribution of the established knowledge is outlined, followed by suggestions for future research.

12.1. Research limitations and uncertainties

Multiple limitations and uncertainties are identified which could have influenced the results of this research. The first limitation is the data used for this research. Data for building the model is available (pumps, storage areas and pipeline characteristics of the WTS of TRANSCO) and is only simplified to allow the model to run more continuous, such as:

- The storage areas per city are modelled together as one tank;
- New pump characteristics are made by combining the two different types of pumps;
- The different pipelines are modelled together;
- Surge tanks areas located at the discharge side of the pumping stations are left out of the analysis due to the timeframe of the model.

However, data needed to run through the model (water flows) is limited. No customer demand pattern is available, only water flows through the system at specific locations such as a limited amount of intermediate demand nodes and inflows into the storage areas. Therefore, assumptions about the water flows are based on the maximum flow scenario through the system (for more information see Appendix A) and are therefore uncertain. Also, only an hourly pattern of one full day in the summer is provided, resulting in the fact that no comparison could have been made between the different seasons in UAE. Predictions about the water usage of the different months could have been made. However, this only results in an increase/decrease of total water usage compared to the data provided by TRANSCO resulting in the fact that the division between the inflows and outflows will stay the same. Variation in water peak demand between the different months are therefore not taken into account since they are unknown. To conclude, the results are based on only one full day of data.

The second limitation of this research is the fact that the future water and electricity demand up till 2050 is not taken into account. For both the water as well as the electricity demand there are predictions up till 2030 available (ADWEC, 2019b) and based on this a forecast could be made up till 2050. However, for the future water demand, this increase will only results in higher absolute costs, power usage and GHG emissions due to the growing water demand. It does not result in different water peaks during the day and thus in different pumping schedules since the division between the inflows and outflows stays equal, as explained in the previous paragraph. Therefore, the costs savings possible (in %) when switching to for example ToU rates will stay the same. The same counts for the future electricity demand profiles. Since there is no data or literature available about future daily electricity demand profiles (only yearly increases), the assumption is made that the electricity demand patterns (peaks) during the day stay the same into the future. Since the absolute number of electricity demand is not used (only the division between the different power sources below the electricity demand profile), this research did not take into account future electricity demand profiles.

The third limitation of this research are the electricity tariffs that are used. Since UAE has currently flat rates tariffs, multiple ToU tariffs scenarios are investigated in which the difference between the on-peak and off-peak increased between the different scenarios. However, no predictions of electricity prices up till 2050 are done and thus the same tariffs are used for each year. This is chosen since there is no historical data of electricity tariffs and/or research into future prices available. However, this results in the fact that there are on-peak electricity tariffs during the day, also for example in 2050 when most of the electricity produced during daytime is coming from solar power and thus a low price is expected. Research into predictions of future electricity prices is relevant, but due to time limitations not completed in this research. Nonetheless, by investigating the GHG emissions and carbon tax scenarios, shifting to day pumping (solar availability) is researched.

The fourth limitation of this research is the fact that the model does not show water variation patterns in the storage areas. The operating horizon (24 hours) is too short to shows the repeating pattern of filling and emptying the different storage areas. Therefore, boundary effects occur in which at the beginning of the time horizon the model first has to find its water pattern and at the end of the time horizon the storage areas are emptied due to the objective function (minimise costs/GHG emissions and thus minimise storage areas). To give an insight in how this can look like, the time-dependent GHG emissions scenario for 2050 is modelled with an operating horizon of three days (meaning: three days consisting of the same water flows), see Figure 12.1.

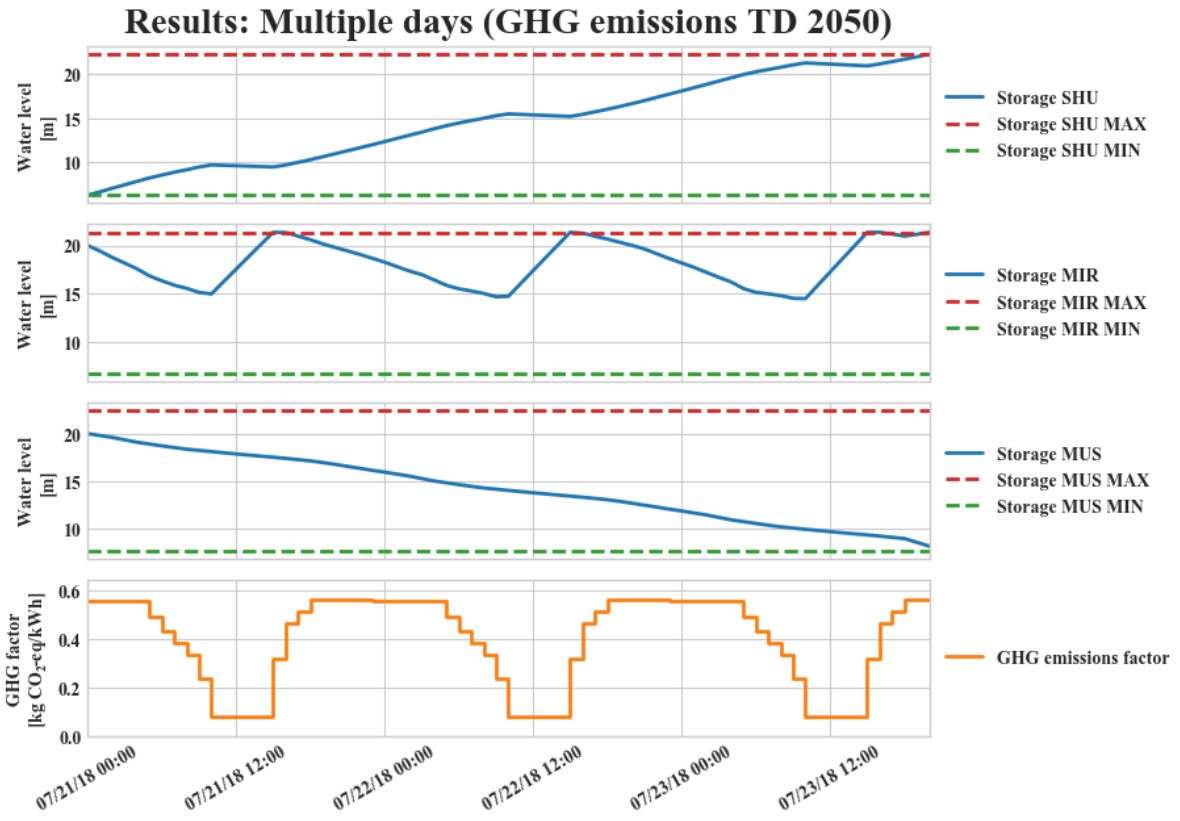

Figure 12.1: Results of 72 hours operating horizon to show the repeating water variation patterns (filling and emptying of the storage areas) of the TD GHG emissions scenario in 2050.

As seen, the storage areas at Mirfa show a repeating pattern (compared to Figure 8.4) where they are emptied during high GHG emissions factors and filled during low GHG emissions factors. For the storage areas at Shuweihat and Mussafah, the operating horizon is still too short to clearly show the water variation pattern.

The fifth limitation of this research is the solver (Gurobi) that is used. First, Gurobi is only for free for academic licences and so commercial licences are really expensive, making the research harder to reproduce when using a different solver. Second, the solver cannot prove what the best solution is, it can only approach

the best solution. This is due to the mixed integer problem where in total thirteen pumps can be on or off at 24 different timesteps, resulting in 13^{24} possible options. To terminate the model to be able to find the corresponding results, or a MIPGap or a time limit must be included. A MIPGap will terminate the model when the gap between the lower and upper objective bound is less than MIPGap times the absolute value of the upper bound (Gurobi, 2019a). A time limit terminates the model when the total time (in seconds) is expended (Gurobi, 2019b). Although the results found in this research are not optimal, the approached solutions are justifiable due to the small gap numbers (< 0.01).

The sixth and final limitation of this research is the fact that there are no reference values available concerning the current power usage, costs or GHG emissions emitted by TRANSCO of one single day and of only this part of the WTS (between Shuweihat and Mussafah). Therefore, the results of this research are not compared with the current numbers of TRANSCO and so no conclusions (or recommendations) can be made about the current situation (base case scenarios). Hard conclusions can only be made about the influence of the infrastructure and on the different scenarios towards the future and thus how the pump schedule responds on ToU rates and time-dependent GHG emissions factors. To state conclusions about the optimal pump schedule now, the current pump schedule of TRANSCO must be analysed together with their current power usage and expenditures to be able to compare it with the results of the optimisation model made in this research.

12.2. Contribution of established knowledge

The results of this research indicate that ToU electricity tariffs and time-dependent GHG emissions factors can change the composition of total costs and emissions significantly, which is in line with previous studies (Biehl & Inman, 2010; Bunn & Reynolds, 2009; Herstein et al., 2009; Ramos et al., 2011; Wu, 2011b). The exact results of course differ due to the different electricity tariffs and power source mixes in the specific countries. However, switching to time-dependent tariffs and factors and thus making use of the available storage areas minimise the total costs and GHG emissions. In line with research conducted by Stokes et al. (2014) and Wu (2011a), trade-offs between the two objectives (minimising total costs and minimising total GHG emissions) are evident. Especially since the fluctuation of the electricity tariffs and GHG emissions factors do not coincide (high electricity tariffs and low GHG emissions factors during day time due to solar power). This especially counts for countries with a high share of solar power in their power source mix but who also have a high electricity tariff during day time.

The results of this research contributes to established knowledge by giving an insight in how the energy market and water management in UAE (and other countries) can achieve a better collaboration. Optimising individual components of a WTS are often named and researched in literature. Combining the multiple facets from a system perspective is limited. The case study used in this research (between Shuweihat and Mussafah of the WTS of TRANSCO) is relatively simple compared with for example the whole WTS of TRANSCO or with water distribution networks which often have many more pumping stations and hundreds of pipelines. However, the impact of the different scenarios on the objective functions and the final results can be generalised to other parts of the system or other water distribution systems with varying complexity.

This research also contributes to the knowledge base of policy makers in UAE. Implementing carbon taxes has indirectly an influence on the sustainability performance of TRANSCO since such a policy will incentivise TRANSCO to pump when most sustainable energy sources are producing during day/night. Therefore, policy makers can use this tool to further reduce the GHG emissions in UAE and thereby contribute to their Green Key Performance Indicators (MOCCAE, 2019).

12.3. Future research

There are four areas which require future research. First, the model that is made is a mixed integer linear model and so pumps can be on or off at every timestep. However, as explained in section 12.1, this results in the fact that the solver cannot find the most optimal solution, it can only approach it. Therefore, instead of implementing a MIPGap or time limit, another approach could be to switch the model from a MILP to a continuous model. Here, a virtual pumping station could be made that represents the multiple pumps but in fact only has a discharge through the pumping station (with a minimum discharge above zero since at least one pump must always be on). This results that every pump will operate at the same head (H) and they share

the capacity. The intersection of the capacity curve (Q-H characteristic) and the system curve (represents the energy that is needed to transport a certain discharge through the system) gives the operating point and thus the total discharge of all pumps. A limitation of this approach is the fact that one efficiency for all discharges must be chosen (around 80%), where normally the efficiency is dependent on the hydraulic energy absorbed by the water and the mechanical energy supplied by the motor of the pump via the drive shaft and is thus not constant. However, this can also be justified since most of the time pumps operate around this efficiency, only during start up and shut down times the efficiency is lower. Another justification for this is the fact that the efficiency has a much smaller effect on the total power than the total head. As seen in equation 2.8, the power usage is influenced by the density, the gravitational acceleration, the discharge, the head and the efficiency. Since the head is written as $H_{stat} + CQ^2$ and is thus a quadratic function, the effect of the head on the power is much larger than the effect of the efficiency. Thus, keeping the efficiency constant will only have a small effect on the power outcome. To conclude, by using a continuous model instead of a MILP model, the run time will decrease extremely and no time limit or MIPGap is necessary to achieve a solution. However, the results are less certain since the pump characteristics are not included in the model and the efficiency of the pumps is assumed to be static. Future research is necessary to calculate the difference between the MILP and the continuous model.

Second, the model did not take into account the amount of time the water stays in the pipelines before it enters the downstream storage farms. The assumption is made that the amount of water flowing into the pipes from the upstream farm automatically results in the same amount of water flowing out of the pipes into the downstream farm. This approach is justified since this study did not take the quality of the water into discussion. However, the quality of the water is an important factor, especially since part of the water is provided as drinking water for the customers. Therefore, future research into the quality of the water is necessary, for example by taking into account the chlorine concentration in the water and thus adding an extra objective function.

Third, water network constraints limit the amount of water that can be delivered to the customers. Before 2012, not all of the water desalination capacity could be fully utilised because of the water network constraints of TRANSCO. Due to the implementation of extra pipelines and pumps, the network constraints were removed. The question rises how this will develop towards 2030 and 2050. The water demand will only further rise due to the population growth and the economic development of UAE. Therefore, future research into the constraints of the current network is necessary in which future water demand predictions should be taken into account. On the other hand, the question also rises if the water resource availability at the source will become an issue or not. As explained in Chapter 1, conventional approaches in UAE (rainfall, river runoff) are limited and therefore, desalination plants play a key roll in narrowing the water demand-supply gap. However, seawater desalination is very energy and cost intensive. Currently the desalination plants make use of the excess heat of gas-fired combined cycle power plants. Since the goal of UAE is to reduce the share of gas of the total energy mix from around 100% to 38% by 2050, the question will be if desalination plants are economic profitable towards the future or that UAE should investigate other options to insure that the water demand is fulfilled. Since a water availability issue (water rationing) at the source can have an impact on the operation and network constraints of TRANSCO, future research into water availability is relevant.

The fourth and final recommendation concerns the electricity prices. Currently the power source mix of UAE consist mainly of natural gas. The water and electricity to distribution and supply companies is sold through an annually adjusted bulk supply tariff. This is possible since no renewable sources are included in the power source mix and therefore the available electricity production is not fluctuating during the day, resulting in the fact that the electricity price is also not fluctuating during the day. However, with the implementation of renewable sources into their power source mix, the electricity price will fluctuate in the future. Therefore, it is interesting to investigate how the pump schedule will react by using for example day ahead market and/or intraday market prices. The network of TRANSCO can already be tested with for example day ahead market and/or intraday market prices of the Netherlands or Germany to investigate the effect of this on the pump schedule.

13

Conclusion

In this research, a quantitative analysis is conducted in which a model is made that established the operational electricity usage, GHG emissions and expenditures related to electricity use of TRANSCOs water supply system. The model consist of two parts: the internal model (represents the water infrastructure of TRANSCO) and the optimisation model. The focus was on optimising the Shuweihat water transmission scheme, which starts at Shuweihat and ends at Mussafah with Mirfa as intermediate pumping station (~ 230 km), see Figure 1.1 for an overview of the WTS of TRANSCO in UAE. The internal model (made with the software OpenModelica) consist of multiple components, which are inflows from desalination plants, (intermediate) demand nodes (outflows), storage areas, pumping stations (consisting of multiple pumps), pipelines and control valves. The component have their own characteristics, all retrieved from TRANSCO. The optimisation model is made with the software RTC-Tools and is used as a Python package. Here, multiple constraints are included which are the water level constraint, pump switching constraint, pump power constraint, pipeline flow constraint and control valve constraint. Also the objective functions are defined, which are minimising the total costs including and excluding a carbon tax [AED], and minimising the total GHG emissions [t CO_2-eq]. Multiple scenarios are constructed which represents how the future water and energy infrastructure of UAE affects the pump schedule of the WTS of TRANSCO and thus their total operating costs, power usage and GHG emissions. The following sections outline the conclusions of the different scenarios researched.

Electricity tariffs

The effect of varying (ToU) versus flat tariffs on the pump schedule is investigated. Three ToU scenarios are compared (low, medium and extreme) with the current flat tariff of 0.20 AED/kWh. The results show that the total costs over the whole time period reduces when taking into account ToU rates. The larger the difference between on-peak and off-peak rates, the larger the costs reduction is. However, an increase in power usage is necessary to achieve this costs savings. The yellow boxes in Figure 13.1 show the overall results of the flat versus the ToU rates.

GHG emissions factors

The effect of average (AV) versus time-dependent (TD) GHG emissions factors is investigated for three different years based on the power source mix goals of UAE: 2017, 2030 and 2050. The results show that for the year 2017, no GHG emissions savings are possible since no renewable sources are included and thus the AV and TD GHG emissions factors are equal. When implementing renewable sources (solar) into the power source mix of UAE (2030, 2050), remarkable savings can be achieved when switching to TD GHG emissions factors. However, also here an increase in power usage is necessary to achieve this saving, possibly due to the fact that during low GHG emissions factors, more pumps are on and they operate closer to their maximum capacity compared to high GHG emissions factors. The green boxes in Figure 13.1 show the overall results of the AV versus TD GHG emissions factors.

Policy driver carbon tax

The effect of the implementation of carbon taxes on the system is investigated for all three years and all four electricity tariff scenarios. Here, the minimum carbon tax needed to shift to daytime (solar availability) is researched. The results show for the year 2017, implementing a carbon tax has no effect on the pump schedule since no renewable sources are included and thus the carbon tax has no effect. For the years 2030 and 2050, implementing carbon taxes do have an effect. However, for the year 2030 when the proportion of renewable sources is still limited, the necessary taxes are disproportional high. The results also show that

how larger the difference is between the ToU rates, more costs must be paid to pump during daytime due to the dominating on-peak rate. The blue boxes in Figure 13.1 show the overall results of the minimum carbon taxed (AED/kg CO_2-eq) needed to shift to day pumping per year and per electricity tariff scenario.

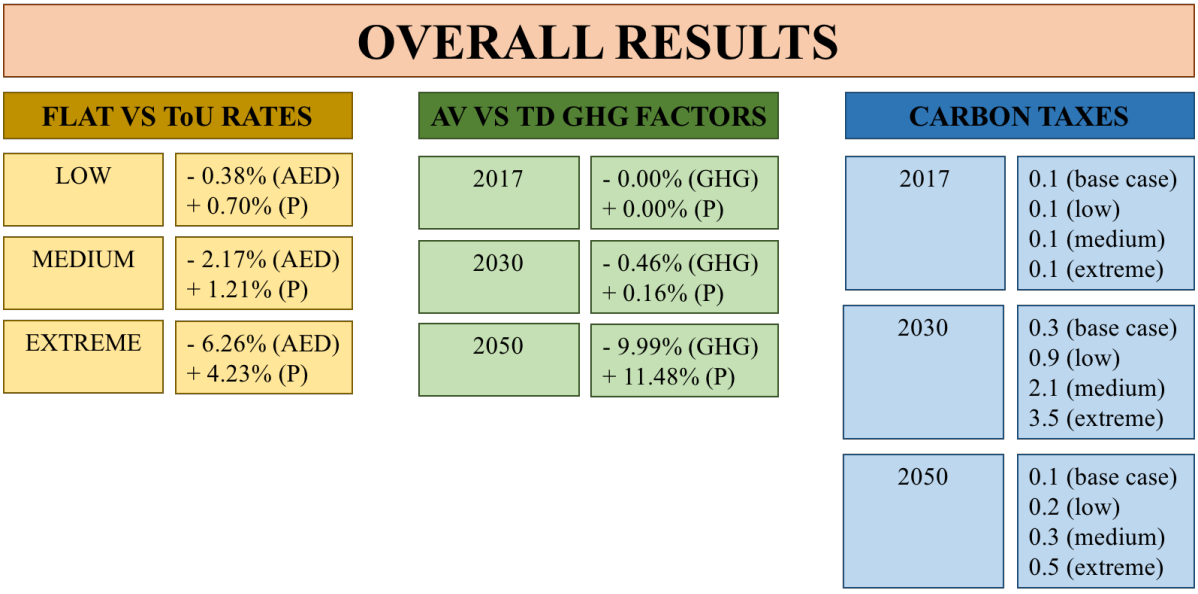

Figure 13.1: Overall results of research: flat vs ToU rates (yellow boxes), AV vs TD GHG emissions factors (green boxes), and minimum carbon taxes (AED/kg CO_2-eq) necessary to shift to daytime (blue boxes).

Infrastructure influence

The effect of the infrastructure of the WTS of TRANSCO on the pump schedule is investigated by increasing the size (+10% and +20%) of two parameters: storage areas and pipelines. The results show that increasing the storage areas and the pipelines both results in total costs and GHG emissions savings. Increasing the pipeline sizes has a larger effect (more reductions possible) than increasing the storage area sizes. Also, more savings are possible at the end of the system (storage area Mussafah and pipeline between Mirfa and Mussafah), possibly due to the fact that the demand of water at the end of the system is the highest resulting in the largest influence on the system.

Sensitivity analysis

Two uncertain parameters are tested: 1) GHG emissions intensities (lower and higher intensities) resulting in different GHG emissions factors, and 2) speed of the water flow through the pipelines (slower and faster speeds), resulting in different resistance coefficients. The results show that changing the speed of the water flow has no significant effect on the costs and power usage when switching to ToU rates. Changing the GHG emissions coefficients has no significant effect on the GHG emissions and power usage when switching to TD GHG emissions factors for the years 2017 and 2030. For the year 2050, higher emissions intensities also have no significant effect. However, lower emissions intensities do have an effect on the GHG emissions and power usage, probably due to the fact that when using low emissions intensities, the hours during day time (solar availability) have GHG emissions factors of almost zero, resulting in the fact that the pumps are even more triggered to work at maximum capacity.

Final remarks

To conclude, switching the pump schedule to times with lower electricity tariffs and/or GHG emissions factors and thereby using the capacity of the storage areas has remarkable effects on the possible costs and/or GHG emissions savings compared to flat electricity tariffs and/or average GHG emissions factors. Also, including a carbon tax has a positive effect on switching the pump schedule to day time (solar availability). However, when the proportion of solar power is small, this carbon tax is disproportional high.

References

ADDC. (2019). *Water and Electricity Tariffs 2017*. Retrieved 2019-04-16, from https://www.addc.ae/en-US/residential/Documents/02-English.pdf.

ADWEC. (2019a). *Abu Dhabi Water and Electricity Company*. Retrieved 2019-04-16, from http://www.adwec.ae/.

ADWEC. (2019b). *Statistical report 2017*. Retrieved 2019-04-23, from http://www.adwec.ae/Documents/Report/2017/2017_Statisticalreport.pdf

AE. (2019). *The energy sector of the UAE*. Retrieved 2019-01-25, from https://government.ae/en/information-and-services/environment-and-energy/water-and-energy/energy.

Alvisi, S., & Franchini, M. (2016). A Methodology for Pumping Control Based on Time Variable Trigger Levels. *Procedia Engineering*, *162*, 365–372.

Amborse, M. (2002). Piping systems embodied energy analysis. *CMIT Doc*, *2*, 302.

Basupi, I., Kapelan, Z., & Butler, D. (2014). Reducing life-cycle carbon footprint in the (re) design of water distribution systems using water demand management interventions. *Urban Water Journal*, *11*(2), 91–107.

Biehl, W., & Inman, J. (2010). Energy optimization for water systems. *Journal-American Water Works Association*, *102*(6), 50–55.

Boulos, P., & Schade, C., T. Baxter. (2008). Locating Leaks in Water Distribution Systems Using Network Modeling. *Journal of Water Management Modeling*, *228*(21), 351–362.

Bunn, S., & Reynolds, L. (2009). The energy-efficiency benefits of pump-scheduling optimization for potable water supplies. *IBM Journal of Research and Development*, *53*(3), 5–13.

Cabrera, E., Pardo, M. A., Cobacho, R., & Cabrera, E. (2010). Energy Audit of Water Networks. *Journal of Water Resources Planning and Management*, *136*(6), 669–677.

CDIAC. (2014). *Ranking of the world's countries by 2014 per capita fossil-fuel CO2 emission rate*. Retrieved 2019-01-24, from https://data.worldbank.org/indicator/EN.ATM.CO2E.PC?end=2014{&}start=1960{&}view=chart{&}year{_}high{_}desc=true.

Dandy, G., Roberst, A., Hewitson, C., & Chrystie, P. (2008). Sustainability objectives for the optimization of water distribution networks. *Water Distribution Systems Analysis Symposium*, 1–11.

Deltares. (2015a). Cursus Pompen Pompenkelders. *Cursussen Hydrodynamica van Leidingsystemen.*.

Deltares. (2015b). *Hydraulic Calculation Report: Shuweihat Phase 2 WTS, Lot A - Steady State*.

Dweiri, F., Khan, S. A., & Almulla, A. (2018). A multi-criteria decision support system to rank sustainable desalination plant location criteria. *Desalination*, *444*, 26–34.

Ertin, E., Dean, A., Moore, M., & Priddy, K. (2001). Dynamic Optimization for Optimal Control of Water Distribution Systems. *Applications and Science of Computational Intelligence IV*, *4390*, 142–150.

Filion. (2008). Impact of Urban Form on Energy Use in Water Distribution Systems. *Journal of Infrastructure Systems*, *14*(4), 337–346.

Filion, MacLean, H., & Karney, B. (2004). Life Cycle Energy Analysis of Water Distribution System. *Journal of Infrastructure Systems*, *10*(3).

Forum, W. E. (2019). *The Global Risks Report 2019, 14th edition* (Tech. Rep.). Geneva, Switzerland: World Economic Forum.

Ghimire, S. R., & Barkdoll, B. D. (2009). Impact of Storage Tanks on Energy Consumption in Municipal Water Distribution Systems. In *World environmental and water resources congress 2009* (pp. 1–7). Reston, VA: American Society of Civil Engineers.

Gude, V. (2017). Desalination and water reuse to address global water scarcity. *Reviews in Environmental Science and Bio/Technology*, *16*(4), 591–609.

Gurobi. (2019a). *MIPGap*. Retrieved 2019-06-24, from `http://www.gurobi.com/documentation/8.1/refman/mipgap2.html`.

Gurobi. (2019b). *Time Limit*. Retrieved 2019-06-24, from `https://www.gurobi.com/documentation/8.1/refman/timelimit.html#parameter:TimeLimit`.

Herstein, L. M., Filion, Y. R., & Hall, K. R. (2009). Evaluating Environmental Impact in Water Distribution System Design. *Journal of Infrastructure Systems*, *15*(3), 241–250.

IPCC. (2014). Energy Systems. In: Climate Change 2014: Mitigation of Climate Change. Contribution of Working Group III to the Fifth Assessment of the Intergovernmental Panel on Climate Change. *Journal of Water Management Modeling*, *Cambridge University Press, Cambridge, United Kingdom and New York, NY, USA.*, 511–397.

Jones, E., Qadir, M., van Vliet, M., Smakhtin, V., & Kang, S. (2018). The state of desalination and brine production: A global outlook. *Science of the Total Environment*, *657*, 1343–1356.

Kang, D., & Lansey, K. (2011). Dual water distribution network design under triple-bottom line objectives. *Journal of Water Resources Planning and Management*, *138*(2), 162–175.

Kelly, T. (2007). *Climate change: An inconvenient truth for the water industry* (Tech. Rep.). Adelaide, Australia.

Kumar, G., & Karney, B. W. (2007). Electricity Usage in Water Distribution Networks. In *2007 ieee canada electrical power conference* (pp. 97–102). IEEE.

MacLeod, S., Roshani, E., & Filion, Y. R. (2011). Impact of Pipe Material Selection on Greenhouse Gas Mitigation in Water Networks under Uncertain Discount Rates and Carbon Prices. In *Water distribution systems analysis 2010* (pp. 1014–1027). Reston, VA: American Society of Civil Engineers.

Mekonnen, M. M., & Hoekstra, A. Y. (2016). Four billion people facing severe water scarcity. *Science Advances*, *2*(2), e1500323.

MOCCAE. (2019). *UAE Green Key Performance Indicators* (Tech. Rep.). United Arab Emirates, Ministry of Climate Change and Environment.

Murad, A. A., Al Nuaimi, H., & Al Hammadi, M. (2007). Comprehensive Assessment of Water Resources in the United Arab Emirates (UAE). *Water Resources Management*, *21*(9), 1449–1463.

OECD. (2016). Effective Carbon Rates: Pricing CO_2 through Taxes and Emissions Trading Systems. *Journal of Water Management Modeling*, *OECD Publishing, Paris.*

Planells-Alandi, P., Carrión-Pérez, P., Ortega-Álvarez, J. F., Moreno-Hidalgo, M. Á., & Tarjuelo Martín-Benito, J. M. (2005). Pumping Selection and Regulation for Water-Distribution Networks. *Journal of Irrigation and Drainage Engineering*, *131*(3), 273–281.

Ramos, H. M., Kenov, K. N., & Vieira, F. (2011). Environmentally friendly hybrid solutions to improve the energy and hydraulic efficiency in water supply systems. *Energy for Sustainable Development*, *15*(4), 436–442.

Roshani, E., MacLeod, S. P., & Filion, Y. R. (2012). Evaluating the Impact of Climate Change Mitigation Strategies on the Optimal Design and Expansion of the Amherstview, Ontario, Water Network: Canadian Case Study. *Journal of Water Resources Planning and Management*, *138*(2), 100–110.

RSB. (2019a). *Drinking Water Section - Transmission.* Retrieved 2019-01-24, from `http://rsb.gov.ae/en/sector/transmission`.

RSB. (2019b). *Physical and financial structure of the water, wastewater and electricity sector.* Retrieved 2019-04-16, from http://rsb.gov.ae/en/sector/overview.

Sensfub, F., Ragwits, M., & Genoese, M. (2009). The merit-order effect: A detailed analysis of the price effect of renewable electricity generation on spot market prices in Germany. *Energy Policy*, *8*(36), 3086–3094.

Shahin, M., & Salem, A. (2015). The Challenges of Water Scarcity and the Future of Food Security in the United Arab Emirates (UAE). *Natural Resources and Conservation*, *3*(1), 1–6.

Sherif, M., Almulla, M., Shetty, A., & Chowdhury, R. K. (2014). Analysis of rainfall, PMP and drought in the United Arab Emirates. *International Journal of Climatology*, *34*(4), 1318–1328.

Simonovic, S. P. (2002). World water dynamics: global modeling of water resources. *Journal of Environmental Management*, *66*(3), 249–267.

Stokes, C., Maier, H., & Simpson, A. (2015). Water Distribution System Pumping Operational Greenhouse Gas Emissions Minimization by Considering Time-Dependent Emissions Factors. *Journal of Water Resources Planning and Management*, *141*(7), 04014088.

Stokes, C., Simpson, A., & Maier, H. (2014). The cost-greenhouse gas emission nexus for water distribution systems including the consideration of energy generating infrastructure: an integrated conceptual optimization framework and review of literature. *Earth Perspectives*, *1*(9), 1–17.

Tarantini, M., & Ferri, F. (2001). LCA of drinking and wastewater treatment systems of Bologna city: Final results. *4th IRCEW Conference, Inter-Regional Conference on Environment-Water Fortaleza, Brazil*.

Trifunovic, N. (2006). Chapter 1: Water Transport and Distribution Systems. In *Introduction to urban water distribution.* CRC Press.

UN. (2019). *Sustainable Development Goals.* Retrieved 2019-01-21, from https://www.un.org/sustainabledevelopment/sustainable-development-goals/.

WNA. (2011). *Comparison of Lifecycle Greenhouse Gas Emissions of Various Electricity Generation Sources.* Retrieved 2019-05-10, from http://www.world-nuclear.org/uploadedFiles/org/WNA/Publications/Working_Group_Reports/comparison_of_lifecycle.pdf.

Wu, W. (2009a). Accounting for greenhouse gas emissions in multiobjective genetic algorithm optimization of water distribution systems. *Journal of Water Resources Planning and Management2*, *136*(2), 146–155.

Wu, W. (2009b). Single-objective versus multiobjective optimization of water distribution systems accounting for greenhouse gas emissions by carbon pricing. *Journal of Water Resources Planning and Management*, *136*(5), 555–565.

Wu, W. (2011a). Incorporation of variable-speed pumping in multiobjective genetic algorithm optimization of the design of water transmission systems. *Journal of Water Resources Planning and Management*, *138*(5), 543–552.

Wu, W. (2011b). Sensitivity of optimal tradeoffs between cost and greenhouse gas emissions for water distribution systems to electricity tariff and generation. *Journal of Water Resources Planning and Management*, *138*(2), 182–186.

V

Appendices

A

Flow patterns Shuweihat scheme

This appendix discusses the flow patterns through the Shuweihat scheme. As seen below in Figure A.1, there are multiple inflows and outflows. For some of the inflows and outflows, an hourly pattern is provided by TRANSCO for one full day (July 21, 2018). Unfortunately, there is only data available for that specific day. Therefore, the data is limited. Also, multiple assumptions are made due to gaps in the data. The assumptions that are made are all explained in the sections below. The numbers written in bold are the numbers that are used as input/output into the model (which are all the elements outside the red dotted rectangle of Figure A.1.

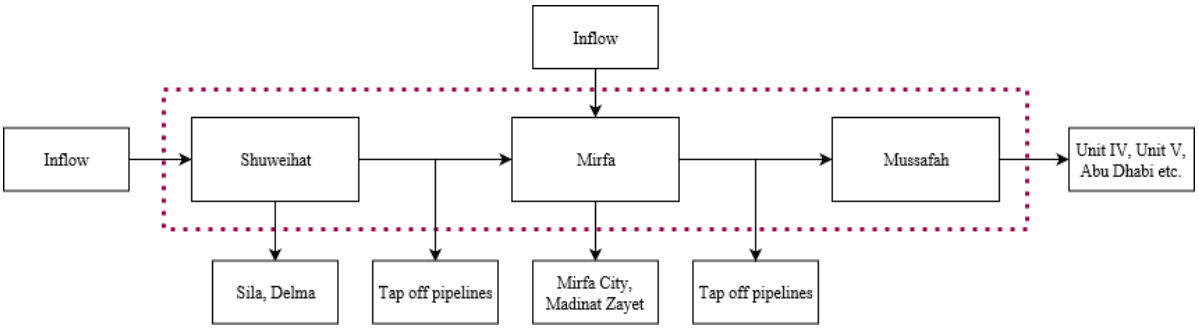

Figure A.1: Flow patterns between Shuweihat, Mirfa and Mussafah.

A.1. Inflow Shuweihat pumping station

The water flowing into the Shuweihat pumping station comes from two co-generation plants, called SHU1 and SHU2. A daily production pattern of the two co-generation plants of July 21, 2018 is provided by TRANSCO. The Shuweihat pumping station pumps the water towards Mirfa (and further towards Mussafah, Abu Dhabi), but also towards Delma and Sila, which is out of the research scope (Figure A.1). Therefore, the distribution between those flows is needed. However, no daily flow patterns from Shuweihat to Delma and Sila are available. Therefore, the distribution of the flows is based on the maximum flow scenario, see table A.1. The maximum flow from the Shuweihat pumping station is 202 MIGD. Of this, 174 MIGD flows through Line A and Line B towards Mirfa. The remaining 28 MIGD is transported to Delma (14.4 MIGD) and Sila (13.6 MIGD) (Deltares, 2015b). As seen in Table A.1, the flow towards Delma and Sila is equal to 13.86 % of the total inflow at the Shuweihat pumping station (called 'outflow SHU'). The remaining part flows towards Mirfa. Table A.2 shows the values of the production patterns of the two Shuweihat co-generation plants of July 21, 2018, the inflow in the model (called 'inflow SHU'), and the flow towards Delma and Sila (called 'outflow SHU').

Table A.1: Maximum flow scenario at Shuweihat pumping station.

Destination	Flow [MIGD]	Flow [m^3/s]	Distribution [%]
Line A Mirfa	93	4.893	46.04
Line B Mirfa	81	4.262	40.10
Delma	14.4	0.758	7.13
Sila	13.6	0.716	6.73
Total	202	10.629	100.00

Table A.2: Production patterns SHU1 and SHU2 (co-generation plants) of July 21, 2018, total inflow at Shuweihat pumping station towards Mirfa (inflow SHU), and total outflow Shuweihat pumping station towards Delma and Sila (outflow SHU). All values are given in [m^3/s].

Time	SHU1	SHU2	**Inflow SHU**	**Outflow SHU**	Unit
00:00	5.332	5.332	**10.665**	**1.478**	[m^3/s]
01:00	5.332	5.332	**10.665**	**1.478**	[m^3/s]
02:00	5.332	5.332	**10.665**	**1.478**	[m^3/s]
03:00	5.332	5.067	**10.399**	**1.441**	[m^3/s]
04:00	5.332	5.067	**10.399**	**1.441**	[m^3/s]
05:00	5.332	5.067	**10.399**	**1.441**	[m^3/s]
06:00	5.332	5.067	**10.399**	**1.441**	[m^3/s]
07:00	5.332	5.067	**10.399**	**1.441**	[m^3/s]
08:00	5.332	5.067	**10.399**	**1.441**	[m^3/s]
09:00	5.332	5.332	**10.665**	**1.478**	[m^3/s]
10:00	5.332	5.332	**10.665**	**1.478**	[m^3/s]
11:00	5.332	5.332	**10.665**	**1.478**	[m^3/s]
12:00	5.332	5.332	**10.665**	**1.478**	[m^3/s]
13:00	5.332	5.332	**10.665**	**1.478**	[m^3/s]
14:00	5.332	5.332	**10.665**	**1.478**	[m^3/s]
15:00	5.332	5.332	**10.665**	**1.478**	[m^3/s]
16:00	5.332	5.332	**10.665**	**1.478**	[m^3/s]
17:00	5.332	5.332	**10.665**	**1.478**	[m^3/s]
18:00	5.332	5.332	**10.665**	**1.478**	[m^3/s]
19:00	5.332	5.332	**10.665**	**1.478**	[m^3/s]
20:00	5.332	5.332	**10.665**	**1.478**	[m^3/s]
21:00	5.332	5.332	**10.665**	**1.478**	[m^3/s]
22:00	5.332	5.332	**10.665**	**1.478**	[m^3/s]
23:00	5.332	5.332	**10.665**	**1.478**	[m^3/s]

A.2. Tap offs between Shuweihat and Mirfa

There are several tap off pipelines providing water to the areas along the pipeline between Shuweihat and Mirfa. There is only data available of four out of the seven tap off pipelines, since not all parts of the WTS of TRANSCO have measurement technologies. Also, the patterns of those tap off pipelines are general, meaning that the available data are steady state demands (every day during the year has the same demand during the day). However, there is data available of the flow patterns at the beginning and at the end of the pipeline between Shuweihat and Mirfa. Therefore, the differences between these flows are assumed as the tap off flows. Table A.3 shows the flows at the start and at the end of the pipeline. It also shows the tap off flows (called 'tap off SHU-MIR'). This flow is implemented into the model as intermediate demand node (outflow) between Shuweihat and Mirfa.

Table A.3: Flows start and end of the pipeline between Shuweihat and Mirfa, and cumulative tap off flow used as model input (tap off SHU-MIR). All values are given in [m^3/s].

Time	Start pipeline	End pipeline	**Tap off SHU-MIR**	Unit
00:00	8.530	8.105	**0.424**	[m^3/s]
01:00	8.524	8.111	**0.414**	[m^3/s]
02:00	8.521	8.115	**0.406**	[m^3/s]
03:00	8.521	8.112	**0.409**	[m^3/s]
04:00	8.528	8.109	**0.419**	[m^3/s]
05:00	8.703	7.723	**0.980**	[m^3/s]
06:00	8.726	7.711	**1.015**	[m^3/s]
07:00	8.776	7.670	**1.106**	[m^3/s]
08:00	8.837	7.592	**1.246**	[m^3/s]
09:00	8.834	7.594	**1.240**	[m^3/s]
10:00	8.841	7.595	**1.246**	[m^3/s]
11:00	8.828	7.603	**1.226**	[m^3/s]
12:00	8.817	7.608	**1.209**	[m^3/s]
13:00	8.815	7.614	**1.201**	[m^3/s]
14:00	8.815	7.613	**1.202**	[m^3/s]
15:00	8.821	7.615	**1.205**	[m^3/s]
16:00	8.781	7.676	**1.105**	[m^3/s]
17:00	8.750	7.717	**1.033**	[m^3/s]
18:00	8.742	7.726	**1.016**	[m^3/s]
19:00	8.661	7.944	**0.171**	[m^3/s]
20:00	8.595	8.105	**0.489**	[m^3/s]
21:00	8.583	8.114	**0.470**	[m^3/s]
22:00	8.568	8.123	**0.445**	[m^3/s]
23:00	8.560	8.125	**0.435**	[m^3/s]

A.3. Inflow Mirfa pumping station

The water flowing into the Mirfa pumping station comes from a co-generation plant (MIR1), a reverse osmosis plant (MIR2) and from the Shuweihat pumping station (flow SHU-MIR), see also section A.1. A daily production pattern of MIR1 and MIR2 of July 21, 2018 is provided by TRANSCO. The Mirfa pumping station pumps the water towards Mussafah (and further towards Abu Dhabi), but also towards Mirfa City and Madinat Zayed, which is out of the research scope (Figure A.1). Therefore, the distribution between those flows is needed. However, no daily flow patterns from Mirfa to Mirfa City and Madinat Zayed are available. Therefore, the distribution of the flows is based on the maximum flow scenario, see Table A.4. The maximum flow from the Mirfa pumping station is 185.26 MIGD. Of this, 166 MIGD flows through Line A and Line B towards Mussafah. The remaining 19.26 MIGD is transported to Mirfa City (7.12 MIGD) and Madinat Zayed (12.14 MIGD) (Deltares, 2015b). As seen in Table A.4, the flow towards Mirfa City and Madinat Zayed is equal to 10.40% of the total inflow at the Mirfa pumping station from the desalination plants (called 'outflow MIR'). The remaining water coming from MIR1, MIR2 and from Shuweihat flows further towards Mussafah. Table A.5 shows the values of the production patterns of MIR1 and MIR2, the inflow in the model from the Mirfa plants (called 'inflow MIR'), the flow coming from Shuweihat (called 'flow SHU-MIR'), and the flow towards Mirfa City and Madinat Zayed (called 'outflow MIR').

Table A.4: Maximum flow scenario at Mirfa pumping station.

Destination	Flow [MIGD]	Flow [m^3/s]	Distribution [%]
Lina A Mussafah	80	4.209	43.18
Line B Mussafah	86	4.525	46.42
Mirfa City	7.12	0.375	3.85
Madinat Zayed	12.14	0.639	6.55
Total	185.26	9.748	100.00

Table A.5: Production patterns MIR1 (co-generation plant) and MIR2 (reverse osmosis plant) of July 21, 2018, total inflow at Mirfa pumping station (inflow MIR), flow between Shuweihat and Mirfa (flow SHU-MIR), and total outflow Mirfa pumping station towards Mirfa City and Madinat Zayed (outflow MIR). All values are given in [m^3/s].

Time	MIR1	MIR2	**Inflow MIR**	Flow SHU-MIR	**Outflow MIR**	Unit
00:00	1.187	1.261	**2.447**	8.105	**0.255**	[m^3/s]
01:00	1.187	1.317	**2.504**	8.111	**0.260**	[m^3/s]
02:00	1.187	1.317	**2.504**	8.115	**0.260**	[m^3/s]
03:00	1.187	1.582	**2.769**	8.112	**0.288**	[m^3/s]
04:00	1.187	1.582	**2.769**	8.109	**0.288**	[m^3/s]
05:00	1.187	1.582	**2.769**	7.723	**0.288**	[m^3/s]
06:00	1.187	1.582	**2.769**	7.711	**0.288**	[m^3/s]
07:00	1.187	1.582	**2.769**	7.670	**0.288**	[m^3/s]
08:00	1.187	1.582	**2.769**	7.592	**0.288**	[m^3/s]
09:00	1.187	1.317	**2.504**	7.594	**0.260**	[m^3/s]
10:00	1.187	1.317	**2.504**	7.595	**0.260**	[m^3/s]
11:00	1.187	1.317	**2.504**	7.603	**0.260**	[m^3/s]
12:00	1.187	1.317	**2.504**	7.608	**0.260**	[m^3/s]
13:00	1.187	1.317	**2.504**	7.614	**0.260**	[m^3/s]
14:00	1.187	1.317	**2.504**	7.613	**0.260**	[m^3/s]
15:00	1.187	1.317	**2.504**	7.615	**0.260**	[m^3/s]
16:00	1.187	1.317	**2.504**	7.676	**0.260**	[m^3/s]
17:00	1.187	1.317	**2.504**	7.717	**0.260**	[m^3/s]
18:00	1.187	1.317	**2.504**	7.726	**0.260**	[m^3/s]
19:00	1.187	1.317	**2.504**	7.944	**0.260**	[m^3/s]
20:00	1.187	1.317	**2.504**	8.105	**0.260**	[m^3/s]
21:00	1.187	1.317	**2.504**	8.114	**0.260**	[m^3/s]
22:00	1.187	1.317	**2.504**	8.123	**0.260**	[m^3/s]
23:00	1.187	1.317	**2.504**	8.125	**0.260**	[m^3/s]

A.4. Tap offs between Mirfa and Mussafah

There are several tap off pipelines (TO - 04, TO - 05, TO - 06, TO - 07, TO - 08) providing water to the areas along the pipeline between Mirfa and Mussafah. There are no daily demand patterns available of those tap off pipelines, since not all parts of the WTS of TRANSCO have measurement technologies. Therefore, the distribution between the flows is based on the maximum flow scenario, see Table A.6 (Deltares, 2015b). As seen, 12.53% (20.80 MIGD) of the total flow between Mirfa and Mussafah flows into the tap off pipelines (modelled together as one intermediate demand node to simplify the model). The remaining 87.47% (65.20 + 80 MIGD) is transported towards Mussafah. Since there is also no hourly pattern available, the assumption is made that the at every hour, the tap off is constant (equal to 12.53% of the total flow between Mirfa and Mussafah). The total flow between Mirfa and Mussafah is calculated with the following formula:

$$Flow_{MIR-MUS} = Flow_{SHU-MIR} + Inflow_{MIR} - Outflow_{MIR} \tag{A.1}$$

Table A.7 shows the tap off flows between Mirfa and Mussafah (called 'tap off MIR-MUS'). It also shows the demand node at Mussafah (called 'outflow MUS'), which is assumed to be 75% of flow towards Mussafah of the maximum flow scenario, since the system almost never works at his maximum capacity. This flow is also the final demand node of this research.

Table A.6: Maximum flow scenario between Mirfa and Mussafah.

Destination	Flow [MIGD]	Flow [m^3/s]	Distribution [%]
TO - 04	1.20	0.063	0.72
TO - 05	5.20	0.274	3.13
TO - 06	2.60	0.137	1.57
TO - 07	6.20	0.326	3.73
TO - 08	5.60	0.295	3.37
Line A Mussafah	80.00	4.209	48.19
Line B Mussafah	65.20	3.340	39.28
Total	166.00	8.734	100.00

Table A.7: Total outflow of the Mirfa pumping station towards Mussafah (flow MIR-MUS), cumulative tap off flow between Mirfa and Mussafah (tap off MIR-MUS), and final demand flow at Mussafah (outflow MUS). All values are given in [m^3/s].

Time	Flow MIR-MUS	**Tap off MIR-MUS**	**Outflow MUS**	Unit
00:00	10.298	**1.290**	**6.756**	[m^3/s]
01:00	10.354	**1.297**	**6.793**	[m^3/s]
02:00	10.358	**1.298**	**6.795**	[m^3/s]
03:00	10.593	**1.327**	**6.949**	[m^3/s]
04:00	10.590	**1.327**	**6.947**	[m^3/s]
05:00	10.204	**1.279**	**6.694**	[m^3/s]
06:00	10.192	**1.277**	**6.686**	[m^3/s]
07:00	10.151	**1.272**	**6.659**	[m^3/s]
08:00	10.073	**1.262**	**6.608**	[m^3/s]
09:00	9.838	**1.233**	**6.454**	[m^3/s]
10:00	9.839	**1.233**	**6.454**	[m^3/s]
11:00	9.846	**1.234**	**6.459**	[m^3/s]
12:00	9.852	**1.234**	**6.463**	[m^3/s]
13:00	9.857	**1.235**	**6.467**	[m^3/s]
14:00	9.856	**1.235**	**6.466**	[m^3/s]
15:00	9.859	**1.235**	**6.468**	[m^3/s]
16:00	9.920	**1.243**	**6.508**	[m^3/s]
17:00	9.960	**1.248**	**6.534**	[m^3/s]
18:00	9.969	**1.249**	**6.540**	[m^3/s]
19:00	10.188	**1.277**	**6.683**	[m^3/s]
20:00	10.349	**1.297**	**6.789**	[m^3/s]
21:00	10.357	**1.298**	**6.794**	[m^3/s]
22:00	10.366	**1.299**	**6.800**	[m^3/s]
23:00	10.368	**1.299**	**6.802**	[m^3/s]

B

Input parameters pumps

This appendix shows pump characteristics and the four input parameters for the pumps, which are the power coefficients, the working area coefficients, the speed coefficients, and the working area direction. Section B.1 gives the characteristics and parameters for the Shuweihat pumping station, section B.2 gives the characteristics and parameters for the Mirfa pumping station.

B.1. Shuweihat pumping station

Tables B.1 and B.2 below show the pump characteristics (Q, H, η, P) for the existing and the new pumps of the Shuweihat pumping station. The Figures are found in section 4.5.1.

Table B.1: Performance characteristics 'existing pumps' Shuweihat pumping station.

Discharge [m^3/h]	Pump head [m]	Efficiency [%]	Power [kW]
0	231.0	0	-
500	229.7	25.17	1243
1000	227.8	46.40	1338
1500	226.2	60.96	1517
2000	223.7	71.73	1700
2500	221.6	79.44	1900
3000	218.4	83.76	2131
3500	214.4	87.30	2342
4000	209.9	88.25	2592
4500	204.4	88.88	2820
5000	198.2	89.66	3012
5500	191.9	89.66	3209
6000	184.2	89.03	3382
6500	175.6	88.09	3531
7000	165.8	85.73	3688
7500	154.6	81.80	3861
7750	146.8	79.04	3921

Table B.2: Performance characteristics 'new pumps' Shuweihat pumping station.

Discharge [m^3/h]	Pump head [m]	Efficiency [%]	Power [kW]
0	228.0	0	-
500	226.8	17.69	1747
1000	225.0	32.31	1898
1500	224.0	45.38	2018
2000	222.0	55.77	2169
2500	217.2	65.19	2299
3000	213.6	71.92	2469
3500	210.0	77.50	2629
4000	205.6	80.38	2848
4500	199.6	82.88	3042
5000	193.6	85.19	3192
5500	190.0	86.54	3353
6000	186.8	87.31	3498
6500	178.8	87.12	3635
7000	169.6	86.92	3722
7500	160.0	85.19	3838
8000	149.2	82.69	3933
8250	145.0	80.70	4039

Below, the four input parameters for the pumps of the Shuweihat pumping station are found, which are the power coefficients, the working area coefficients, the speed coefficients, and the working area direction.

$$\text{Power coefficients Shuweihat pumps} = \begin{bmatrix} -423,682.62902 & 589,175.61553 \\ 8,694.19307 & 0.0 \\ -2,429,644.32826 & 1,623,332.63787 \\ 16,355.82263 & 0.0 \\ -937,550.22454 & 870,470.90349 \\ 11,855.69327 & 0.0 \\ -1,260541.75415 & 1,064,952.17028 \\ 13,269.33806 & 0.0 \\ -1,157,214.83752 & 1,1001,680.34748 \\ 12,907.40232 & 0.0 \\ -2,226,770.77265 & 1,520,414.95408 \\ 16,370.65563 & 0.0 \\ -2,266,889.23731 & 1,533,695.41415 \\ 16,571.71892 & 0.0 \\ -2,965,085.90406 & 1,773,712.33110 \\ 18,807.21945 & 0.0 \\ -4,167,977.62211 & 2,318,958.12878 \\ 19,613.36731 & 0.0 \end{bmatrix}$$

$$\text{Speed coefficients Shuweihat pumps} = \begin{bmatrix} 88.3224 & 281.642 & 143.011 \\ 58.8183 & -24.9845 & 0.0 \\ -1.45483 & 0.0 & 0.0 \end{bmatrix}$$

$$\text{Working area coefficients Shuweihat pumps} = \begin{bmatrix} 471.44014 & -143.83742 \\ -1.0 & 0.0 \\ 372.22434 & -102.48711 \\ -1.0 & 0.0 \\ 247.78929 & -33.53068 \\ -1.0 & 0.0 \\ 296.79639 & -64.98132 \\ -1.0 & 0.0 \\ 229.96309 & -16.40839 \\ -1.0 & 0.0 \\ -41.10896 & 40.79260 \\ -1.0 & 0.0 \\ 68.29681 & -29.94475 \\ -1.0 & 0.0 \\ -130.67394 & 736.77605 \\ -1.0 & 0.0 \end{bmatrix}$$

$$\text{Working area direction Shuweihat pumps} = \begin{bmatrix} 1 & 1 & 1 & 1 & 1 & -1 & -1 & 1 \end{bmatrix}$$

B.2. Mirfa pumping station

Tables B.3 and B.4 below show the pump characteristics (Q, H, η, P) for the existing and the new pumps of the Mirfa pumping station. The Figures are found in section 4.5.2.

Table B.3: Performance characteristics 'existing pumps' Mirfa pumping station.

Discharge [m^3/h]	Pump head [m]	Efficiency [%]	Power [kW]
0	300.0	0	-
1000	296.0	37.60	2124
2000	290.4	60.00	2612
3000	280.0	75.00	3022
4000	267.2	82.80	3483
5000	249.6	86.60	3889
6000	230.4	87.60	4258
7000	209.6	86.40	4582

Table B.4: Performance characteristics 'new pumps' Mirfa pumping station.

Discharge [m^3/h]	Pump head [m]	Efficiency [%]	Power [kW]
0	292.0	0	-
1000	288.0	35.00	2220
2000	284.0	58.00	2642
3000	276.0	73.50	3040
4000	265.0	81.00	3531
5000	244.0	84.00	3919
6000	219.0	85.00	4171
7000	187.0	84.00	4205
8000	155.0	79.00	4235
8500	137.0	75.00	4190

Below, the four input parameters for the pumps of the Mirfa pumping station are found, which are the power coefficients, the working area coefficients, the speed coefficients, and the working area direction.

$$\text{Power coefficients Mirfa pumps} = \begin{bmatrix} -1,061,921.75072 & 1,020,960.64776 \\ 11,322.18684 & 0.0 \\ -507,544.02173 & 689,823.48224 \\ 8,589.11259 & 0.0 \\ -1,493,638.14362 & 1,289,517.93104 \\ 12,821.47662 & 0.0 \\ -2,780,659.38823 & 1,894.262.42795 \\ 16,126.85765 & 0.0 \\ -1,311,916.23777 & 1,177,202.19015 \\ 12,251.61860 & 0.0 \\ -2,554,217.75311 & 1,802,920.56694 \\ 15,564.56709 & 0.0 \\ -2,705,227.20793 & 1,867,063.36927 \\ 15,930.55374 & 0.0 \\ -3,458,444.62301 & 2,170,003.95537 \\ 17,707.52753 & 0.0 \\ -4,780,690.70889 & 2,710,896.90964 \\ 19,344.54479 & 0.0 \end{bmatrix}$$

$$\text{Speed coefficients Mirfa pumps} = \begin{bmatrix} 88.3224 & 281.642 & 143.011 \\ 58.8183 & -24.9845 & 0.0 \\ -1.45483 & 0.0 & 0.0 \end{bmatrix}$$

$$\text{Working area coefficients Mirfa pumps} = \begin{bmatrix} 374.81975 & -93.60473 \\ -1.0 & 0.0 \\ 303.75048 & -33.85859 \\ -1.0 & 0.0 \\ 332.67147 & -64.05772 \\ -1.0 & 0.0 \\ 433.19098 & -124.59028 \\ -1.0 & 0.0 \\ 505.92104 & -155.73538 \\ -1.0 & 0.0 \\ -41.44460 & 42.25987 \\ -1.0 & 0.0 \\ 88.83442 & -44.89979 \\ -1.0 & 0.0 \\ -174.46026 & 1,030.66490 \\ -1.0 & 0.0 \end{bmatrix}$$

$$\text{Working area direction Mirfa pumps} = \begin{bmatrix} 1 & 1 & 1 & 1 & 1 & -1 & -1 & 1 \end{bmatrix}$$

C

GHG emissions factors

This appendix shows the daily electricity demand profiles, the daily sun profile and the intermediate results of the calculation of the average and time-dependent GHG emissions factors for the three different scenario years: 2017, 2030 and 2050.

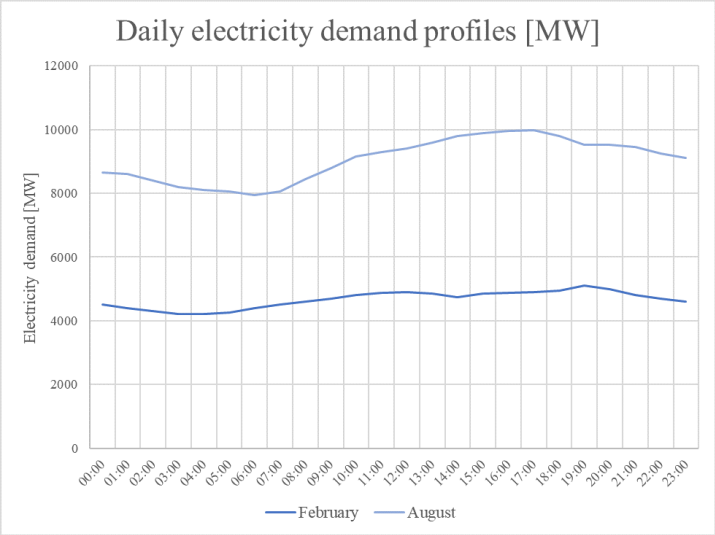

Figure C.1: Electricity demand profiles of an average day in February and in August, 2017.

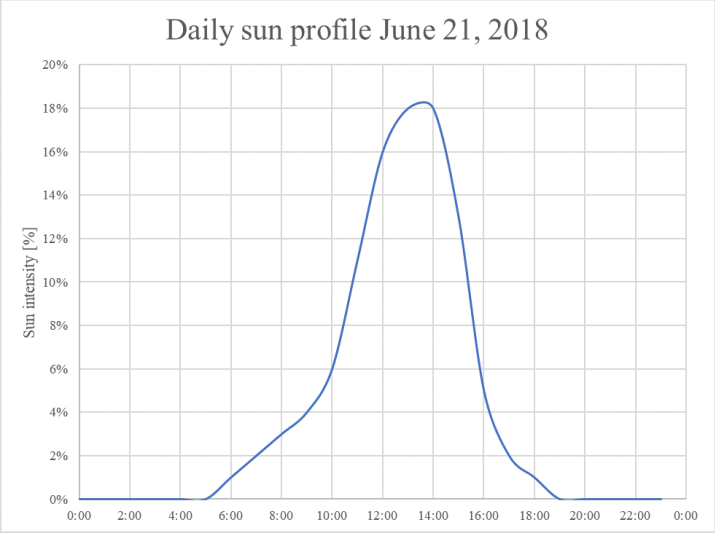

Figure C.2: Sun profile of June 21, 2018 in UAE.

Hourly electricity demand and total electricity produced per source in 2017

Table C.1: Hourly electricity demand and total electricity produced by the different sources [MW & %] of an average day in August, 2017.

From	To	Natural gas	%	Gas oil	%	Demand	%
00:00	01:00	8628	99.75	22	0.25	8650	100.00
01:00	02:00	8579	99.75	22	0.25	8600	100.00
02:00	03:00	8379	99.75	21	0.25	8400	100.00
03:00	04:00	8180	99.75	21	0.25	8200	100.00
04:00	05:00	8080	99.75	20	0.25	8100	100.00
05:00	06:00	8030	99.75	20	0.25	8050	100.00
06:00	07:00	7930	99.75	20	0.25	7950	100.00
07:00	08:00	8030	99.75	20	0.25	8050	100.00
08:00	09:00	8429	99.75	21	0.25	8450	100.00
09:00	10:00	8778	99.75	22	0.25	8800	100.00
10:00	11:00	9127	99.75	23	0.25	9150	100.00
11:00	12:00	9277	99.75	23	0.25	9300	100.00
12:00	13:00	9377	99.75	24	0.25	9400	100.00
13:00	14:00	9576	99.75	24	0.25	9600	100.00
14:00	15:00	9776	99.75	25	0.25	9800	100.00
15:00	16:00	9875	99.75	25	0.25	9900	100.00
16:00	17:00	9925	99.75	25	0.25	9950	100.00
17:00	18:00	9950	99.75	25	0.25	9975	100.00
18:00	19:00	9776	99.75	25	0.25	9800	100.00
19:00	20:00	9501	99.75	24	0.25	9525	100.00
20:00	21:00	9501	99.75	24	0.25	9525	100.00
21:00	22:00	9426	99.75	24	0.25	9450	100.00
22:00	23:00	9227	99.75	23	0.25	9250	100.00
23:00	00:00	9077	99.75	23	0.25	9100	100.00

Hourly electricity demand and total electricity produced per source in 2030

Table C.2: Hourly electricity demand and total electricity produced by the different sources [MW & %] of an average day in August, 2030.

From	To	Nuclear	%	Solar	%	Coal	%	Natural gas	%	Demand	%
00:00	01:00	1085	12.54	0	0.00	1038	12.00	6527	75.46	8650	100.00
01:00	02:00	1085	12.61	0	0.00	1032	12.00	6483	75.39	8600	100.00
02:00	03:00	1085	12.92	0	0.00	1008	12.00	6307	75.08	8400	100.00
03:00	04:00	1085	13.23	0	0.00	984	12.00	6131	74.77	8200	100.00
04:00	05:00	1085	13.39	0	0.00	972	12.00	6043	74.61	8200	100.00
05:00	06:00	1085	13.48	0	0.00	966	12.00	5999	74.52	8050	100.00
06:00	07:00	1085	13.65	108	1.36	954	12.00	5803	72.99	7950	100.00
07:00	08:00	1085	13.48	217	2.70	966	12.00	5782	71.83	8050	100.00
08:00	09:00	1085	12.84	325	3.85	1014	12.00	6026	71.31	8450	100.00
09:00	10:00	1085	12.33	434	4.93	1056	12.00	6225	70.74	8800	100.00
10:00	11:00	1085	11.86	651	7.11	1098	12.00	6316	69.03	9150	100.00
11:00	12:00	1085	11.67	1193	12.83	1116	12.00	5906	63.50	9300	100.00
12:00	13:00	1085	11.54	1736	18.47	1128	12.00	5451	57.99	9400	100.00
13:00	14:00	1085	11.30	1953	20.34	1152	12.00	5410	56.36	9600	100.00
14:00	15:00	1085	11.07	1953	19.93	1176	12.00	5586	57.00	9800	100.00
15:00	16:00	1085	10.96	1410	14.25	1188	12.00	6217	62.80	9900	100.00
16:00	17:00	1085	10.90	542	5.45	1194	12.00	7129	71.65	9950	100.00
17:00	18:00	1085	10.88	217	2.18	1197	12.00	7476	74.95	9975	100.00
18:00	19:00	1085	11.07	108	1.11	1176	12.00	7431	75.82	9800	100.00
19:00	20:00	1085	11.39	0	0.00	1143	12.00	7297	76.61	9525	100.00
20:00	21:00	1085	11.39	0	0.00	1143	12.00	7297	76.61	9525	100.00
21:00	22:00	1085	11.48	0	0.00	1134	12.00	7231	76.52	9450	100.00
22:00	23:00	1085	11.73	0	0.00	1110	12.00	7055	76.27	9250	100.00
23:00	00:00	1085	11.92	0	0.00	1092	12.00	6923	76.08	9100	100.00

Hourly electricity demand and total electricity produced per source in 2050

Table C.3: Hourly electricity demand and total electricity produced by the different sources [MW & %] of an average day in August, 2050.

From	To	Nuclear	%	Solar	%	Coal	%	Natural gas	%	Demand	%
00:00	01:00	542	6.27	0	0.00	1946	22.49	6162	71.23	8650	100.00
01:00	02:00	542	6.31	0	0.00	1934	22.49	6124	71.21	8600	100.00
02:00	03:00	542	6.46	0	0.00	1886	22.45	5972	71.09	8400	100.00
03:00	04:00	542	6.62	0	0.00	1838	22.41	5820	70.97	8200	100.00
04:00	05:00	542	6.70	0	0.00	1814	22.39	5744	70.91	8200	100.00
05:00	06:00	542	6.74	0	0.00	1802	22.38	5706	70.88	8050	100.00
06:00	07:00	542	6.82	955	12.01	1549	19.48	4904	61.69	7950	100.00
07:00	08:00	542	6.74	1909	23.72	1344	16.69	4255	52.85	8050	100.00
08:00	09:00	542	6.42	2864	33.89	1210	14.32	3833	45.36	8450	100.00
09:00	10:00	542	6.16	3819	43.40	1065	12.11	3373	38.34	8800	100.00
10:00	11:00	542	5.93	5728	62.60	691	7.55	2188	23.92	9150	100.00
11:00	12:00	542	5.83	8758	94.17	0	0.00	0	0.00	9300	100.00
12:00	13:00	542	5.77	8858	94.23	0	0.00	0	0.00	9400	100.00
13:00	14:00	542	5.65	9058	94.35	0	0.00	0	0.00	9600	100.00
14:00	15:00	542	5.54	9258	94.46	0	0.00	0	0.00	9800	100.00
15:00	16:00	542	5.48	9358	94.52	0	0.00	0	0.00	9900	100.00
16:00	17:00	542	5.45	4773	47.97	1112	11.18	3522	35.40	9950	100.00
17:00	18:00	542	5.44	1909	19.14	1806	18.10	5718	57.32	9975	100.00
18:00	19:00	542	5.54	955	9.74	1993	20.33	6310	64.39	9800	100.00
19:00	20:00	542	5.69	0	0.00	2156	22.63	6827	71.67	9525	100.00
20:00	21:00	542	5.69	0	0.00	2156	22.63	6827	71.67	9525	100.00
21:00	22:00	542	5.74	0	0.00	2138	22.62	6770	71.64	9450	100.00
22:00	23:00	542	5.86	0	0.00	2090	22.59	6618	71.54	9250	100.00
23:00	00:00	542	5.96	0	0.00	2054	22.57	6504	71.47	9100	100.00

D

Values infrastructure influence

Tables D.1, D.2, D.3 and D.4 below shows the exact savings possible when increasing the storage area sizes and pipe sizes for the different electricity and GHG emissions scenarios. Figures are found in Chapter 10.

Table D.1: Changes (of costs and power) of the increased storage area sizes compared to the original sizes, in [%].

Change	Costs BC	Power BC	Costs S1	Power S1	Costs S2	Power S2	Costs S3	Power S3
SHU + 10%	-0.06%	-0.06%	-0.12%	-0.10%	-0.14%	-0.18%	-0.13%	-0.37%
SHU + 20%	-0.17%	-0.17%	-0.22%	-0.17%	-0.25%	-0.32%	-0.25%	0.31%
MIR + 10%	-0.68%	-0.68%	-0.69%	-0.63%	-0.76%	-0.95%	-0.60%	-0.97%
MIR + 10%	-1.33%	-1.33%	-1.39%	-1.36%	-1.46%	-1.60%	-1.21%	-1.63%
MUS + 10%	-4.45%	-4.45%	-4.54%	-4.28%	-5.11%	-4.37 %	-5.95%	-4.29%
MUS + 20%	-8.81%	-8.81%	-8.77%	-8.92%	-9.53%	-7.89%	-11.22%	-8.14%

Table D.2: Changes (of GHG emissions and power) of the increased storage area sizes compared to the original sizes, in [%].

Change	Costs AV'17	Power AV'17	Costs TD'17	Power TD'17	Costs AV'30	Power AV'30
SHU + 10%	-0.11%	-0.11%	-0.11%	-0.11%	-0.08%	-0.08%
SHU + 20%	-0.20%	-0.20%	-0.20%	-0.20%	-0.20%	-0.20%
MIR + 10%	-0.69%	-0.69%	-0.69%	-0.69%	-0.68%	-0.68%
MIR + 20%	-1.35%	-1.35%	-1.35%	-1.35%	-1.35%	-1.35%
MUS + 10%	-4.46%	-4.46%	-4.46%	-4.46%	-4.46%	-4.46%
MUS + 20%	-8.81%	-8.81%	-8.81%	-8.81%	-8.81%	-8.81%
Change	Costs TD'30	Power TD'30	Costs AV'50	Power AV'50	Costs TD'50	Power TD'50
SHU + 10%	-0.07%	-0.09%	-0.11%	-0.11%	-0.17%	-0.05%
SHU + 20%	-0.21%	-0.19%	-0.20%	-0.20%	-0.25%	-0.95%
MIR + 10%	-0.69%	-0.73%	-0.69%	-0.69%	-0.66%	-0.56%
MIR + 20%	-1.37%	-1.42%	-1.33%	-1.33%	-1.25%	-1.23%
MUS + 10%	-4.47%	-4.40%	-2.49%	-4.46%	-5.63%	-3.43%
MUS + 20%	-8.85%	-8.73%	-8.81%	-8.81%	-10.79%	-7.13%

Table D.3: Changes (of costs and power) of the increased pipe area sizes compared to the original sizes, in [%].

Change	Costs BC	Power BC	Costs S1	Power S1	Costs S2	Power S2	Costs S3	Power S3
SHU-MIR + 10%	-3.07%	-3.07%	-3.12%	-3.18%	-3.16%	-3.22%	-3.26%	-0.21%
SHU-MIR + 20%	-4.66%	-4.66%	-4.63%	-4.69%	-4.89%	-4.64%	-5.73%	-2.34%
MIR-MUS + 10%	-11.57%	-11.57%	-11.63%	-11.57%	-12.73%	-10.06%	-15.58%	-10.45%
MIR-MUS + 20%	-18.28%	-18.28%	-18.17%	-18.38%	-18.89%	-15.25%	-23.02%	-15.24%

Table D.4: Changes (of GHG emissions and power) of the increased pipe area sizes compared to the original sizes, in [%].

Change	Costs AV'17	Power AV'17	Costs TD'17	Power TD'17	Costs AV'30	Power AV'30
SHU-MIR + 10%	-3.07%	-3.07%	-3.07%	-3.07%	-3.07%	-3.07%
SHU-MIR + 20%	-4.66%	-4.66%	-4.66%	-4.66%	-4.66%	-4.66%
MIR-MUS + 10%	-11.60%	-11.60%	-11.60%	-11.60%	-11.57%	-11.57%
MIR-MUS + 20%	-18.28%	-18.28%	-18.28%	-18.28%	-18.28%	-18.28%
Change	Costs TD'30	Power TD'30	Costs AV'50	Power AV'50	Costs TD'50	Power TD'50
SHU-MIR + 10%	-2.96%	-3.07%	-3.07%	-3.07%	-3.07%	0.02%
SHU-MIR + 20%	-4.59%	-4.72%	-4.66%	-4.66%	-5.29%	-3.39%
MIR-MUS + 10%	-11.78%	-11.44%	-11.60%	-11.60%	-9.22%	-15.32%
MIR-MUS + 20%	-18.39%	-18.02%	-18.28%	-18.28%	-23.17%	-14.89%